

074 71085

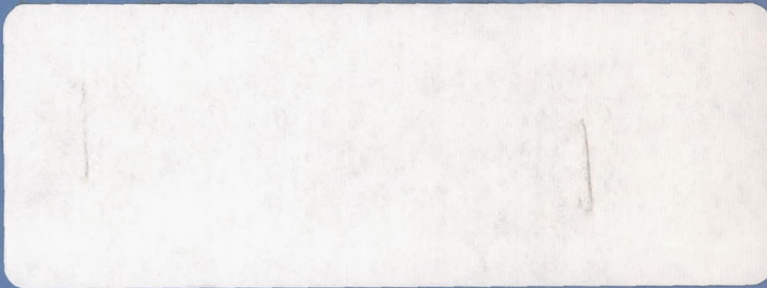
CONFIDENTIAL

NASA TECHNICAL
MEMORANDUM



NASA TM X-3024

NASA TM X-3024



DECLASSIFIED
BY AUTHORITY OF NASA CLASSIFICATION
CHANGE NOTICES NO. 240 DATED 30 SEP 76.
ITEM NO. 52

EFFECTS OF WING TRAILING-EDGE TRUNCATION
ON AERODYNAMIC CHARACTERISTICS OF
AN NASA SUPERCRITICAL-WING
RESEARCH AIRPLANE MODEL

by Dennis W. Bartlett and Charles D. Harris

Langley Research Center
Hampton, Va. 23665



NATIONAL AERONAUTICS AND SPACE ADMINISTRATION • WASHINGTON, D. C. • AUGUST 1974

CONFIDENTIAL

~~CONFIDENTIAL~~

1. Report No. NASA TM X-3024	2. Government Accession No.	3. Recipient's Catalog No.
4. Title and Subtitle EFFECTS OF WING TRAILING-EDGE TRUNCATION ON AERODYNAMIC CHARACTERISTICS OF AN NASA SUPERCritical-WING RESEARCH AIRPLANE MODEL (U)		5. Report Date August 1974
7. Author(s) Dennis W. Bartlett and Charles D. Harris		6. Performing Organization Code
9. Performing Organization Name and Address NASA Langley Research Center Hampton, Va. 23665		8. Performing Organization Report No. L-9158
12. Sponsoring Agency Name and Address National Aeronautics and Space Administration Washington, D.C. 20546		10. Work Unit No. 766-73-60-04
15. Supplementary Notes		11. Contract or Grant No.
		13. Type of Report and Period Covered Technical Memorandum
		14. Sponsoring Agency Code
16. Abstract		

An investigation has been conducted in the Langley 8-foot transonic pressure tunnel at Mach numbers from 0.80 to 1.00 to determine the effects of wing trailing-edge truncation on the aerodynamic characteristics of a 0.0625-scale model of an NASA supercritical-wing research airplane. Presented are the effects of wing trailing-edge truncations of 1, 2, and 3 percent of the local streamwise chord on the longitudinal aerodynamic characteristics and the wing section characteristics.

CLASSIFICATION CHANGE

To UNCLASSIFIED

By authority of NASA HQ. T.D. 77-163
Changed by L. Shirley Date 6-15-76
Classified Document Master Control Station, NASA
Scientific and Technical Information Facility

17. Key Words (Suggested by Author(s))

TF-8A supercritical-wing research aircraft
Transonic aerodynamics
Supercritical technology
Wing trailing-edge truncation

21. No. of Pages 103	22. Price
--------------------------------	-----------

EFFECTS OF WING TRAILING-EDGE TRUNCATION
ON AERODYNAMIC CHARACTERISTICS OF AN
NASA SUPERCRITICAL-WING RESEARCH
AIRPLANE MODEL*

By Dennis W. Bartlett and Charles D. Harris
Langley Research Center

SUMMARY

An investigation has been conducted in the Langley 8-foot transonic pressure tunnel at Mach numbers from 0.80 to 1.00 to determine the effects of wing trailing-edge truncation on the aerodynamic characteristics of a 0.0625-scale model of an NASA supercritical-wing research airplane.

The results of this investigation indicate that truncations to the wing trailing edge reduce the aft camber of the wing resulting in losses in lift and positive pitching-moment shifts. The drag polars are also altered such that the minimum drag is reduced but the drag at higher lift coefficients is increased; however, at the higher Mach numbers ($M = 0.96$ to 1.00) the drag is essentially unchanged in the region of the design lift coefficient of 0.40.

Wing pressure distributions indicate that truncations to the wing trailing edge reduce the aft velocity peak on the wing upper surface, the effect being most noticeable at the lower angles of attack (near those for minimum drag) for Mach numbers from about 0.96 to 1.00. The loss of lift associated with the truncated-trailing-edge configurations occurs primarily over the aft section of the wing (evident in the wing pressure distributions), and this in turn causes the positive shifts in pitching-moment coefficient.

INTRODUCTION

For the past several years, a general research effort has been underway at the National Aeronautics and Space Administration to explore and develop the technology for the design of wings which incorporate the NASA supercritical airfoil; investigations have been conducted on both wind-tunnel models and full-scale research airplanes. (See refs. 1 to 4.)

*Title, Unclassified.

Comparisons of wind-tunnel and flight data for the TF-8A supercritical-wing research airplane (ref. 1) have generally shown good agreement, particularly in drag-divergence Mach number. Certain discrepancies are evident, however, when comparing the drag polars, the pitching moments, and the wing pressure distributions; these discrepancies apparently result from the full-scale wing having more effective aft camber than the model wing. This apparent increase in effective aft wing camber at flight conditions causes the full-scale airplane to have higher minimum drag but lower drag due to lift, more negative pitching moments, and higher induced velocities over the aft region of the wing upper surface. At Mach numbers below 0.95, this difference in effective aft wing camber is probably a consequence of the reduced viscous uncambering effect associated with the higher flight Reynolds numbers. As sonic velocity is approached, however, a combination of Reynolds number and wind-tunnel boundary interference effects is probably responsible for the effects noted.

As a result of these earlier unknown influences, the model wing was optimized in an environment that resulted in an excessive amount of aft camber for the most efficient operation at cruise for full-scale flight conditions. As a basis for a possible future modification to the full-scale airplane, a wind-tunnel investigation has been conducted in the Langley 8-foot transonic pressure tunnel to investigate the effects of reducing aft camber by truncating the wing trailing edge. Presented herein are the effects of wing trailing-edge truncations of 1, 2, and 3 percent of the local streamwise chords on the longitudinal aerodynamic characteristics and the wing section characteristics of a 0.0625-scale model of the research airplane. Data are presented over an angle-of-attack range of approximately 0° to 5° and at Mach numbers from 0.80 to 1.00; however, data were obtained only at a Mach number of 0.95 for the 1-percent trailing-edge truncation.

SYMBOLS

Results presented herein are referred to the stability-axis system for the longitudinal aerodynamic characteristics. Total force and moment data have been reduced to conventional coefficient form based on the geometry of the reference wing planform, that is, the planform produced by extending the straight leading and trailing edges of the outboard sections of the wing to the fuselage center line. (See fig. 1(a).) The total pitching-moment coefficients are referenced to the quarter-chord point (model fuselage station 71.482 cm (28.143 in.)) of the mean geometric chord of the reference wing panel. Wing-section pitching-moment coefficients are referenced to a point located at 25 percent of the local total streamwise chord for the particular wing station at which data are presented.

In this report, all orifice locations are presented in terms of the local total streamwise chord, and these locations (x/c) are designated by unprimed symbols. In previous

reports (refs. 2 to 4, for example), primed symbols (i.e., x' and c') were used in conjunction with chords associated with the total wing planform which includes the leading-edge glove and the trailing-edge extension, and unprimed symbols (x and c) were used in conjunction with chords associated with the reference wing planform. (See fig. 1(a).) Outside the glove region, of course, the total and reference wing planforms are identical.

It should be noted that, although the actual wing area and chords were decreased slightly with each succeeding trailing-edge truncation, a constant reference area (S) and mean geometric chord (\bar{c}) based on the geometry of the initial or basic wing (0-percent T.E. truncation) were used to reduce the total airplane forces and moments of all configurations to coefficient form. However, the x/c locations for the pressure orifices on the wing were computed by using the actual chord lengths which resulted from each trailing-edge truncation; these locations are given in table I.

All dimensional values are given in both SI and U.S. Customary Units; however, measurements and calculations were made in U.S. Customary Units.

b wing span, 82.15 centimeters (32.34 inches)

C_D drag coefficient, $\frac{\text{Drag}}{qS}$

C_L lift coefficient, $\frac{\text{Lift}}{qS}$

C_m pitching-moment coefficient, $\frac{\text{Pitching moment}}{qS\bar{c}}$

C_p pressure coefficient, $\frac{p_l - p}{q}$

$C_{p,L}$ wing lower-surface pressure coefficient

$C_{p,U}$ wing upper-surface pressure coefficient

c local total streamwise chord of wing, centimeters (inches)

\bar{c} mean geometric chord of reference wing panel (0-percent T.E. truncation), 13.00 centimeters (5.12 inches)

c_m wing-section pitching-moment coefficient, $\int_0^1 (C_{p,L} - C_{p,U})(0.25 - \frac{x}{\bar{c}}) d \frac{x}{\bar{c}}$

c_n wing-section normal-force coefficient, $\int_0^1 (C_{p,L} - C_{p,U}) d \frac{x}{\bar{c}}$

M	free-stream Mach number
m	surface slope, $\frac{dz}{dx}$
p	free-stream static pressure, pascals (pounds per foot ²)
p_l	local static pressure, pascals (pounds per foot ²)
q	free-stream dynamic pressure, pascals (pounds per foot ²)
S	area of reference wing panels (0-percent T.E. truncation) including fuselage intercept, 0.0996 meter ² (1.0719 feet ²)
x	streamwise distance measured from leading edge of total wing planform, positive toward wing trailing edge, centimeters (inches)
y	spanwise distance measured normal to model plane of symmetry, 0 at fuselage center line, centimeters (inches)
z	vertical distance measured from reference water line, 18.83 cm (7.415 in.), centimeters (inches)
α	angle of attack, referred to fuselage water line, degrees
β	angle of sideslip, referred to fuselage center line, degrees
δ_h	horizontal-tail deflection angle, referred to fuselage water line (positive when trailing edge is down), degrees

Abbreviations:

L.S.	wing lower surface
U.S.	wing upper surface
T.E.	wing trailing edge

APPARATUS AND PROCEDURES

Geometric characteristics of the 0.0625-scale model of the TF-8A supercritical-wing research airplane are presented in figure 1 and photographs are presented as figure 2.

The sweptback supercritical wing was constructed of an aluminum core with plastic fill on the upper-right and lower-left wing panels in which steel pressure tubing was embedded. The wing was mounted at a root-chord incidence angle of 1.5° with respect to the fuselage and has approximately 5° of twist (washout) from root to tip in the unloaded condition. The reference wing planform (0-percent T.E. truncation) has an aspect ratio of 6.8, a taper ratio of 0.36, and sweepback of 42.24° at the quarter-chord. Furthermore, the area of the reference wing planform including the fuselage intercept is 0.0996 m^2 (1.072 ft^2), and the mean geometric chord of a reference wing panel is 12.9997 cm (5.118 in.) (fig. 1(a)). Nondimensional coordinates for the basic wing (0-percent T.E. truncation) can be found in references 2 and 3.

The truncations to the wing trailing edge extended from the wing tip to the 40-percent semispan station and were then linearly faired into the original trailing edge to provide a point of tangency. As the percent of truncation increased, the point of tangency of the linear fairing with the original trailing edge moved inboard. It should be noted that each percentage of T.E. truncation is based on the initial streamwise chords of the basic wing. The supercritical wing panel with the 3-percent trailing-edge truncation shown as a dashed line is presented in figure 1(e), and a comparison of the airfoil section, the airfoil upper surface slopes, and the airfoil lower surface slopes at the 85-percent semispan station is presented in figures 1(f), 1(g), and 1(h), respectively, for the 0- and 3-percent T.E. truncations. The coordinates for the truncated airfoil were generated by recomputing z/c and x/c for the basic airfoil with a 3-percent shorter chord.

The basic fuselage and tails are scaled versions of those utilized on the test-bed airplane (TF-8A). The model fuselage is equipped with flow-through ducts which discharge at the base of the model on either side of the flat-sided model support sting.

Side fuselage area-rule additions were added to the basic fuselage (fig. 1(a)), and aileron-hinge fairings (figs. 1(c) and 1(d)) were included on the model wing for the present investigation. The side fuselage area-rule additions improve the longitudinal progression of the model cross-sectional area, and their effects on the longitudinal aerodynamic characteristics and wing pressure distributions of an 0.087-scale model of the research airplane are presented in reference 2. It should be pointed out that the majority of wind-tunnel investigations previously reported on the TF-8A supercritical-wing research airplane (refs. 2 to 4, for example) utilized a 0.087-scale model, whereas the present investigation utilized a 0.0625-scale model.

Test Facility

The investigation was conducted in the Langley 8-foot transonic pressure tunnel (ref. 5). This facility is a continuous-flow, single-return, rectangular slotted-throat tunnel having controls that allow for the independent variation of Mach number, density, temperature, and dewpoint. The test section is square in cross section with the upper and lower walls radially slotted (each wall having an open ratio of approximately 0.06) to permit changing the test-section Mach number continuously through the transonic speed range. The stagnation pressure in the tunnel can be varied from a minimum value of about 0.25 atmosphere (1 atmosphere = 101 325 Pa) at all Mach numbers to a maximum value of approximately 1.5 atmospheres at transonic Mach numbers and approximately 2.0 atmospheres at Mach numbers of 0.40 or less.

In an effort to reduce subsonic blockage effects, special test-section sidewall inserts were employed for this investigation (fig. 1(i)). (See refs. 4 and 6.) These sidewall inserts were indented to account for 40 percent of the longitudinal development of model cross-sectional area. This resulted, effectively, in a "scalloping" of the sidewalls of the tunnel test section adjacent to the model. Fore and aft of the model, these inserts reduced the cross-sectional area of the tunnel test section by approximately 0.24 percent.

Boundary-Layer Transition

Boundary-layer transition was fixed on the model components for the entire investigation. The boundary-layer trip locations and carborundum grain sizes used on the wing are shown in figure 3. These locations were generally determined by the procedures of reference 7 in an effort to simulate the full-scale Reynolds number boundary-layer characteristics at the wing trailing edge. It should be pointed out that the boundary-layer trips were not moved during the test from their original location on the basic wing as shown in figure 3 even though the relative location of the trips in terms of percent chord did vary slightly as a result of truncating the trailing edge.

For all test Mach numbers, No. 120 carborundum grains were located on the horizontal and vertical tails at 5 percent of the local streamwise chords. Trips of No. 120 carborundum grains were also applied around the fuselage 2.54 cm (1.00 in.) aft of the model nose and 1.27 cm (0.50 in.) rearward of the inlet lip on both the inner and outer surfaces. All boundary-layer trips were applied to the model in bands that were 0.127 cm (0.05 in.) wide, and the leading edge of the bands was located by measurements taken in the streamwise direction. The carborundum grains were sized by the techniques of reference 8.

Measurements and Test Conditions

Six-component force and moment data were obtained with an electrical strain-gage balance housed within the fuselage cavity, and flush-surface static-pressure orifices were distributed in streamwise rows over the upper right and lower left wing panels. (See table I.) The wing pressures were recorded with differential-pressure, scanning-valve units mounted in the nose section of the model allowing balance force and scanning-valve data to be obtained simultaneously.

For determination of the base drag, the static pressures in the balance chamber and in the plane of the model base were recorded with differential-pressure transducers referenced to the free-stream static pressure, and the model attitude was determined from an accelerometer attached to the balance block.

Measurements were taken over a Mach number range varying from 0.80 to 1.00 for angles of attack that varied from approximately 0° to 5° at a sideslip angle of 0° . The horizontal tail was deflected -2.5° for all tests.

The entire investigation was conducted at a stagnation temperature of 322 K (120° F) and at a dewpoint low enough to avoid significant condensation effects. (See ref. 9.)

The tunnel test conditions for the present investigation are summarized in table II.

Corrections

Drag results presented herein have been adjusted to correspond to free-stream static pressure acting in the balance mounting block chamber and at the model base. No adjustments, however, have been made to the drag for internal flow through the ducts. It might be noted that the model base area for the base pressure correction included the sting cross-sectional area at the model base but did not include the exit area of the ducts.

No corrections have been applied to the data for sting interference effects other than the exclusion of the base drag from the total measured drag; however, the model support sting was designed on the basis of the results in reference 10 to minimize sting interference effects at near-sonic Mach numbers.

Corrections have been made to the measured angle of attack to account for tunnel airflow angularity.

PRESENTATION OF RESULTS

The results of this investigation are presented in the following figures:

	Figure
Effect of wing trailing-edge truncation on longitudinal aerodynamic characteristics	4
Effect of wing trailing-edge truncation on wing pressure distributions at -	
Mach number 0.80	5
Mach number 0.90	6
Mach number 0.95	7
Mach number 0.96	8
Mach number 0.97	9
Mach number 0.98	10
Mach number 0.99	11
Mach number 1.00	12
Effect of wing trailing-edge truncation on spanwise distribution of wing-section normal-force coefficient	13
Effect of wing trailing-edge truncation on spanwise distribution of wing-section pitching-moment coefficient	14

DISCUSSION OF RESULTS

Longitudinal Aerodynamic Characteristics

Truncating the wing trailing-edge results in a small increase in the thickness-chord ratios along the wing and a slight loss of wing area, but the predominant effect on the longitudinal aerodynamic characteristics appears to result from the decrease in camber and surface slopes near the trailing edge of the wing. (See figs. 1(f), 1(g), and 1(h).) For each succeeding truncation there is a favorable positive $C_{m,0}$ (pitching-moment coefficient when $C_L = 0$) shift and a negative $C_{L,0}$ (lift coefficient when $\alpha = 0^\circ$) shift at all the Mach numbers for which data are presented in figure 4, and these pitching-moment and lift increments are generally constant throughout the angle-of-attack range.

With regard to the drag characteristics, truncating the wing trailing edge results in a rotation of the drag polars. The direction of the rotation produces lower minimum drag but higher drag due to lift as would be expected with a reduction in camber. (See fig. 4.) The lift coefficient about which the polars are rotated varies from approximately

0.10 at a Mach number of 0.80 to about 0.40 at the higher Mach numbers for which data are presented in figure 4.

Wing Section Characteristics

Pressure distributions. - From the pressure distributions of figures 5 to 12, it is evident that the loss of lift associated with the truncations to the trailing edge primarily occurs over the aft section of the wing. This loss, of course, results in the positive pitching-moment shifts and the losses in lift noted previously in the total airplane force and moment data of figure 4.

Minimum drag levels for the truncated trailing-edge configurations are significantly lower particularly at Mach numbers 0.96 and above. (See fig. 4.) These reductions in minimum drag are felt to be associated with changes in the region of expanding flow (increasingly more negative pressure coefficient) on the wing upper surface in the vicinity of the 80-percent chord. (See figs. 5 to 12, $\alpha = 1^\circ$ and 2° .) This region of relatively high induced velocities (corresponding to more negative pressure coefficients) produces a strong adverse pressure gradient over the rear of the wing upper surface, and it is in this region of pressure recovery that the boundary-layer development is most sensitive. At the higher Mach numbers ($M = 0.95$ to 1.00), these induced velocities become supersonic and develop into a shock system with attendant wave losses. (See figs. 7 to 12, $\alpha = 1^\circ$ and 2° .) As the trailing edge is progressively truncated, the resulting decrease in wing upper surface slopes (fig. 1(g)) attenuate the local induced velocities on this region of the wing; thereby, not only is the adverse pressure gradient reduced but also the associated boundary-layer and shock losses.

At angles of attack of 4° and 5° , a slight improvement in trailing-edge pressure recovery is also indicated for the truncated trailing-edge configurations at Mach numbers above 0.95; although, no significant differences are evident in the strength of the wing upper-surface shock wave. (See figs. 7 to 12.)

Section normal-force and pitching-moment coefficients. - As would be expected, the wing section normal-force and pitching-moment coefficients (figs. 13 and 14, respectively) indicate the same effects of trailing-edge truncation as the total model lift and pitching-moment coefficients (fig. 4). The reductions in lift and the increases in pitching moment associated with the truncated-trailing-edge configurations are confined to that part of the wing outboard of semispan station $(\frac{y}{b/2}) 0.3$. This is not unexpected since the truncations to the trailing edge did not extend inboard of semispan station 0.26. (See fig. 1(e).)

SUMMARY OF RESULTS

The present wind-tunnel investigation of effects of wing trailing-edge truncation on the aerodynamic characteristics of an NASA supercritical-wing research airplane configuration has shown the following results:

1. Truncations to the wing trailing edge reduce the aft camber of the wing and result in losses in lift and positive pitching-moment increments.
2. Truncations to the wing trailing edge alter the shape of the drag polars such that the minimum drag is reduced but the drag at higher lift coefficients is increased; however, at the higher Mach numbers ($M = 0.96$ to 1.00), the drag is essentially unchanged in the region of the design lift coefficient of 0.40.
3. Wing pressure distributions indicate that truncations to the wing trailing edge reduce the aft velocity peak on the wing upper surface, the effect being most noticeable at angles of attack near minimum drag for Mach numbers of about 0.96 to 1.00.
4. The loss of lift associated with the truncated-trailing-edge configurations occurs primarily over the aft section of the wing, as seen in the pressure distributions, and this results in the positive pitching-moment increments.

Langley Research Center,
National Aeronautics and Space Administration,
Hampton, Va., April 25, 1974.

~~SECRET~~

REFERENCES

1. Anon.: Supercritical Wing Technology - A Progress Report on Flight Evaluations. NASA SP-301, 1972.
2. Bartlett, Dennis W.; and Harris, Charles D.: Aerodynamic Characteristics of an NASA Supercritical-Wing Research Airplane Model With and Without Fuselage Area-Rule Additions at Mach 0.25 to 1.00. NASA TM X-2633, 1972.
3. Bartlett, Dennis W.; and Re, Richard J.: Wind-Tunnel Investigation of Basic Aerodynamic Characteristics of a Supercritical-Wing Research Airplane Configuration. NASA TM X-2470, 1972.
4. Harris, Charles D.; and Bartlett, Dennis W.: Wind-Tunnel Investigation of Effects of Underwing Leading-Edge Vortex Generators on a Supercritical-Wing Research Airplane Configuration. NASA TM X-2471, 1972.
5. Schaefer, William T., Jr.: Characteristics of Major Active Wind Tunnels at the Langley Research Center. NASA TM X-1130, 1965.
6. Goethert, Bernhard H.: Transonic Wind Tunnel Testing. AGARDograph No. 49, Pergamon Press, 1961, pp. 41-56.
7. Blackwell, James A., Jr.: Preliminary Study of Effects of Reynolds Number and Boundary-Layer Transition Location on Shock-Induced Separation. NASA TN D-5003, 1969.
8. Braslow, Albert L.; and Knox, Eugene C.: Simplified Method for Determination of Critical Height of Distributed Roughness Particles for Boundary-Layer Transition of Mach Numbers From 0 to 5. NACA TN 4363, 1958.
9. Jordan, Frank L., Jr.: Investigation at Near-Sonic Speed of Some Effects of Humidity on the Longitudinal Aerodynamic Characteristics of an NASA Supercritical Wing Research Airplane Model. NASA TM X-2618, 1972.
10. Lee, George; and Summers, James L.: Effects of Sting-Support Interference on the Drag of an Ogive-Cylinder Body With and Without a Boattail at 0.6 to 1.4 Mach Number. NACA RM A57I09, 1957.

TABLE I.- LOCATION OF WING PRESSURE ORIFICES

(a) Layout of pressure orifices on wing

c(0-percent T.E. truncation)

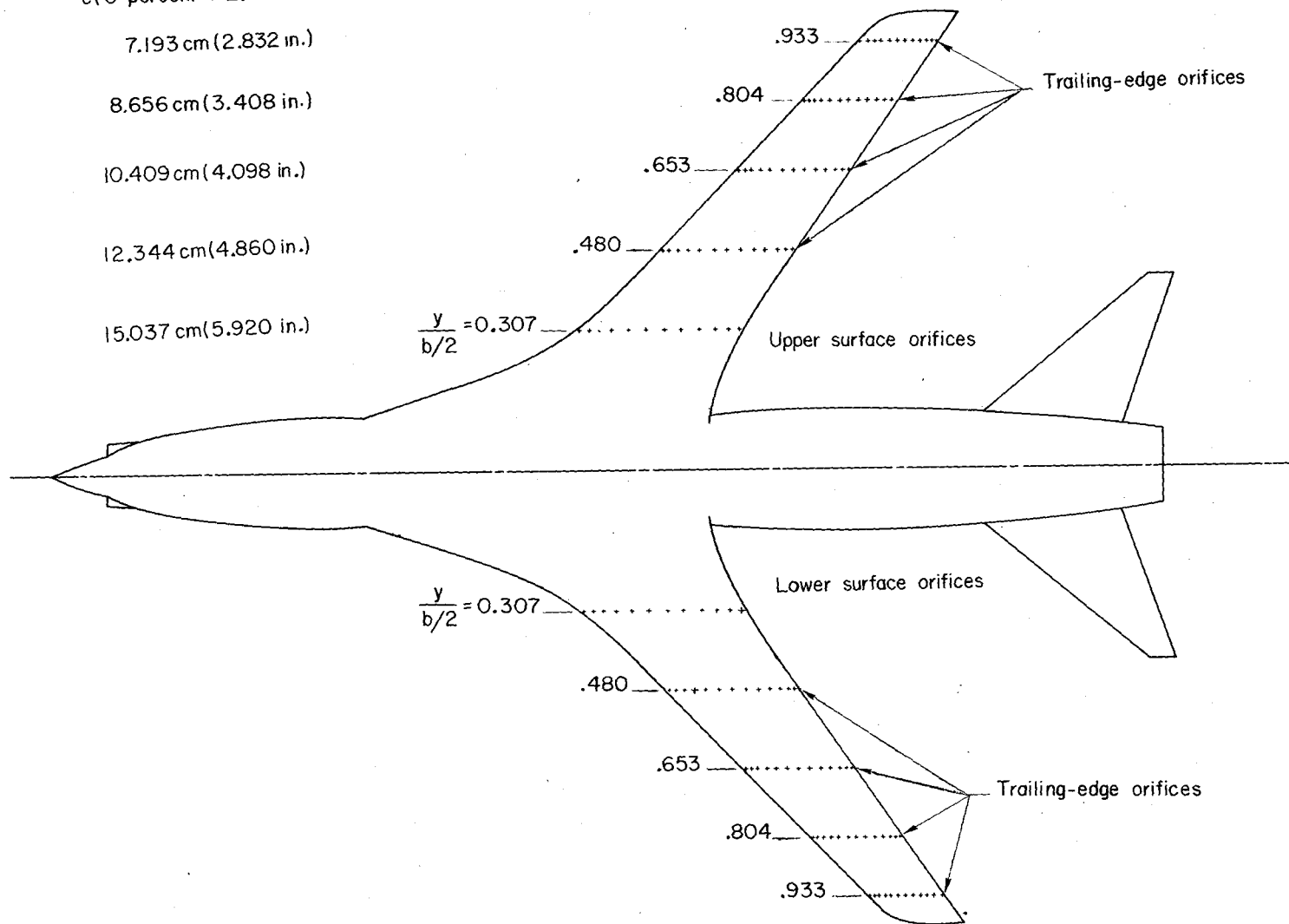
7.193 cm (2.832 in.)

8.656 cm (3.408 in.)

10.409 cm (4.098 in.)

12.344 cm (4.860 in.)

15.037 cm (5.920 in.)



~~CONFIDENTIAL~~

TABLE I.-LOCATION OF WING PRESSURE ORIFICES - Continued

(b) 0-percent T.E. truncation

Wing orifice location, $\frac{x}{c}$, at semispan station, $\frac{y}{b/2}$, of -				
0.307	0.480	0.653	0.804	0.933
Right-wing upper surface				
0.021	0.024	0.026	0.022	0.022
.035	.071	.078	.076	.083
.105	.132	.135	.124	.138
.171	.205	.214	.198	.217
.282	.294	.296	.297	.305
.399	.399	.404	.394	.408
.511	.496	.497	.493	.497
.617	.597	.601	.596	.591
.734	.699	.700	.697	.696
.832	.778	.779	.790	.785
.918	.865	.864	.858	.869
.987	.925	.920	.929	.932
	1.000	1.000	1.000	1.000
Left-wing lower surface				
0.020	0.023	0.023	0.022	0.014
.035	.065	.090	.078	.084
.100	.133	.133	.129	.135
.173	.209	.214	.208	.213
.289	.297	.291	.299	.296
.402	.402	.404	.403	.401
.517	.497	.501	.499	.503
.618	.598	.602	.602	.588
.734	.697	.697	.699	.693
.834	.777	.776	.791	.782
.916	.863	.860	.865	.869
.985	.927	.917	.926	.920
	1.000	1.000	1.000	1.000

~~CONFIDENTIAL~~

~~CONFIDENTIAL~~

TABLE I.- LOCATION OF WING PRESSURE ORIFICES – Continued

(c) 1-percent T.E. truncation

Wing orifice location, $\frac{x}{c}$, at semispan station, $\frac{y}{b/2}$, of –				
0.307	0.480	0.653	0.804	0.933
Right-wing upper surface				
0.021	0.024	0.026	0.022	0.022
.035	.072	.079	.077	.083
.105	.134	.137	.125	.139
.171	.208	.217	.200	.219
.282	.297	.299	.300	.309
.399	.403	.408	.398	.412
.511	.501	.502	.498	.502
.617	.603	.607	.602	.597
.734	.707	.707	.704	.703
.832	.786	.787	.798	.793
.918	.873	.873	.866	.877
.987	.935	.929	.938	.941
	1.000	1.000	1.000	1.000
Left-wing lower surface				
0.020	0.023	0.023	0.022	0.014
.035	.066	.080	.079	.084
.100	.135	.135	.130	.136
.173	.211	.216	.210	.216
.289	.300	.294	.302	.299
.402	.406	.409	.407	.405
.517	.502	.506	.504	.508
.618	.604	.608	.608	.593
.734	.704	.704	.707	.700
.834	.784	.784	.799	.789
.916	.872	.868	.873	.878
.985	.936	.926	.936	.925
	1.000	1.000	1.000	1.000

~~CONFIDENTIAL~~

~~CONFIDENTIAL~~

TABLE I.- LOCATION OF WING PRESSURE ORIFICES - Continued

(d) 2-percent T.E. truncation

Wing orifice location, $\frac{x}{c}$, at semispan station, $\frac{y}{b/2}$, of -				
0.307	0.480	0.653	0.804	0.933
Right-wing upper surface				
0.021	0.025	0.026	0.022	0.022
.035	.072	.080	.077	.084
.105	.135	.138	.126	.141
.171	.210	.219	.202	.222
.282	.300	.302	.303	.312
.399	.407	.413	.402	.416
.511	.506	.507	.503	.507
.617	.609	.613	.608	.603
.734	.714	.714	.711	.710
.832	.794	.795	.807	.801
.918	.882	.882	.875	.886
.987	.944	.938	.947	.951
	1.000	1.000	1.000	1.000
Left-wing lower surface				
0.020	0.024	0.024	0.022	0.014
.035	.066	.081	.080	.085
.100	.136	.136	.131	.137
.173	.213	.218	.212	.218
.289	.303	.297	.305	.302
.402	.410	.412	.411	.410
.517	.507	.512	.508	.513
.618	.610	.614	.614	.600
.734	.711	.711	.714	.707
.834	.792	.792	.807	.797
.916	.881	.877	.882	.887
.985	.946	.935	.945	.939
	1.000	1.000	1.000	1.000

~~CONFIDENTIAL~~

~~CONFIDENTIAL~~

TABLE I.- LOCATION OF WING PRESSURE ORIFICES - Concluded

(e) 3-percent T.E. truncation

Wing orifice location, $\frac{x}{c}$, at semispan station, $\frac{y}{b/2}$, of -				
0.307	0.480	0.653	0.804	0.933
Right-wing upper surface				
0.021	0.025	0.026	0.022	0.022
.035	.073	.081	.078	.085
.105	.136	.140	.128	.142
.171	.212	.221	.204	.224
.282	.303	.305	.306	.315
.399	.411	.417	.406	.421
.511	.511	.512	.508	.512
.617	.616	.619	.615	.609
.734	.721	.721	.719	.717
.832	.802	.803	.815	.810
.918	.891	.891	.884	.896
.987	.954	.948	.957	.960
	1.000	1.000	1.000	1.000
Left-wing lower surface				
0.020	0.024	0.024	0.022	0.014
.035	.067	.082	.080	.086
.100	.138	.137	.133	.139
.173	.216	.220	.214	.220
.289	.306	.300	.308	.305
.402	.414	.417	.415	.414
.517	.512	.517	.515	.518
.618	.617	.620	.621	.606
.734	.719	.718	.721	.715
.834	.801	.800	.815	.806
.916	.890	.886	.891	.896
.985	.956	.945	.955	.949
	1.000	1.000	1.000	1.000

~~CONFIDENTIAL~~

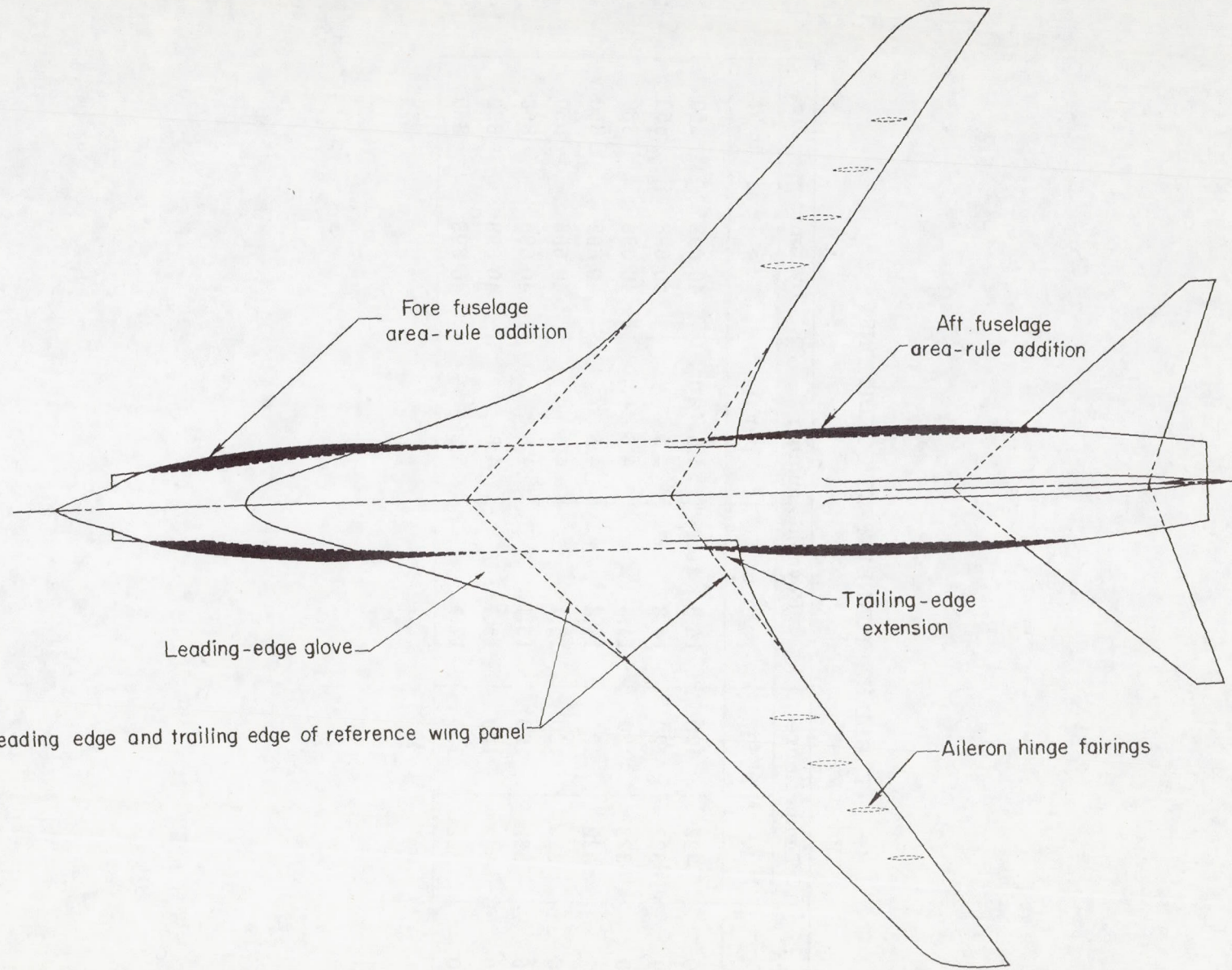
TABLE II.- TUNNEL TEST CONDITIONS

Mach number	Temperature		Reynolds number		Dynamic pressure	
	K	°F	per m	per ft	Pa	lb/ft ²
1.00	322	120	14.8×10^6	4.5×10^6	40 698	850
.99	322	120	14.8	4.5	40 698	850
.98	322	120	14.8	4.5	40 698	850
.97	322	120	14.8	4.5	40 698	850
.96	322	120	15.1	4.6	40 698	850
.95	322	120	15.1	4.6	40 698	850
.90	322	120	15.7	4.8	40 698	850
.80	322	120	17.1	5.2	40 698	850

~~CONFIDENTIAL~~

CONFIDENTIAL

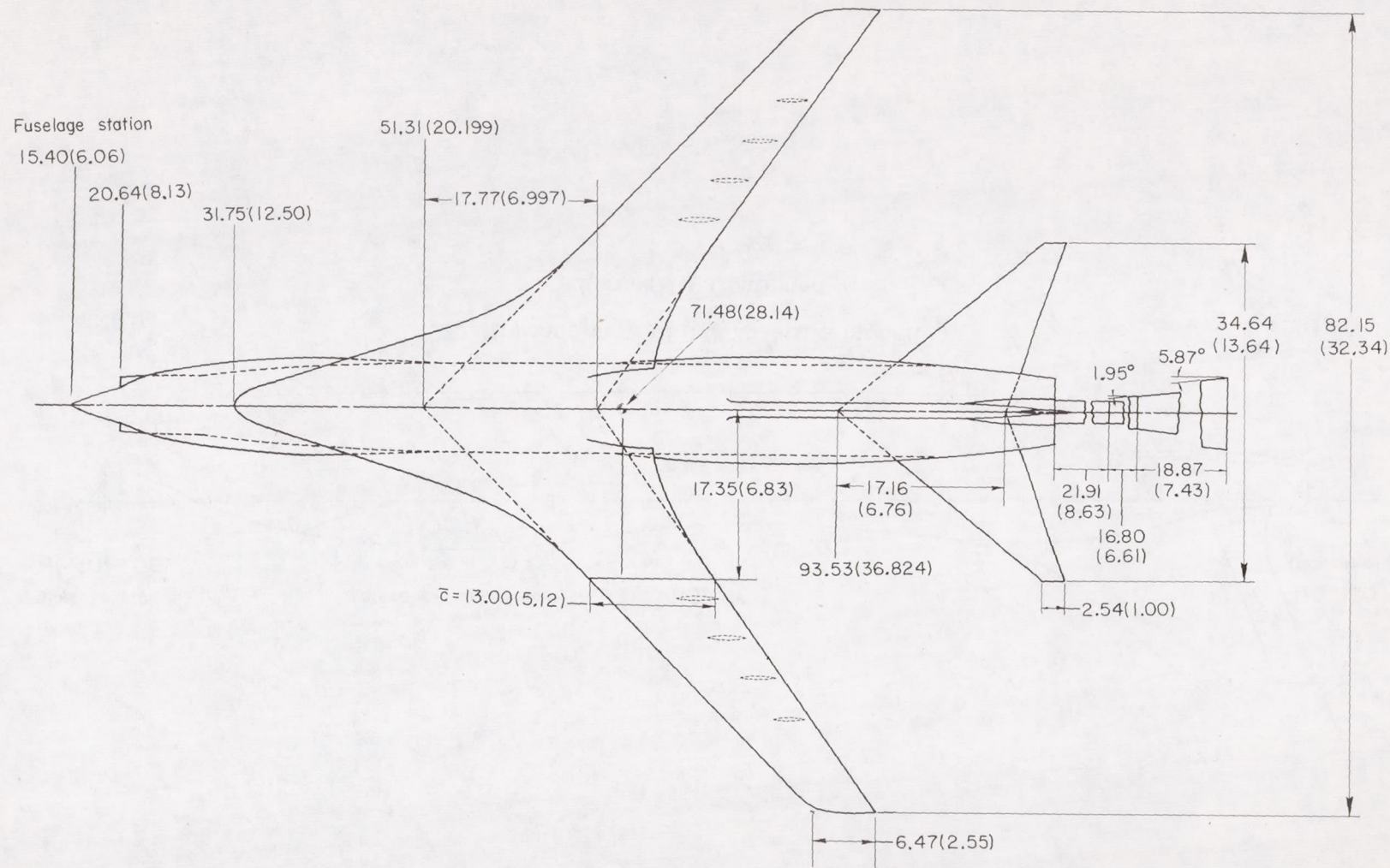
CONFIDENTIAL



(a) General planform arrangement of 0.0625-scale model.

Figure 1.- Model details. Linear dimensions are in cm (in.).

CONFIDENTIAL

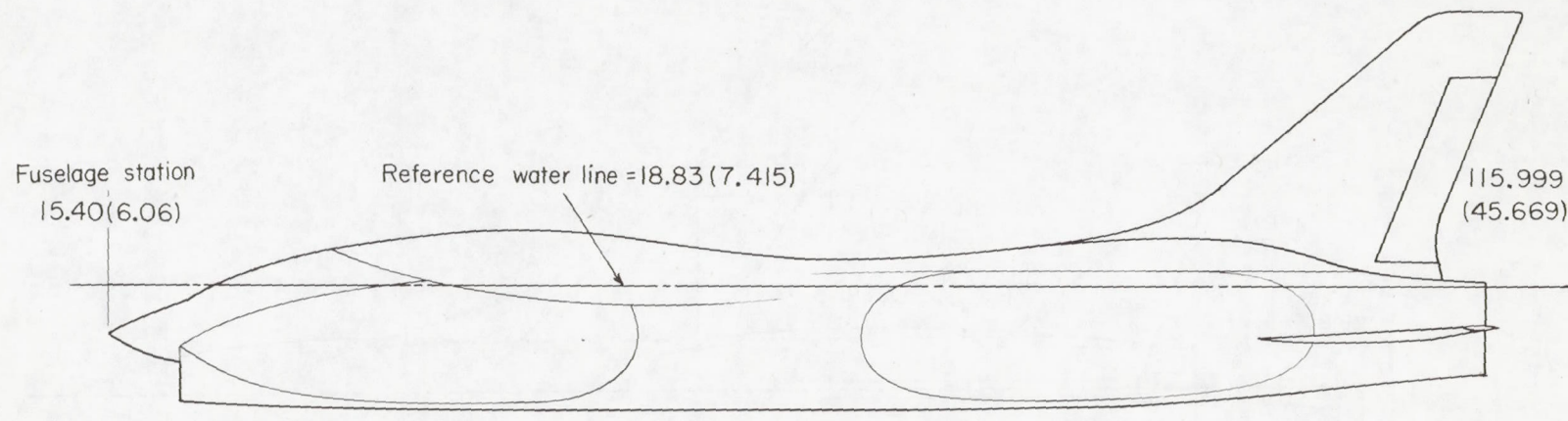


(a) Concluded.

Figure 1.- Continued.

CONFIDENTIAL

~~CONFIDENTIAL~~

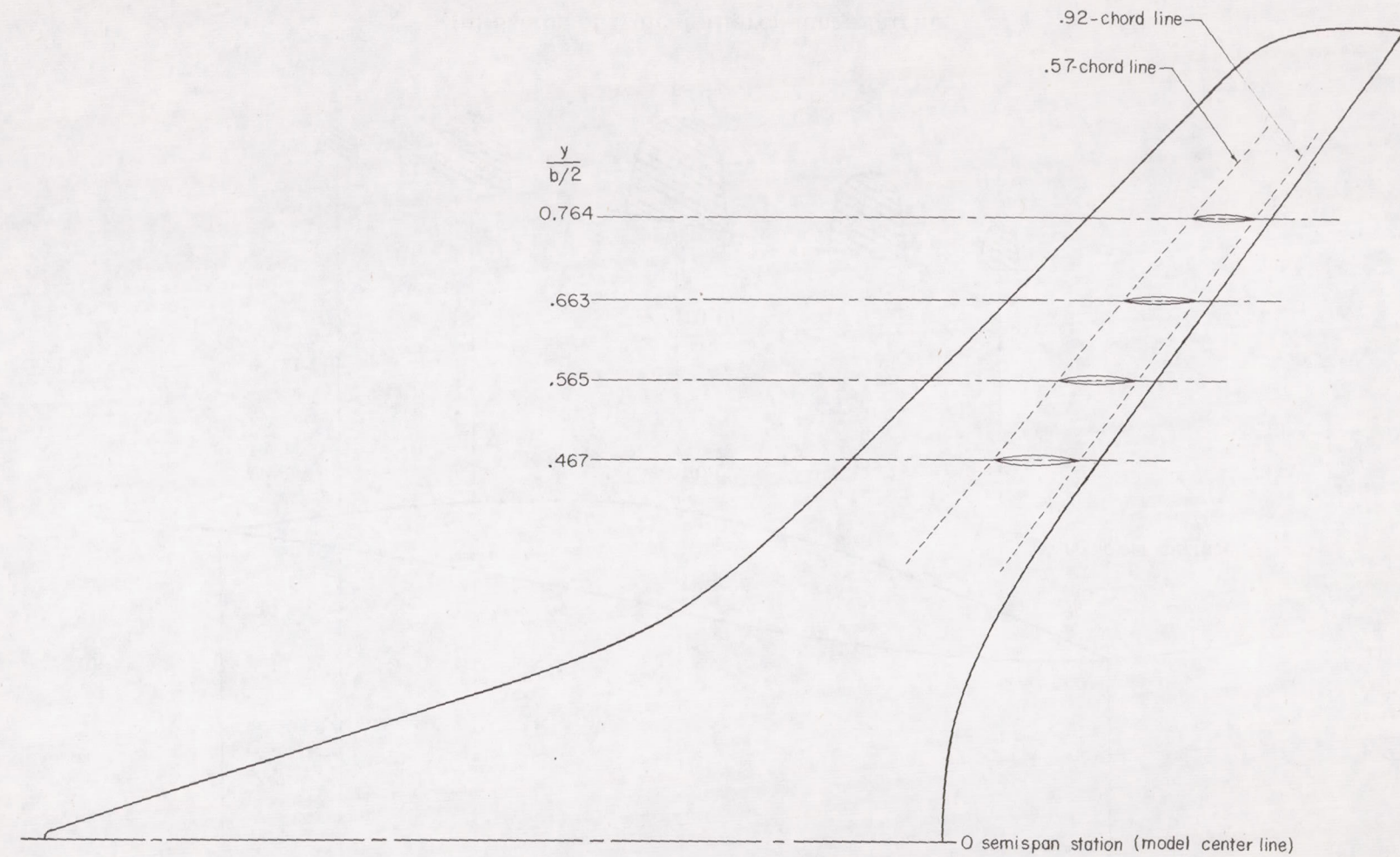


~~CONFIDENTIAL~~

(b) Side view of 0.0625-scale model.

Figure 1.- Continued.

~~CONFIDENTIAL~~



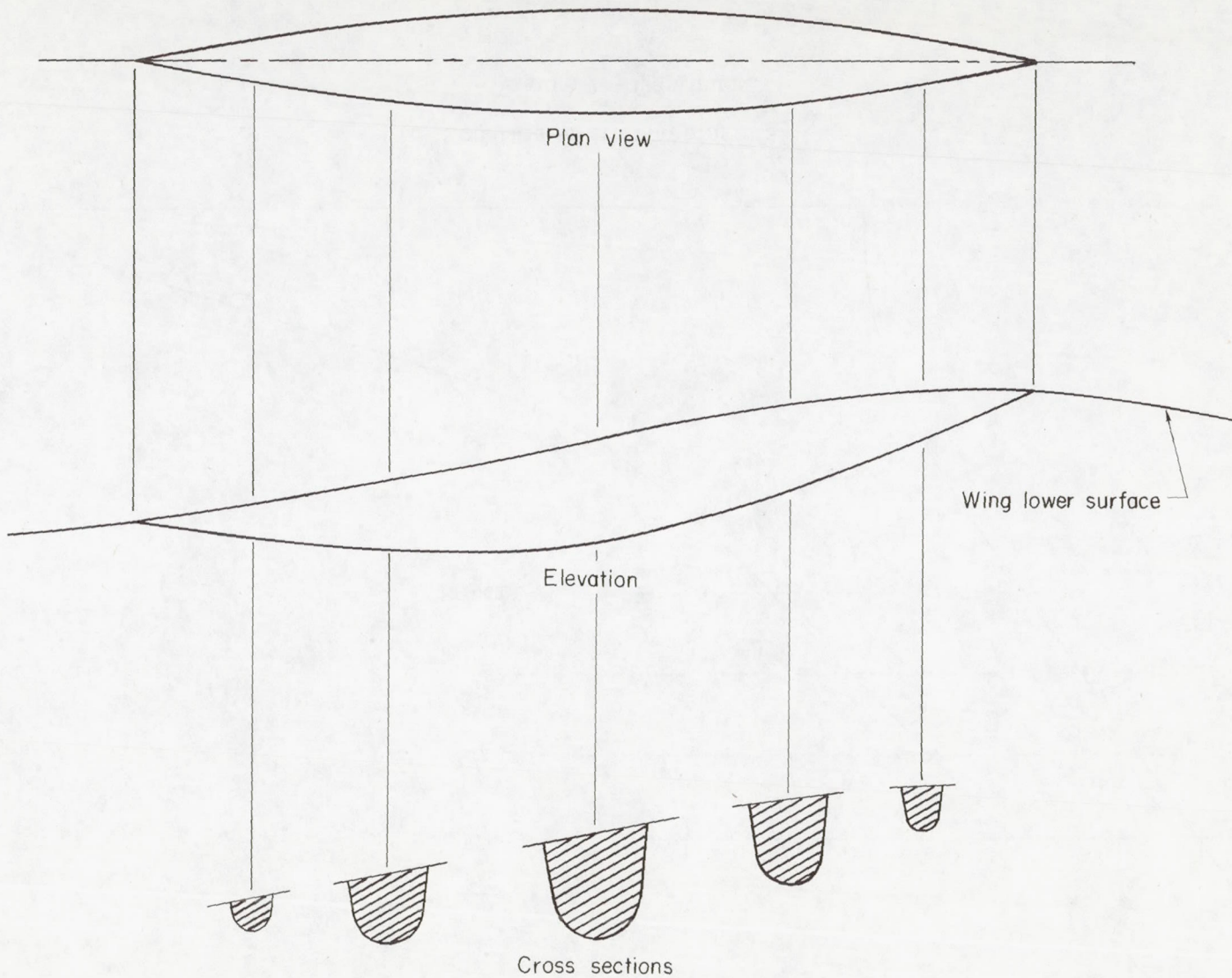
~~CONFIDENTIAL~~

(c) Location of aileron hinge fairings.

Figure 1.- Continued.

CONFIDENTIAL

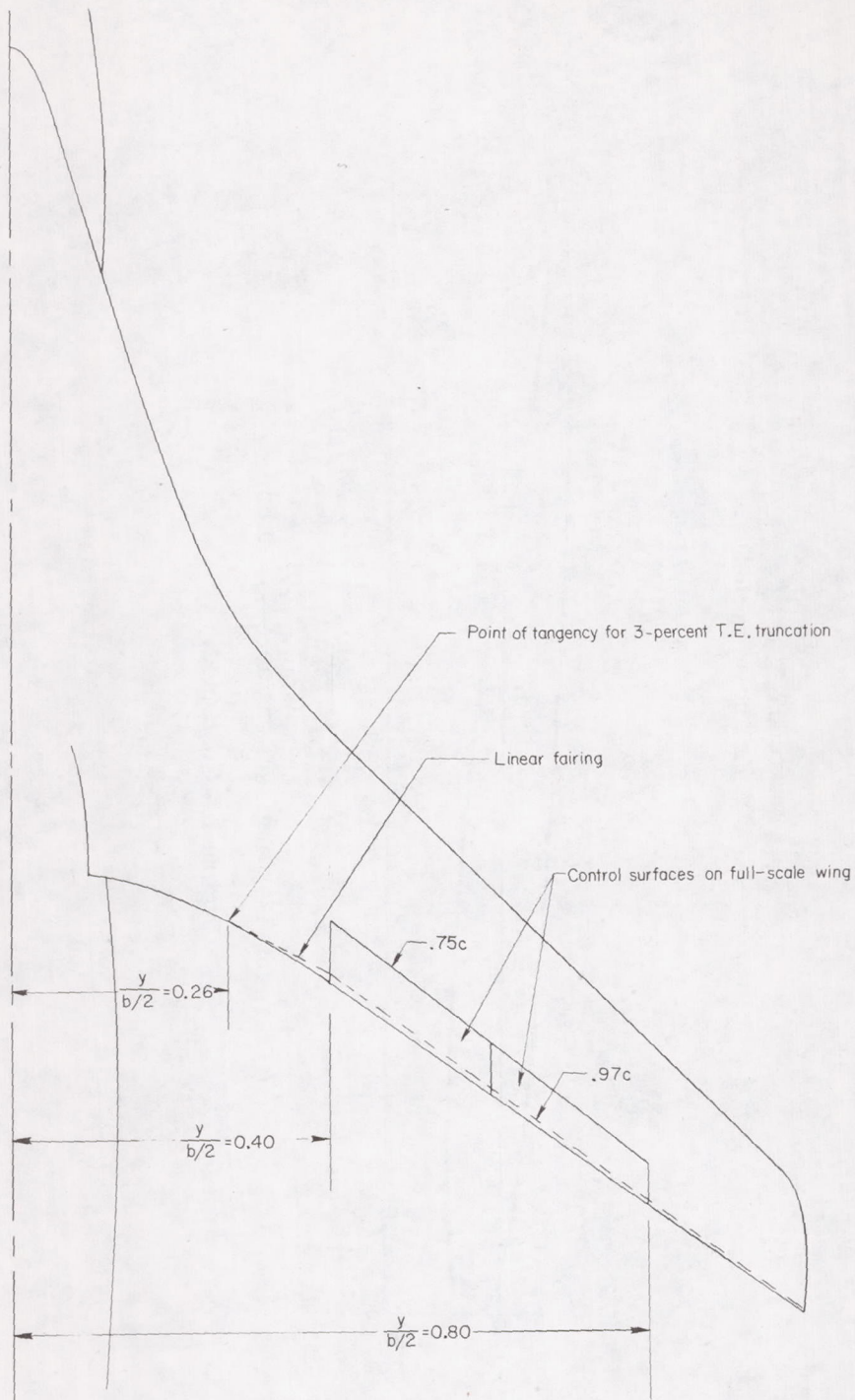
CONFIDENTIAL



(d) Sketch of typical aileron hinge fairing.

Figure 1.- Continued.

~~CONFIDENTIAL~~



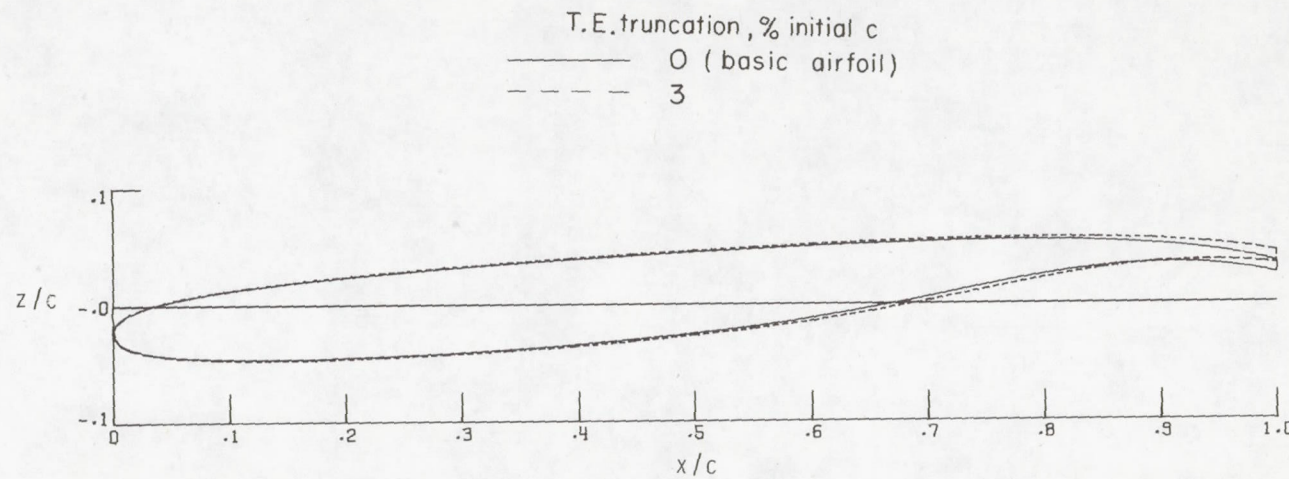
(e) Supercritical-wing panel with 3-percent T.E. truncation.

Figure 1.- Continued.

~~CONFIDENTIAL~~

CONFIDENTIAL

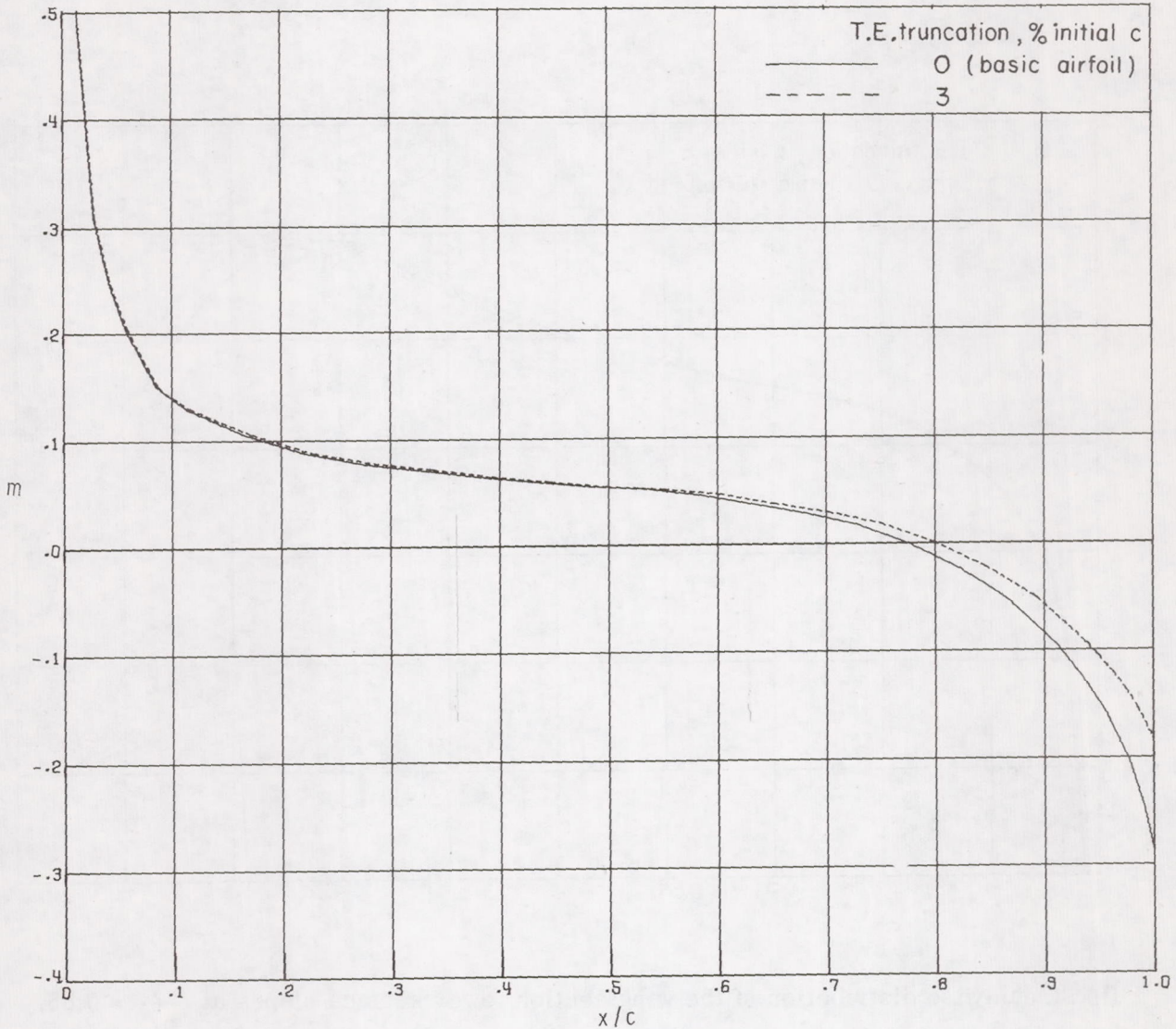
CONFIDENTIAL



(f) Streamwise wing sections at $\frac{y}{b/2} = 0.85.$

Figure 1.- Continued.

~~CONFIDENTIAL~~

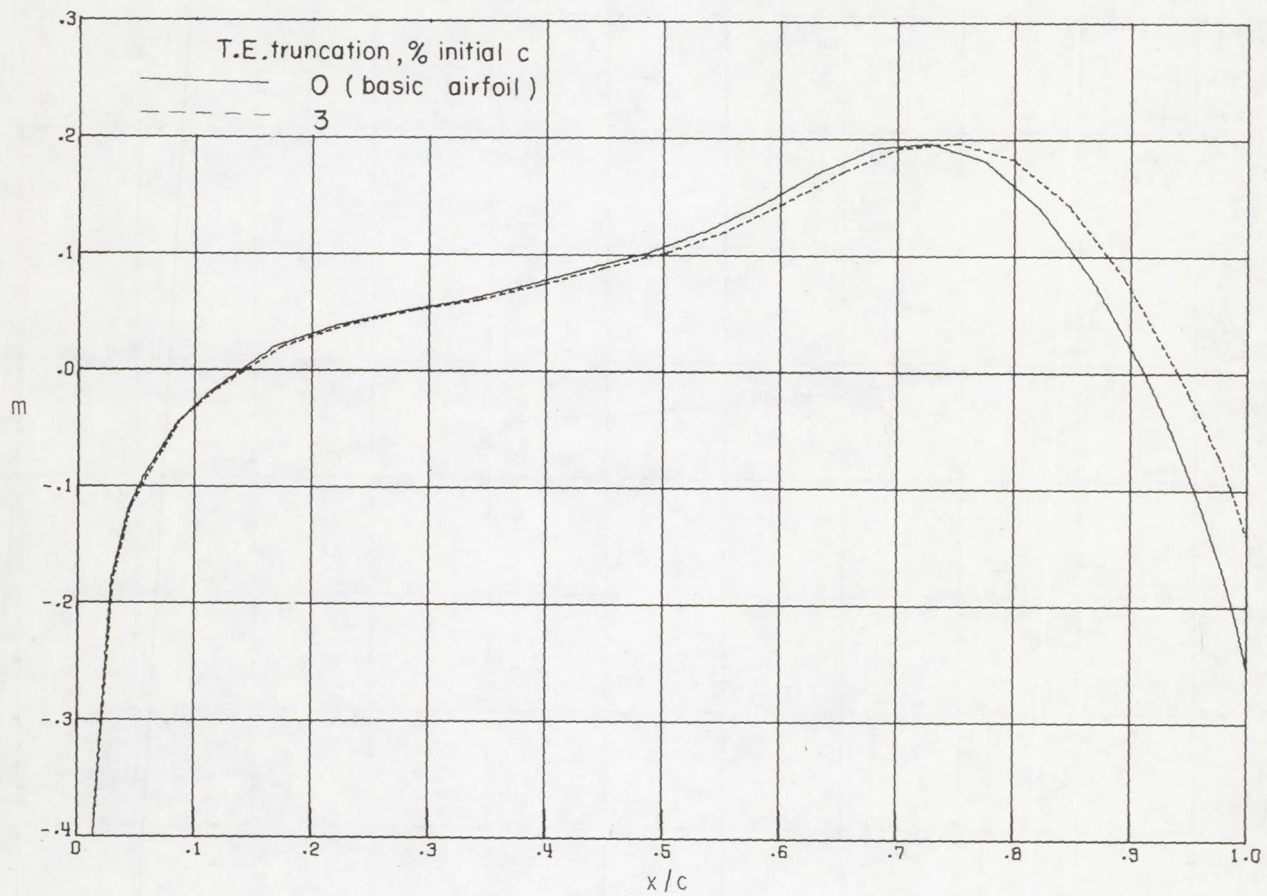


(g) Streamwise distribution of wing section upper surface slopes at $\frac{y}{b/2} = 0.85$.

Figure 1.- Continued.

~~CONFIDENTIAL~~

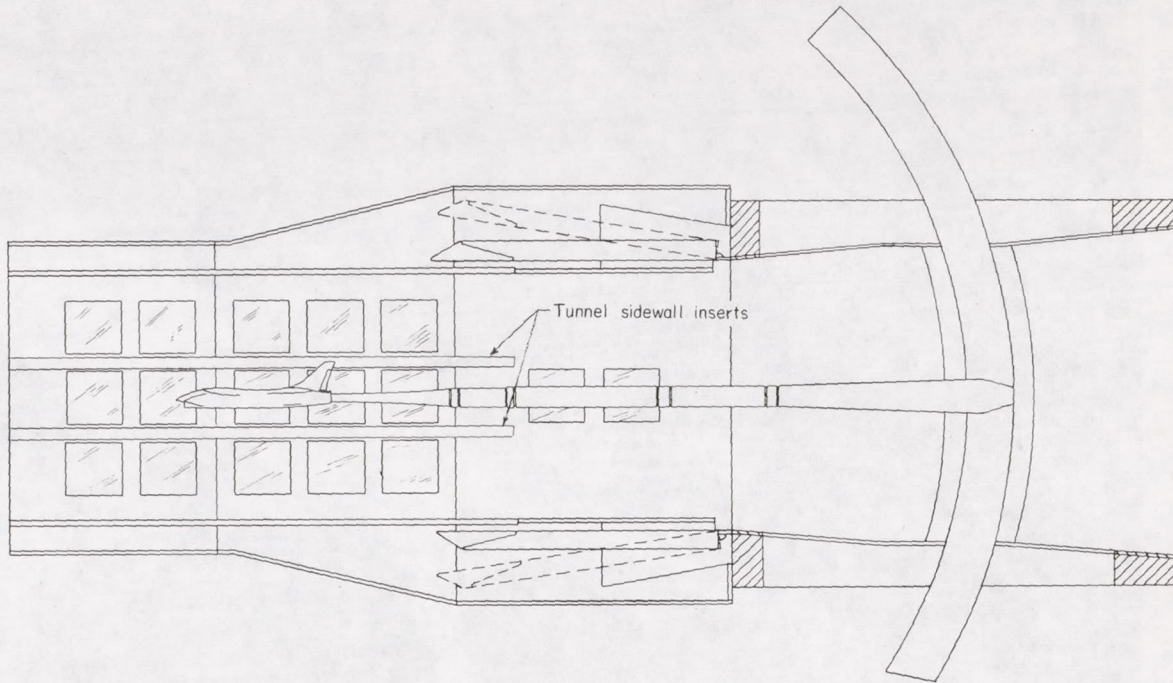
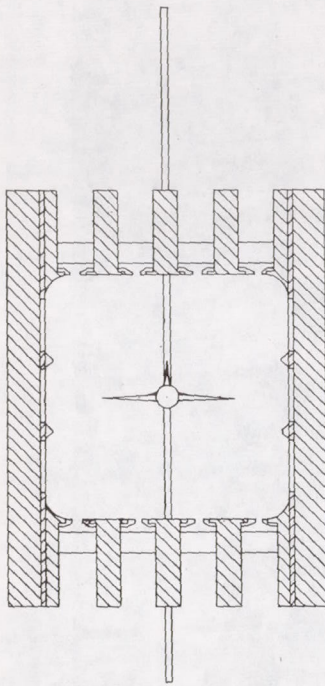
~~CONFIDENTIAL~~



(h) Streamwise distribution of the wing section lower surface slopes at $\frac{y}{b/2} = 0.85$.

Figure 1.- Continued.

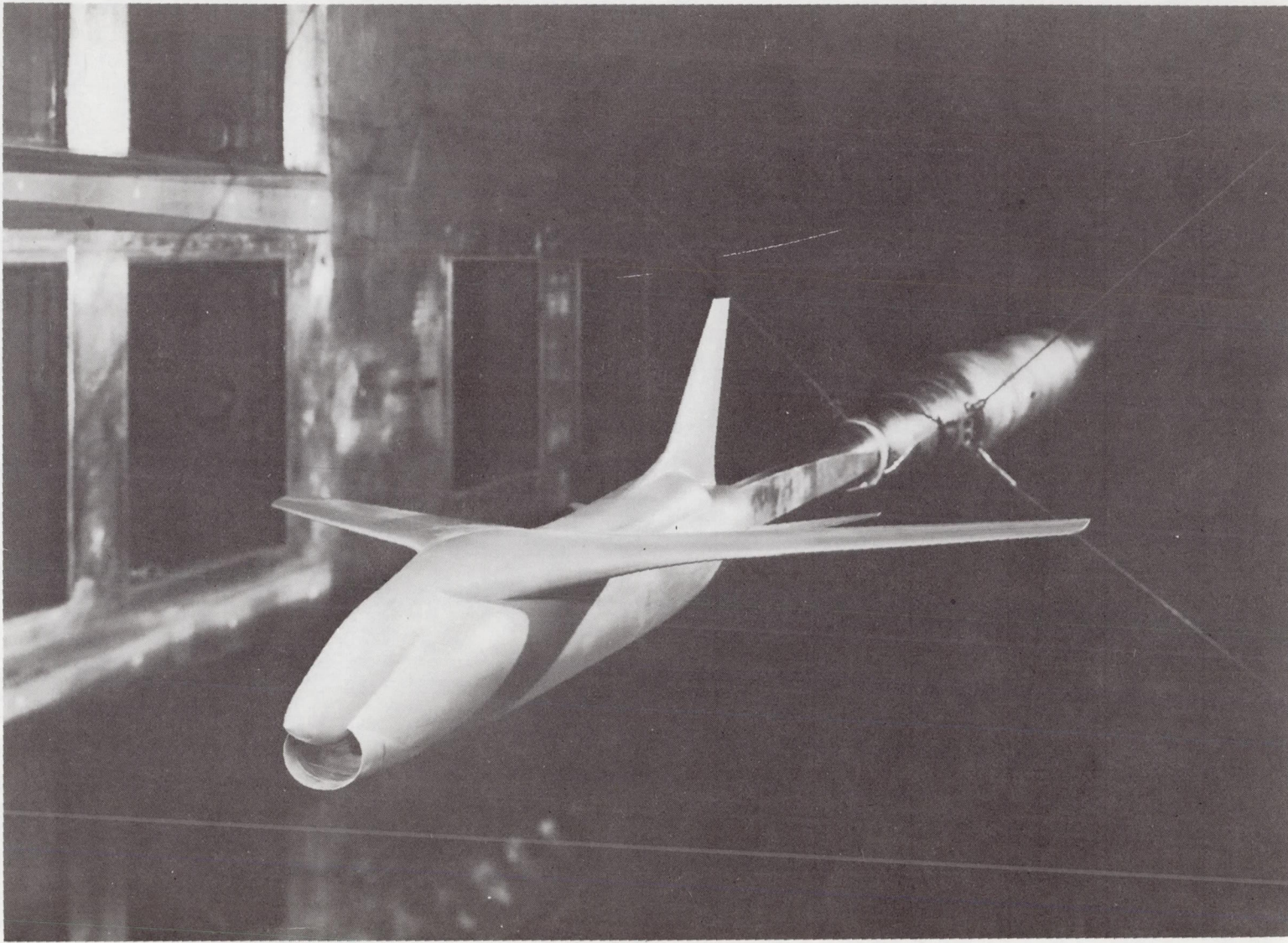
CONFIDENTIAL



CONFIDENTIAL

(i) Tunnel test section with sidewall inserts.

Figure 1.- Concluded.

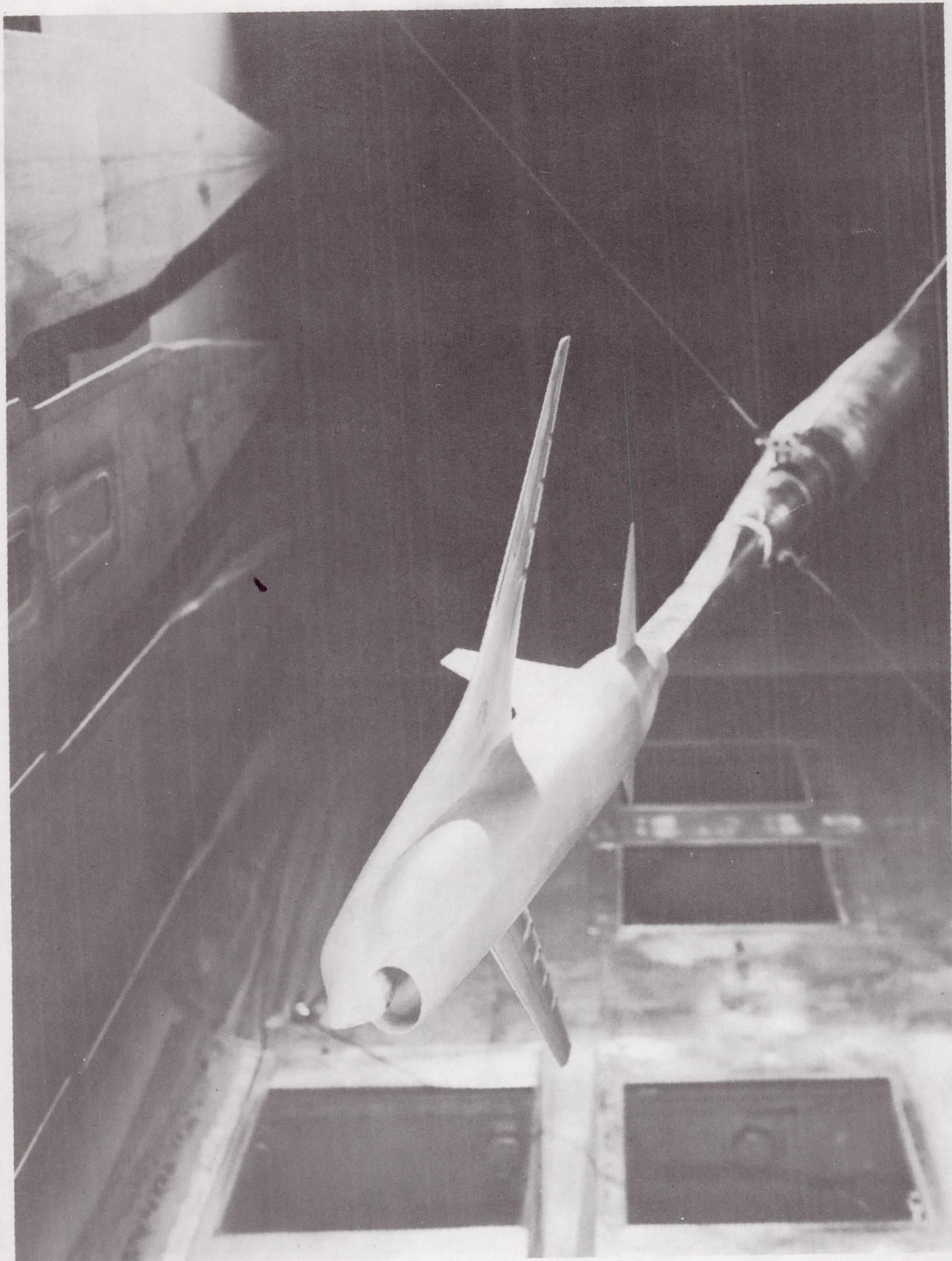
~~CONFIDENTIAL~~

L-73-1017

Figure 2.- Photographs of the 0.0625-scale model installed in the Langley 8-foot transonic pressure tunnel.

~~CONFIDENTIAL~~

~~CONFIDENTIAL~~

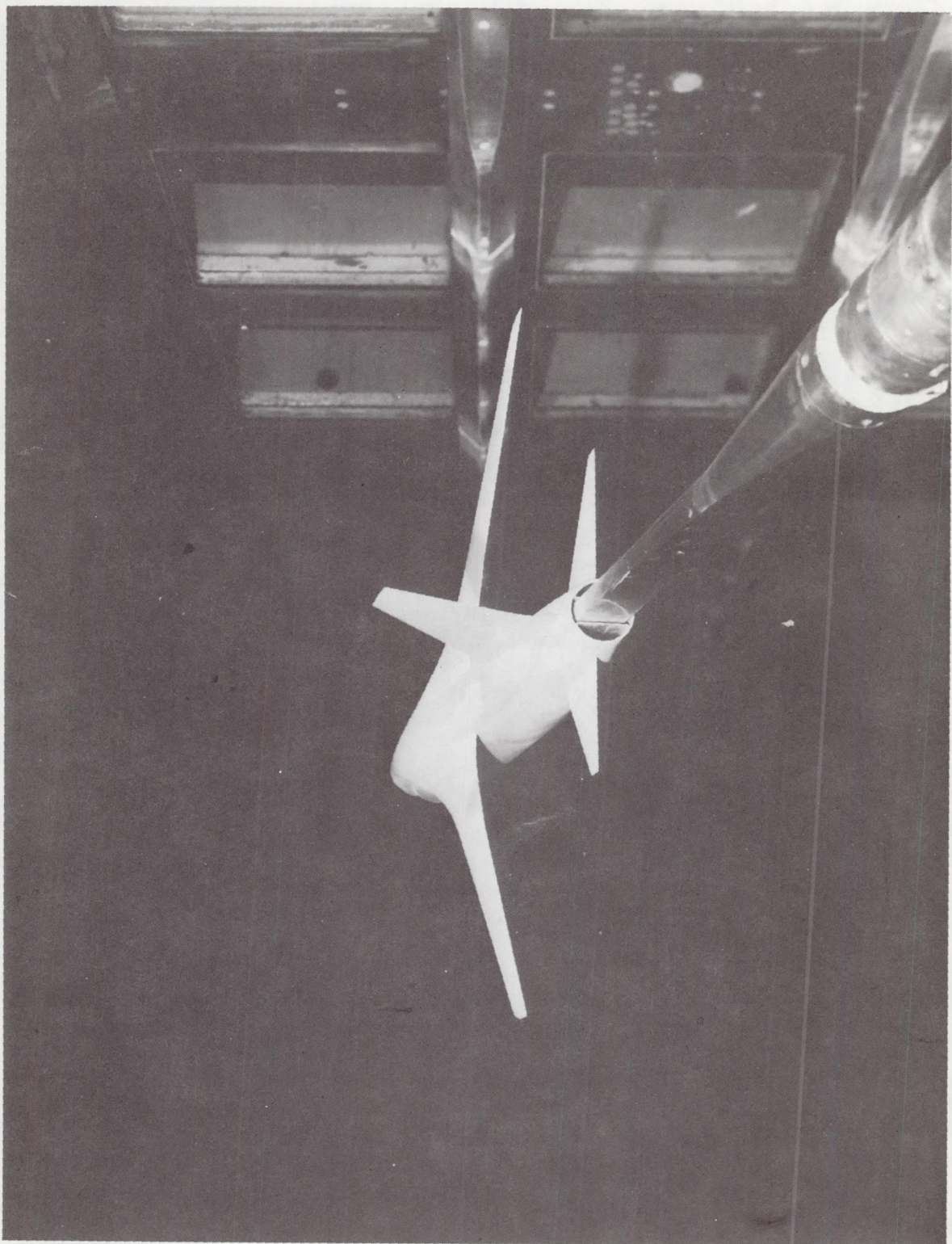


L-73-1018

Figure 2.- Continued.

~~CONFIDENTIAL~~

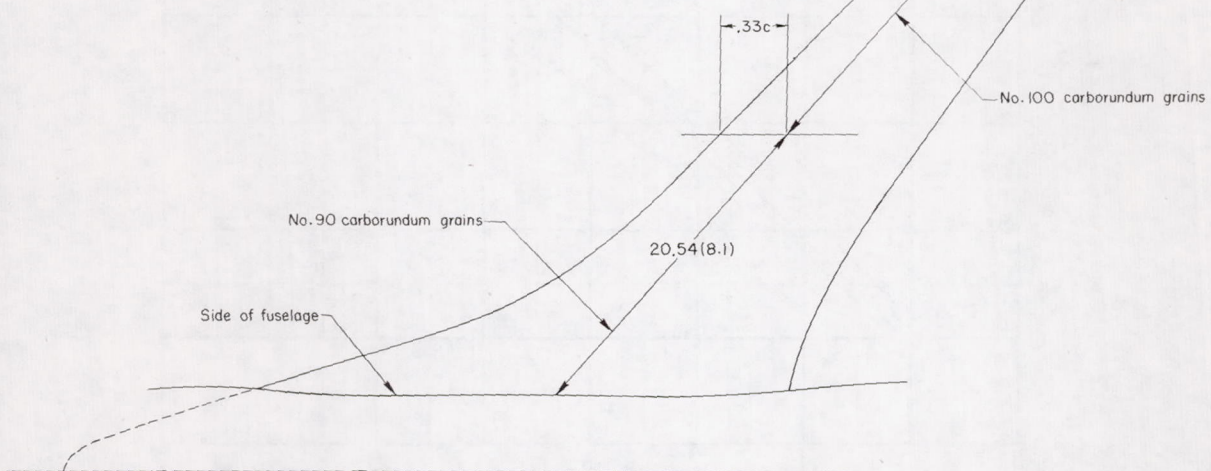
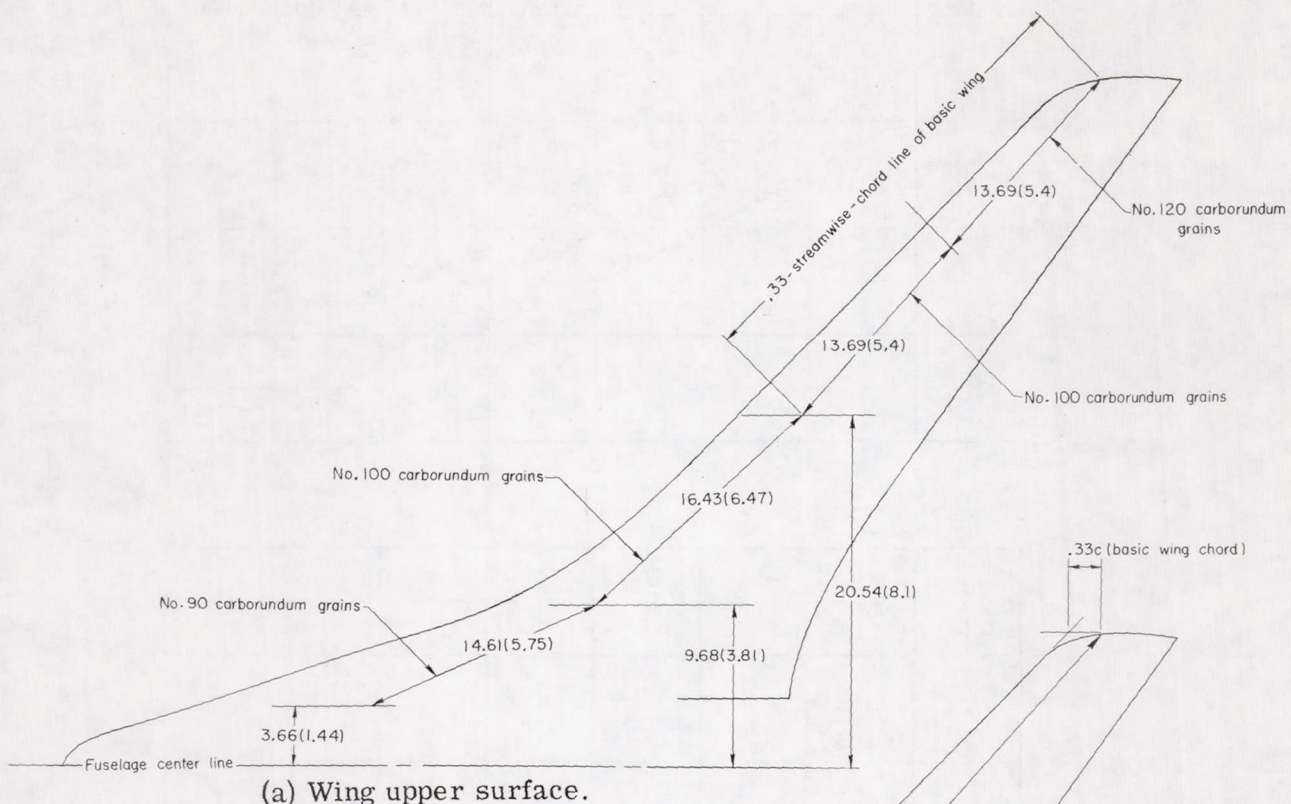
~~CONFIDENTIAL~~



L-73-1016

Figure 2. - Concluded.

~~CONFIDENTIAL~~

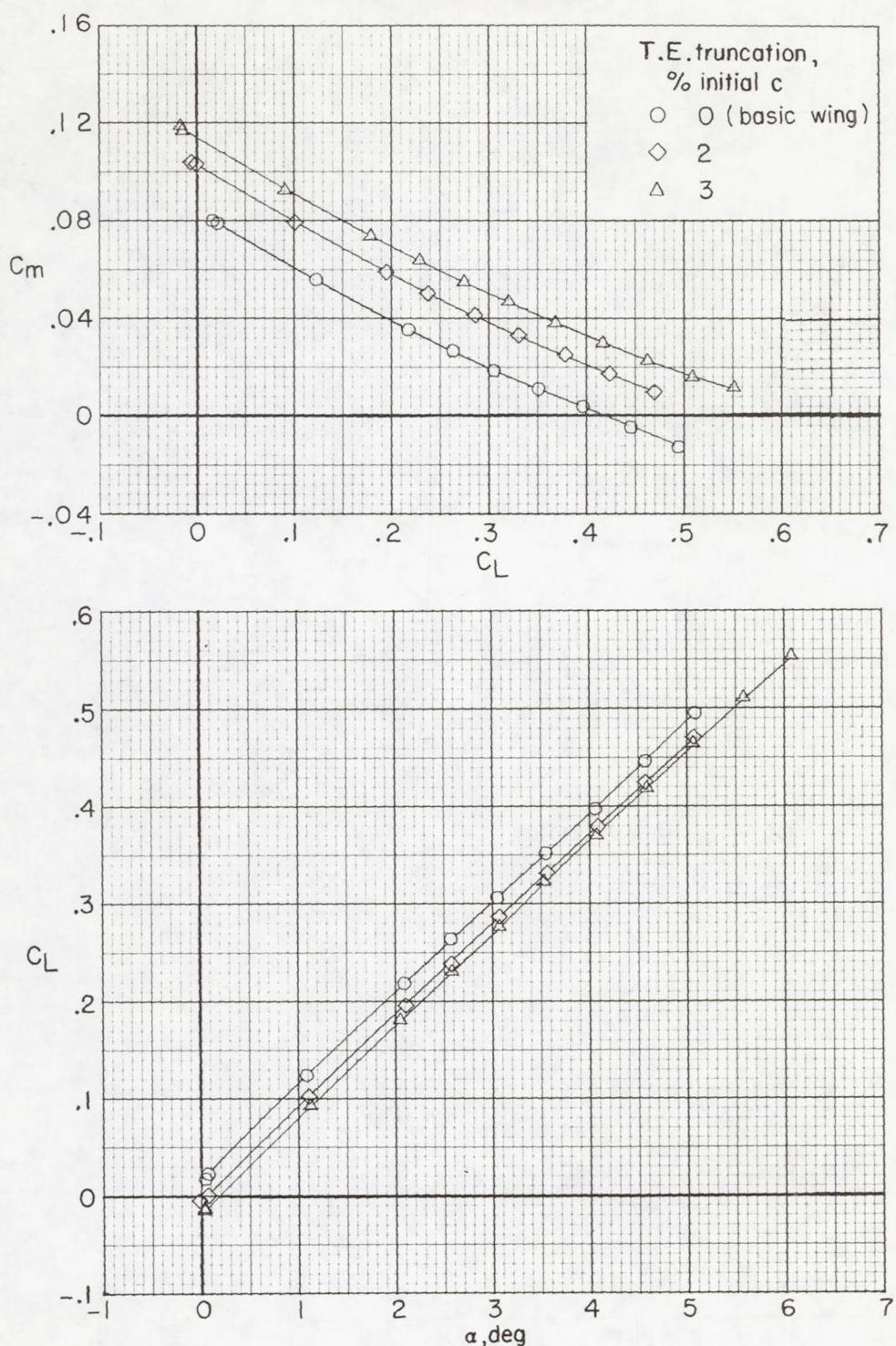


(b) Wing lower surface.

Figure 3.- Boundary-layer trip arrangements. Dimensions are in cm (in.).

~~CONFIDENTIAL~~

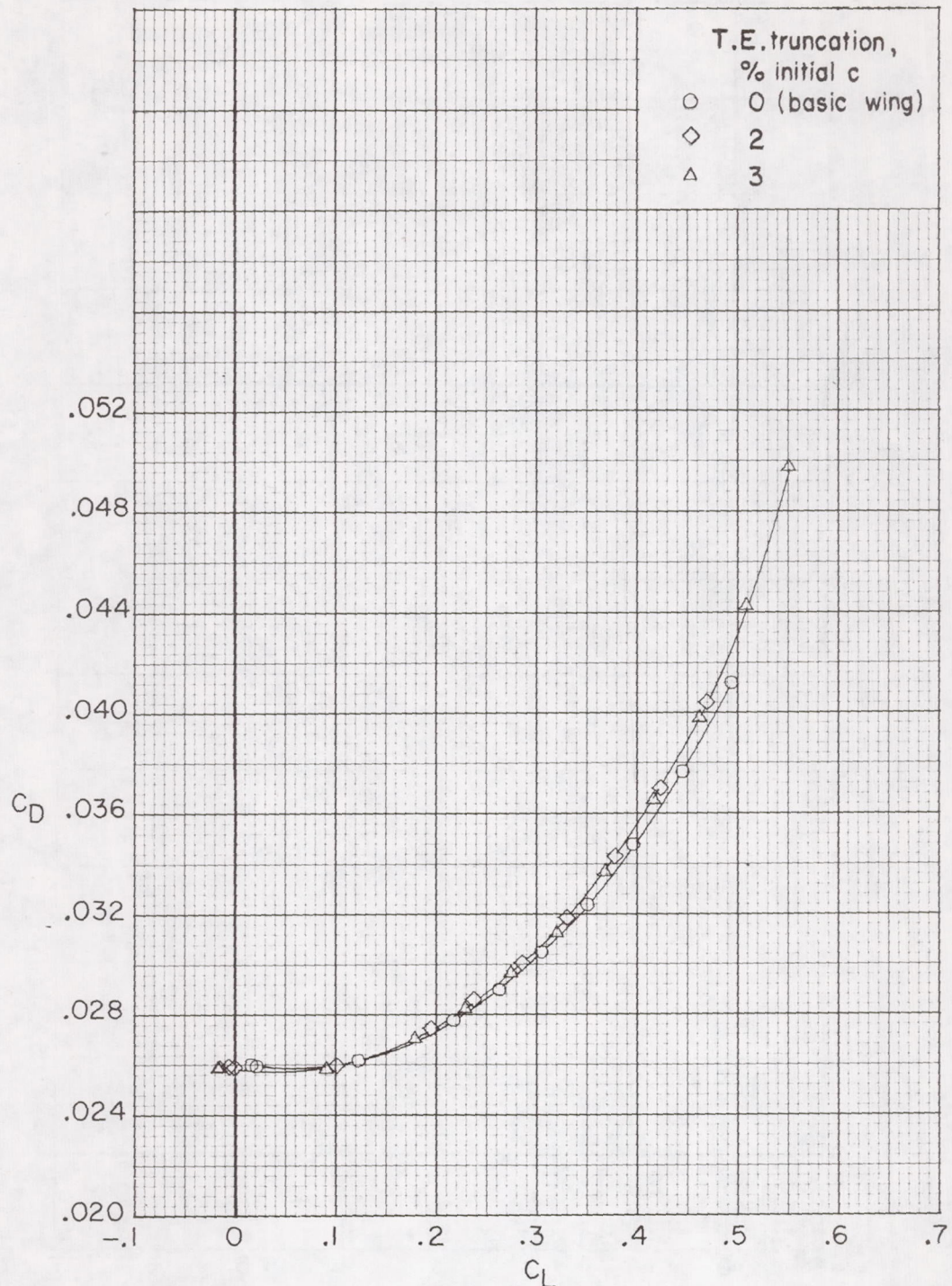
~~CONFIDENTIAL~~



(a) $M = 0.80$.

Figure 4.- Effect of wing trailing-edge truncation on longitudinal aerodynamic characteristics. $\beta = 0^\circ$; $\delta_h = -2.5^\circ$.

~~CONFIDENTIAL~~

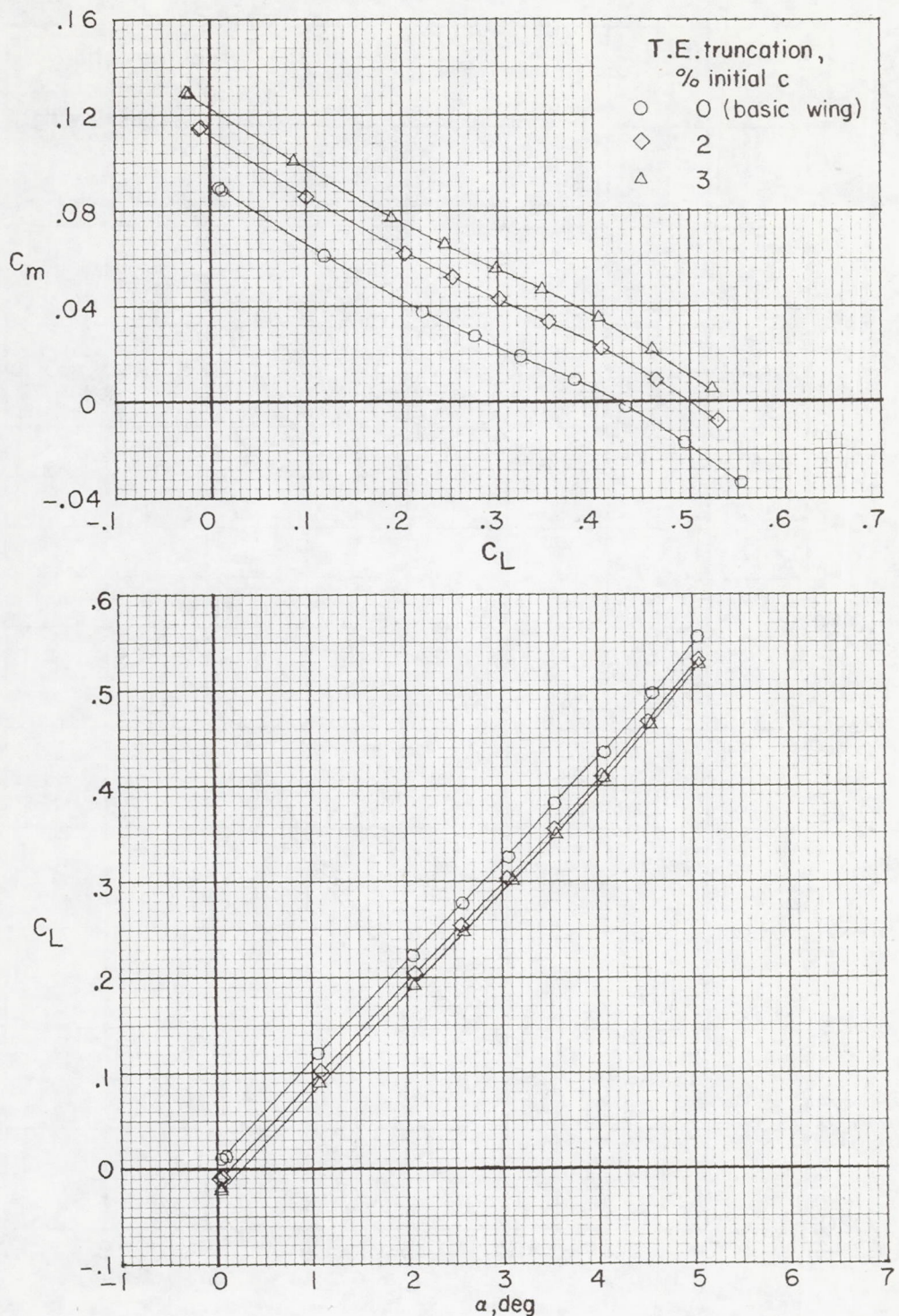


(a) $M = 0.80$. Concluded.

Figure 4.- Continued.

~~CONFIDENTIAL~~

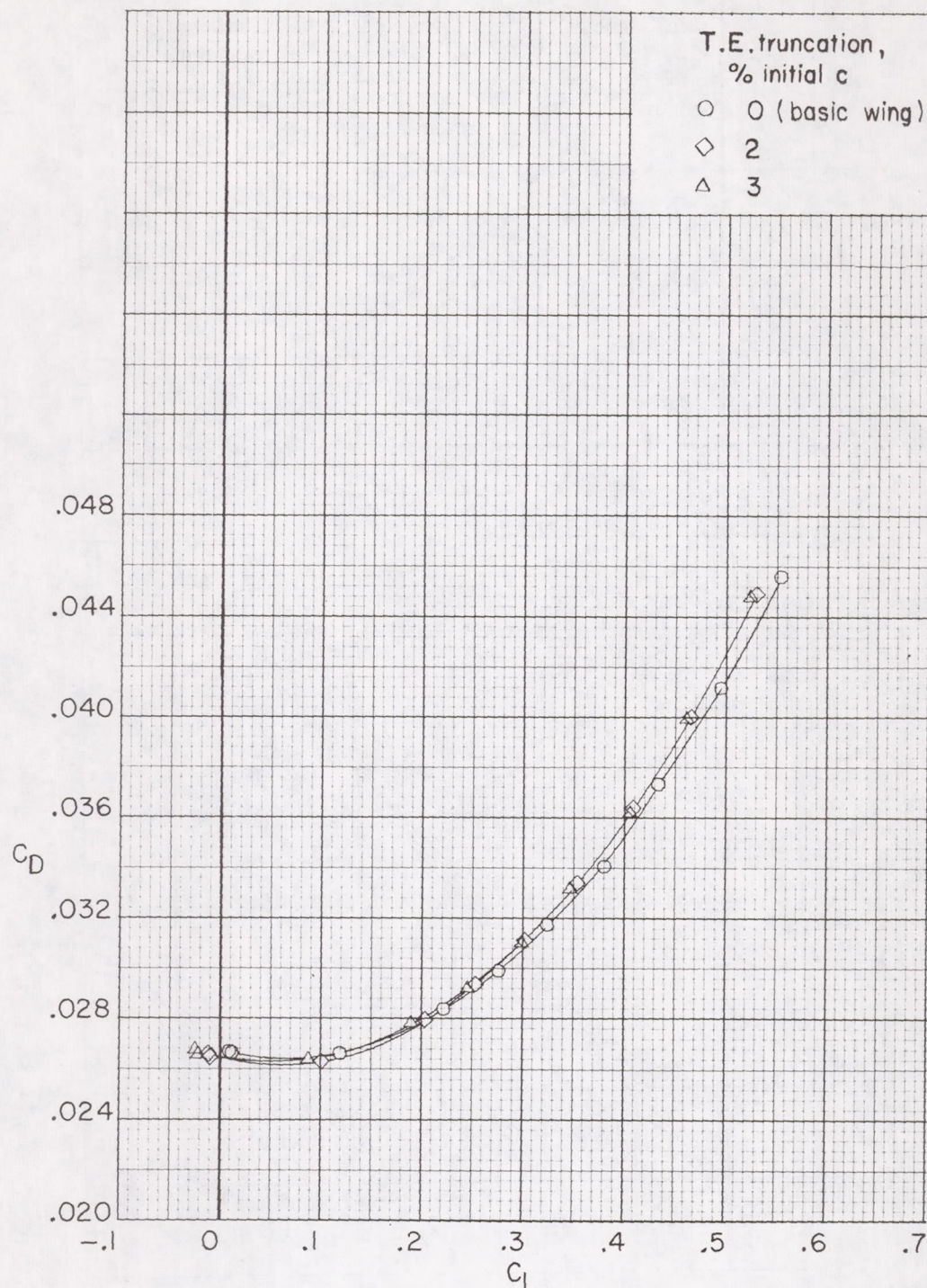
~~CONFIDENTIAL~~



(b) $M = 0.90.$

Figure 4.- Continued.

~~CONFIDENTIAL~~

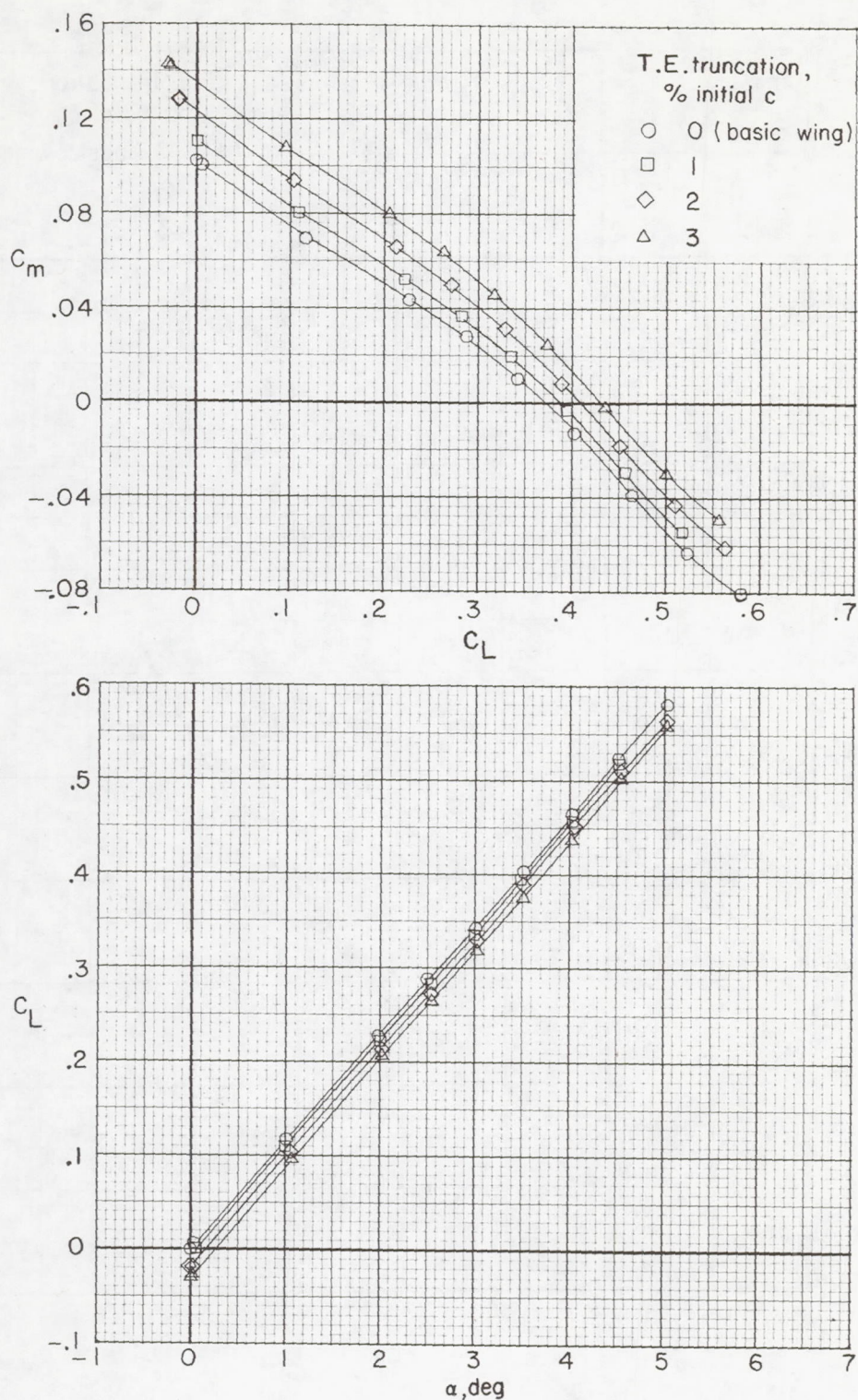


(b) $M = 0.90$. Concluded.

Figure 4.- Continued.

~~CONFIDENTIAL~~

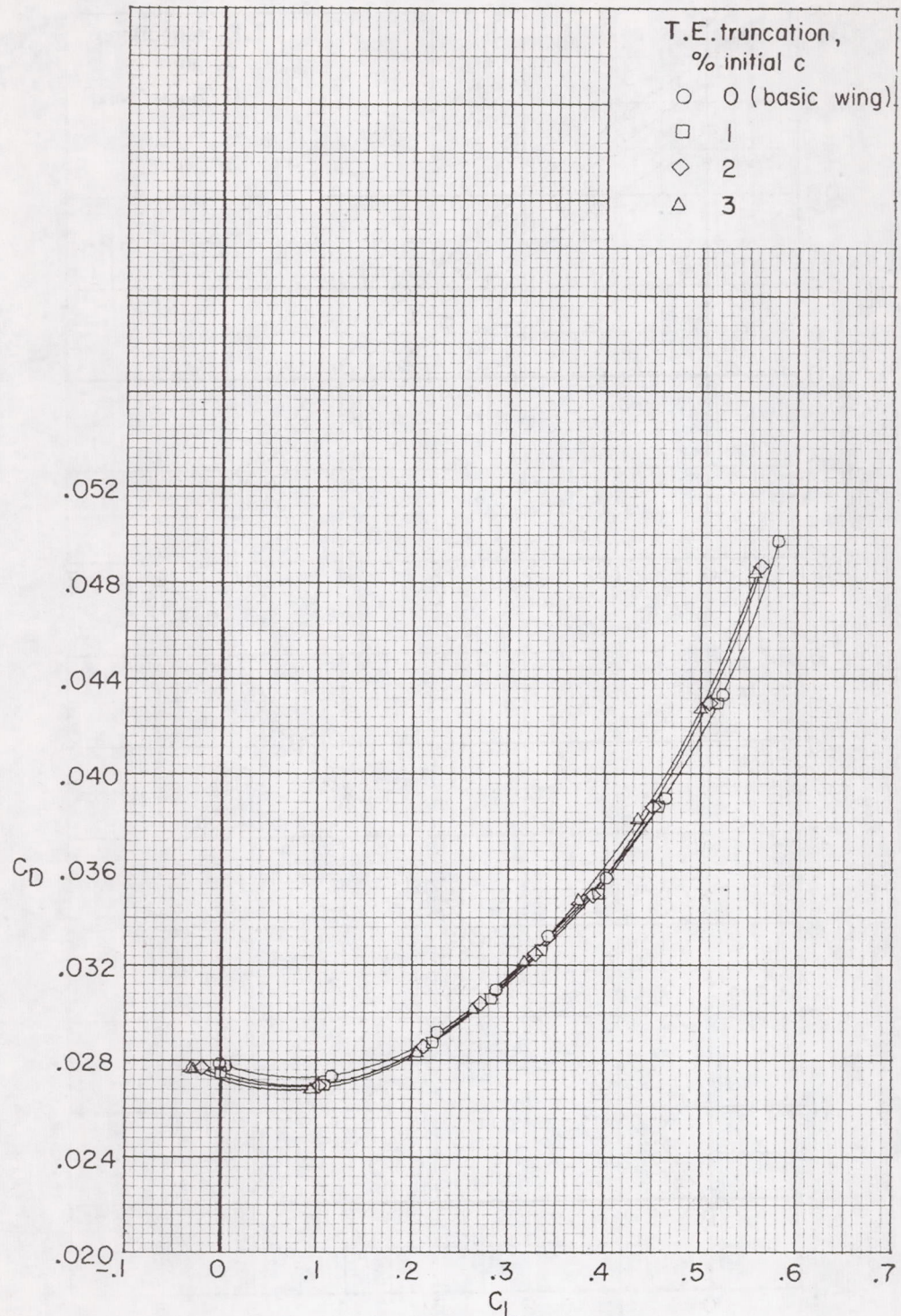
~~CONFIDENTIAL~~



(c) $M = 0.95$.

Figure 4.- Continued.

~~CONFIDENTIAL~~

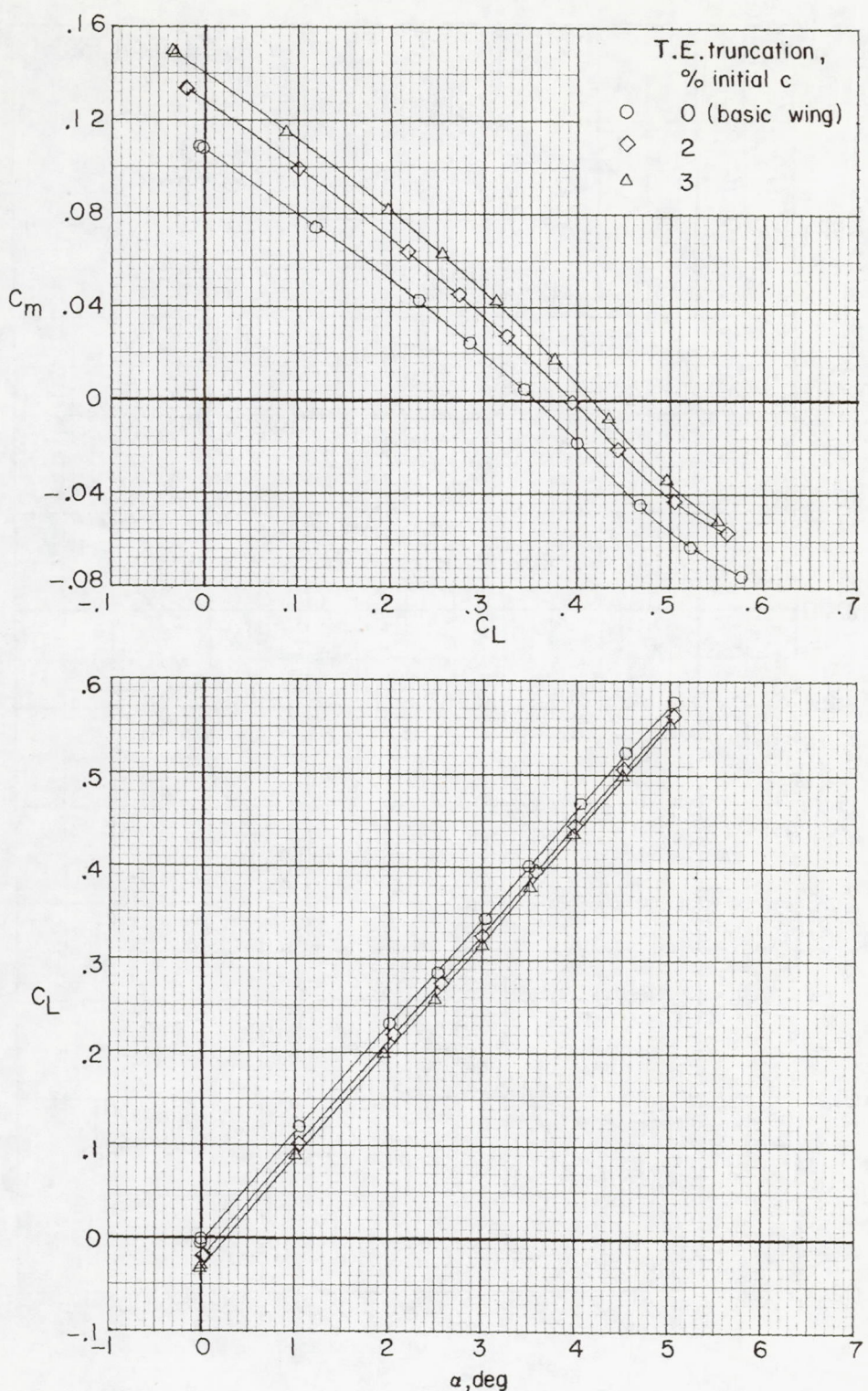


(c) $M = 0.95$. Concluded.

Figure 4.- Continued.

~~CONFIDENTIAL~~

~~CONFIDENTIAL~~

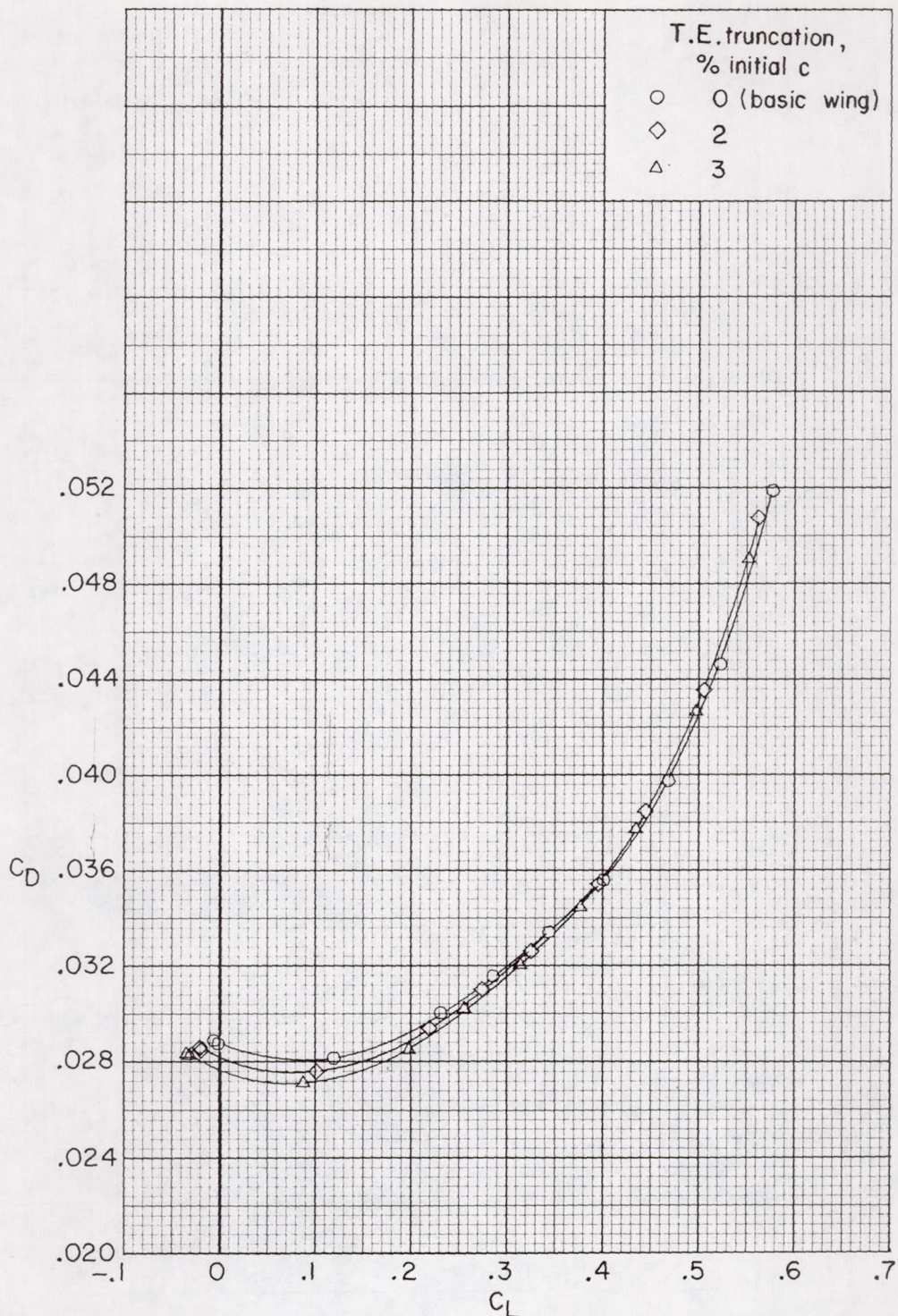


(d) $M = 0.96$.

Figure 4.- Continued.

~~CONFIDENTIAL~~

~~CONFIDENTIAL~~

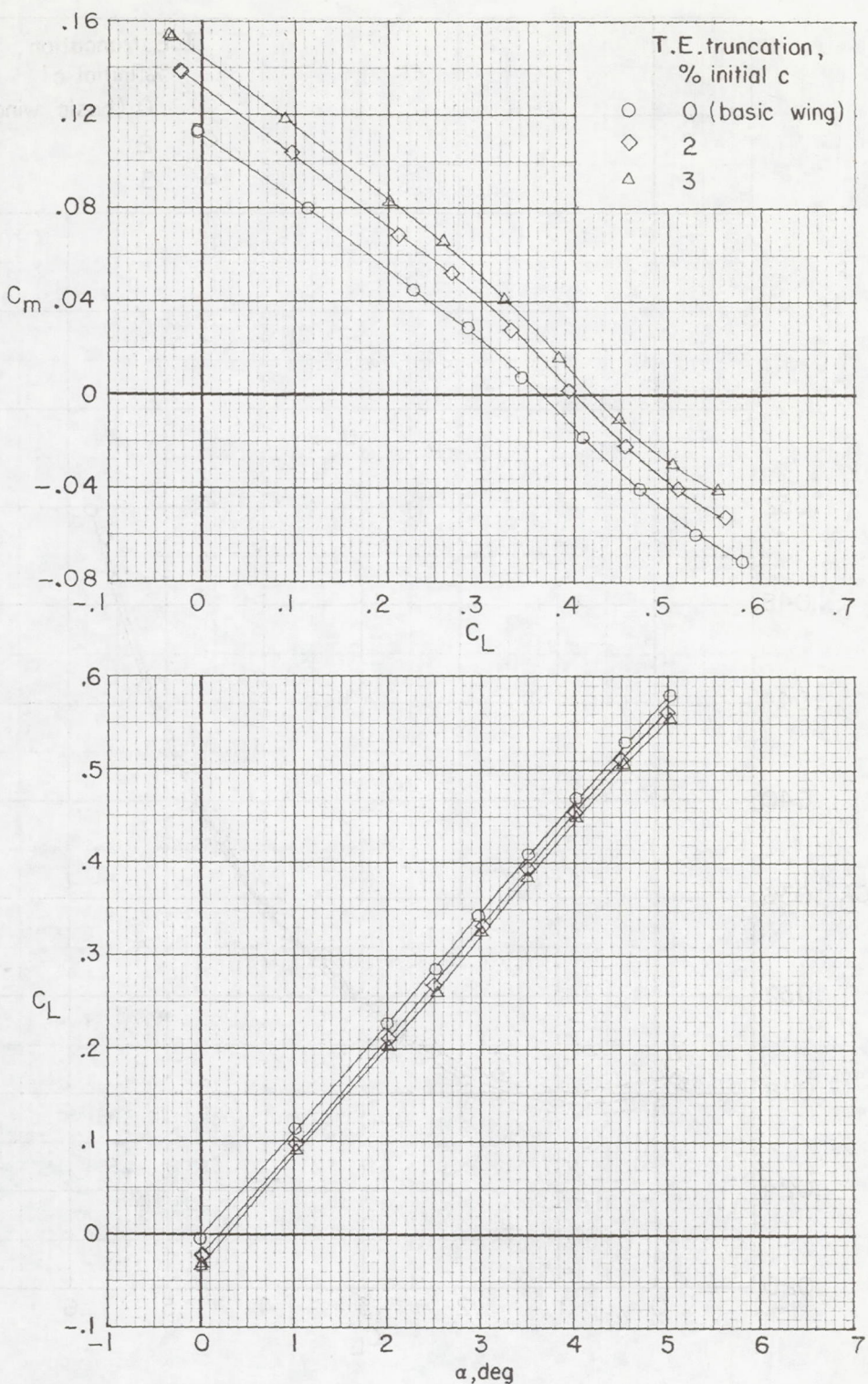


(d) $M = 0.96$. Concluded.

Figure 4.- Continued.

~~CONFIDENTIAL~~

~~CONFIDENTIAL~~

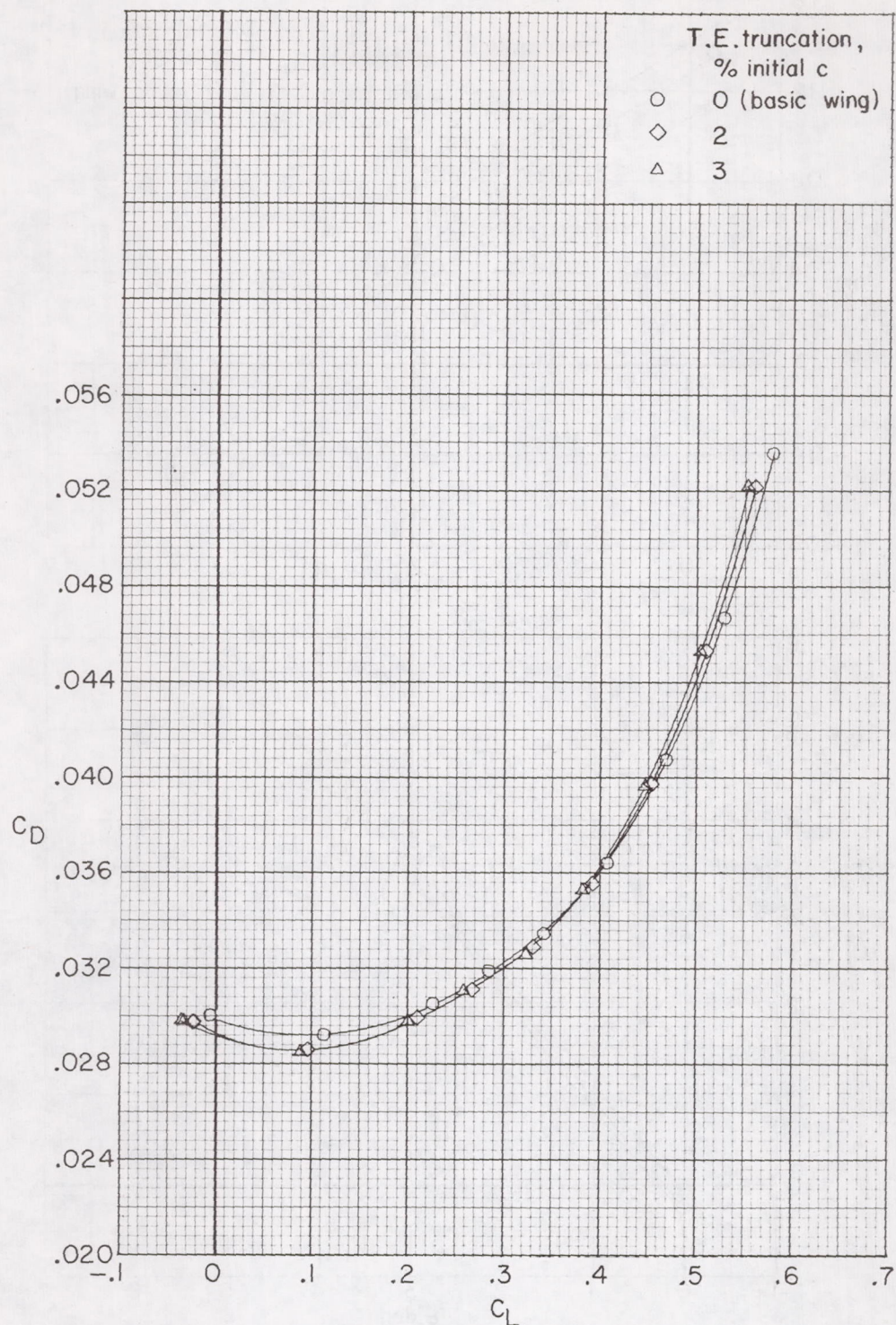


(e) $M = 0.97$.

Figure 4.- Continued.

~~CONFIDENTIAL~~

~~CONFIDENTIAL~~

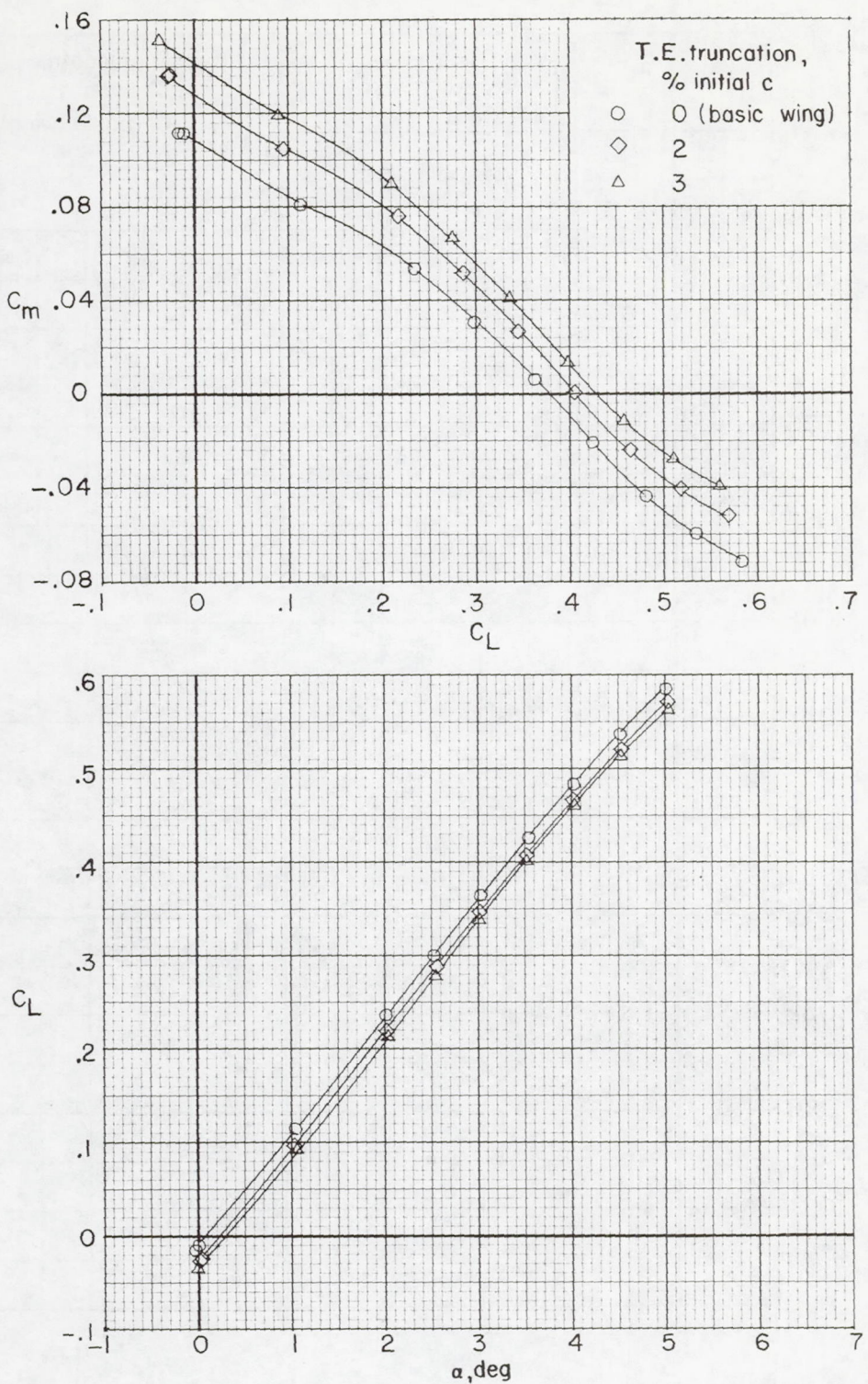


(e) $M = 0.97$. Concluded.

Figure 4.- Continued.

~~CONFIDENTIAL~~

~~CONFIDENTIAL~~

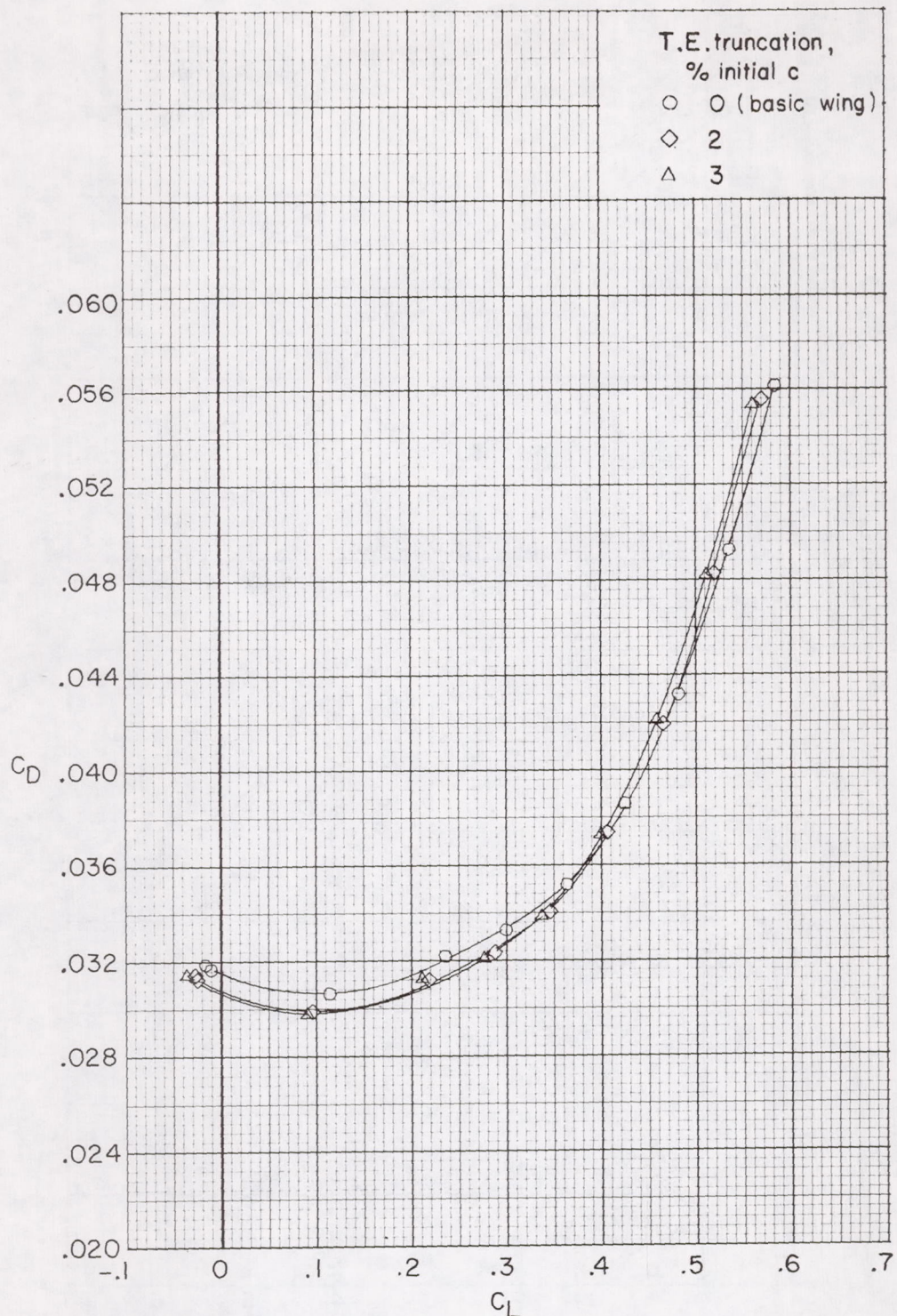


(f) $M = 0.98$.

Figure 4.- Continued.

~~CONFIDENTIAL~~

~~CONFIDENTIAL~~

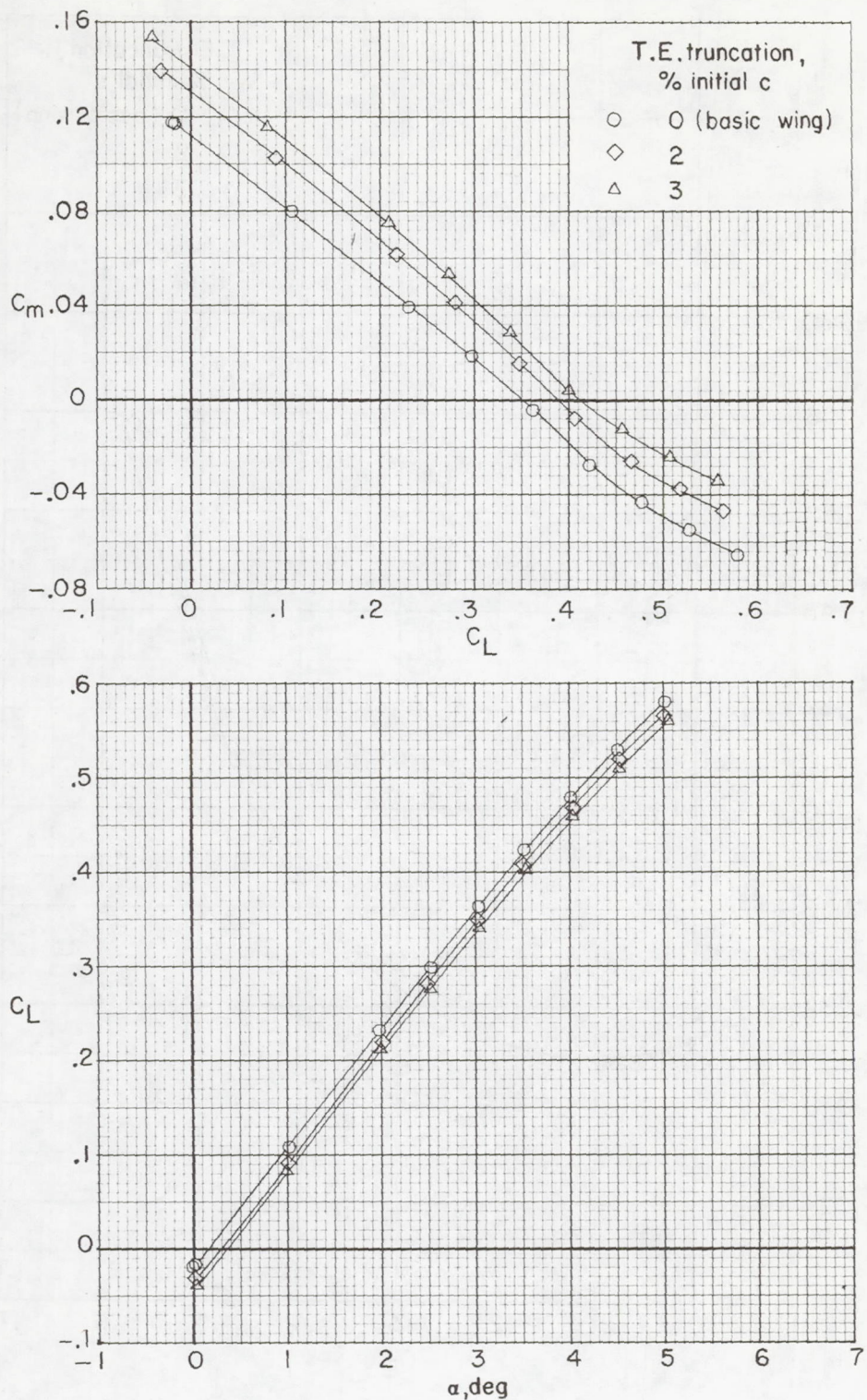


(f) $M = 0.98$. Concluded.

Figure 4.- Continued.

~~CONFIDENTIAL~~

~~CONFIDENTIAL~~

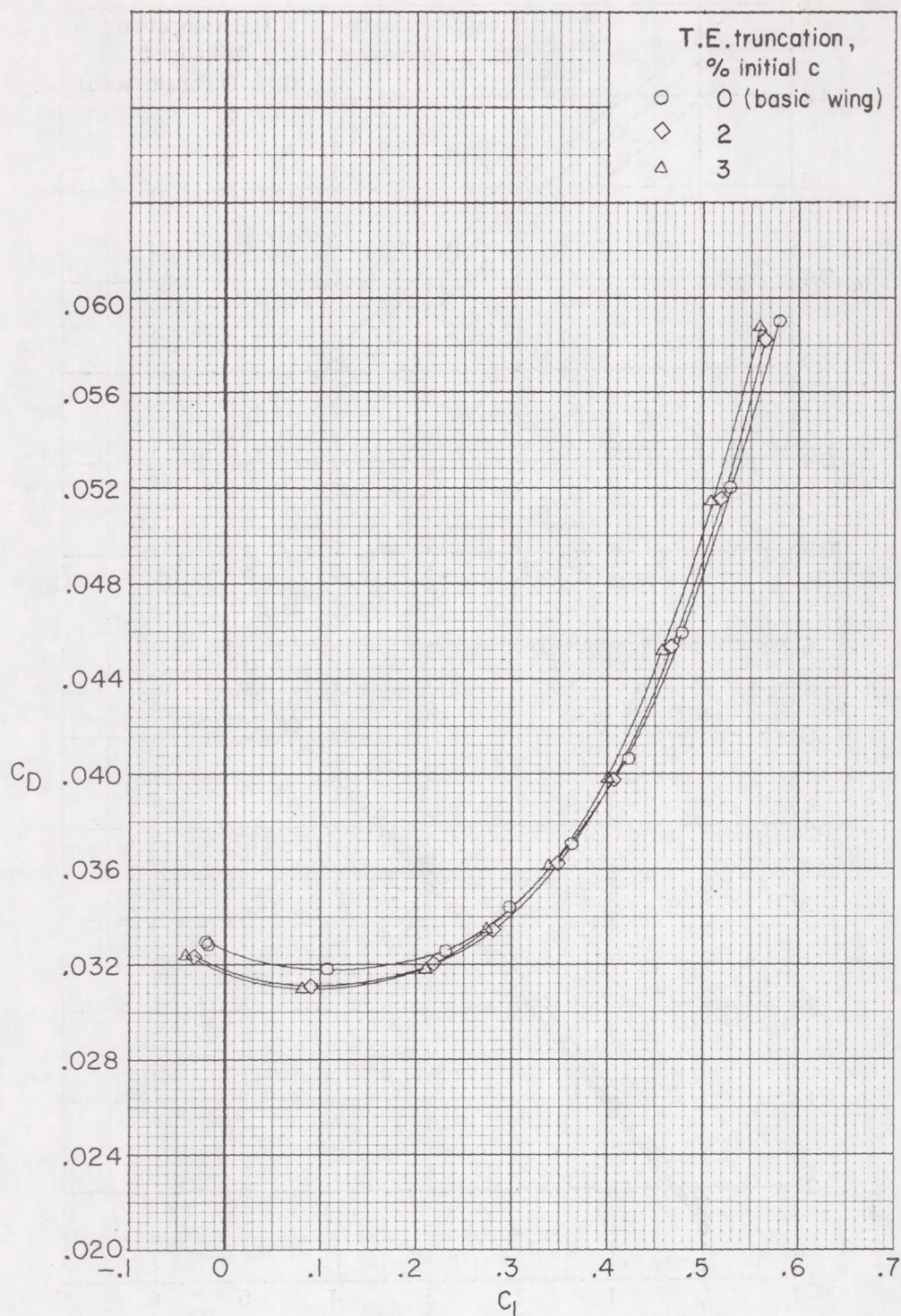


(g) $M = 0.99$.

Figure 4.- Continued.

~~CONFIDENTIAL~~

~~CONFIDENTIAL~~

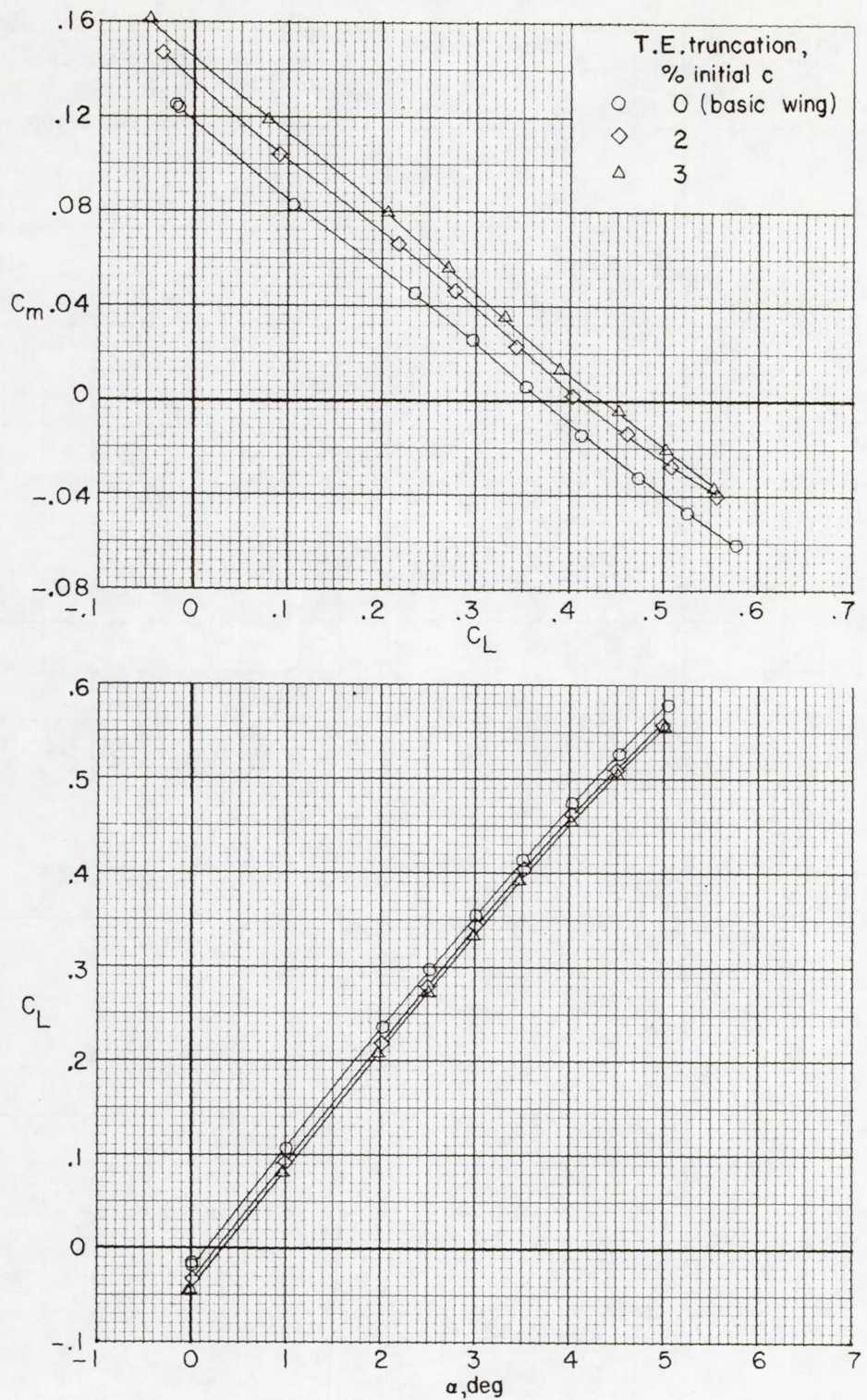


(g) $M = 0.99$. Concluded.

Figure 4.- Continued.

~~CONFIDENTIAL~~

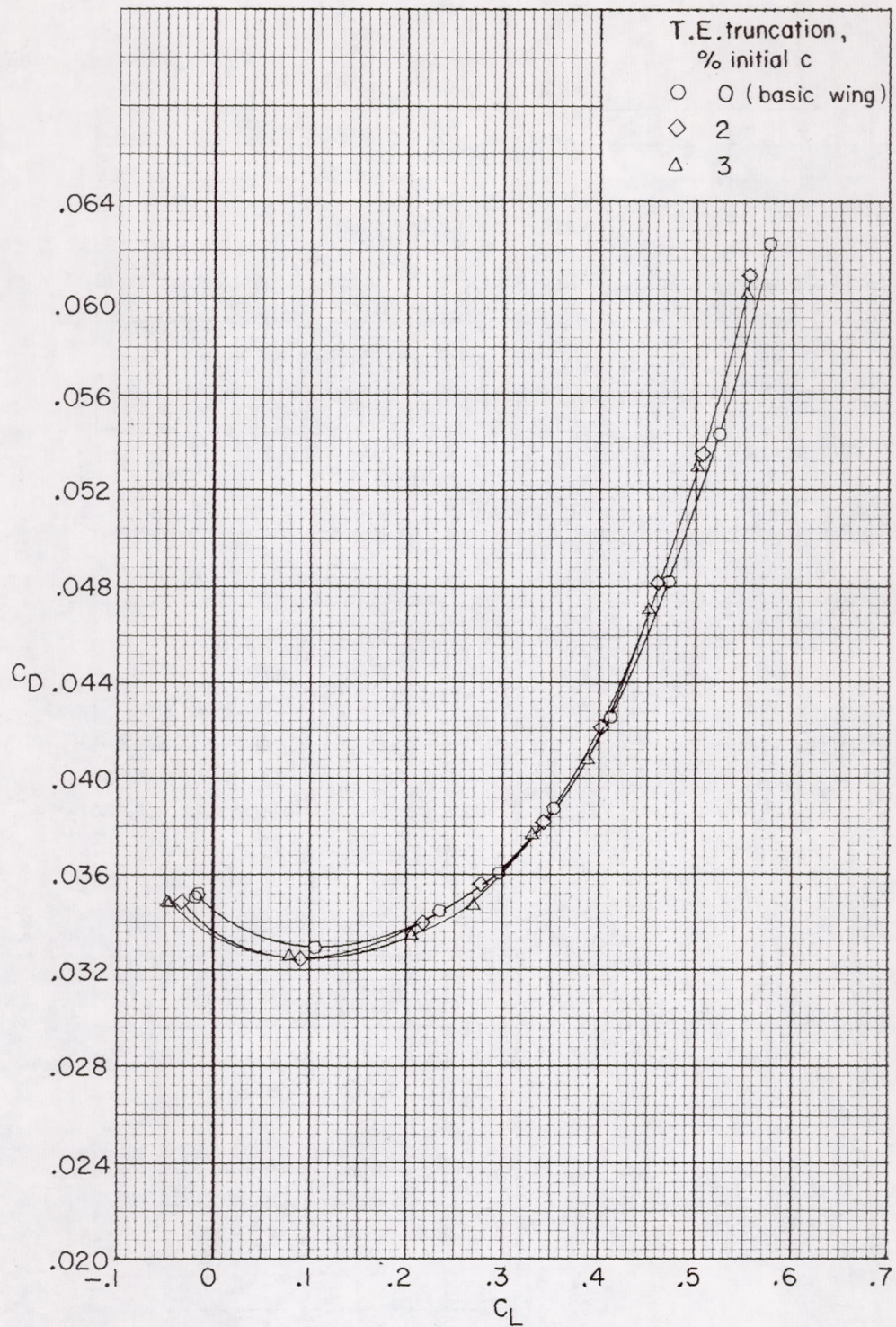
~~CONFIDENTIAL~~



(h) $M = 1.00.$

Figure 4.- Continued.

~~CONFIDENTIAL~~



(h) $M = 1.00$. Concluded.

Figure 4.- Concluded.

~~CONFIDENTIAL~~

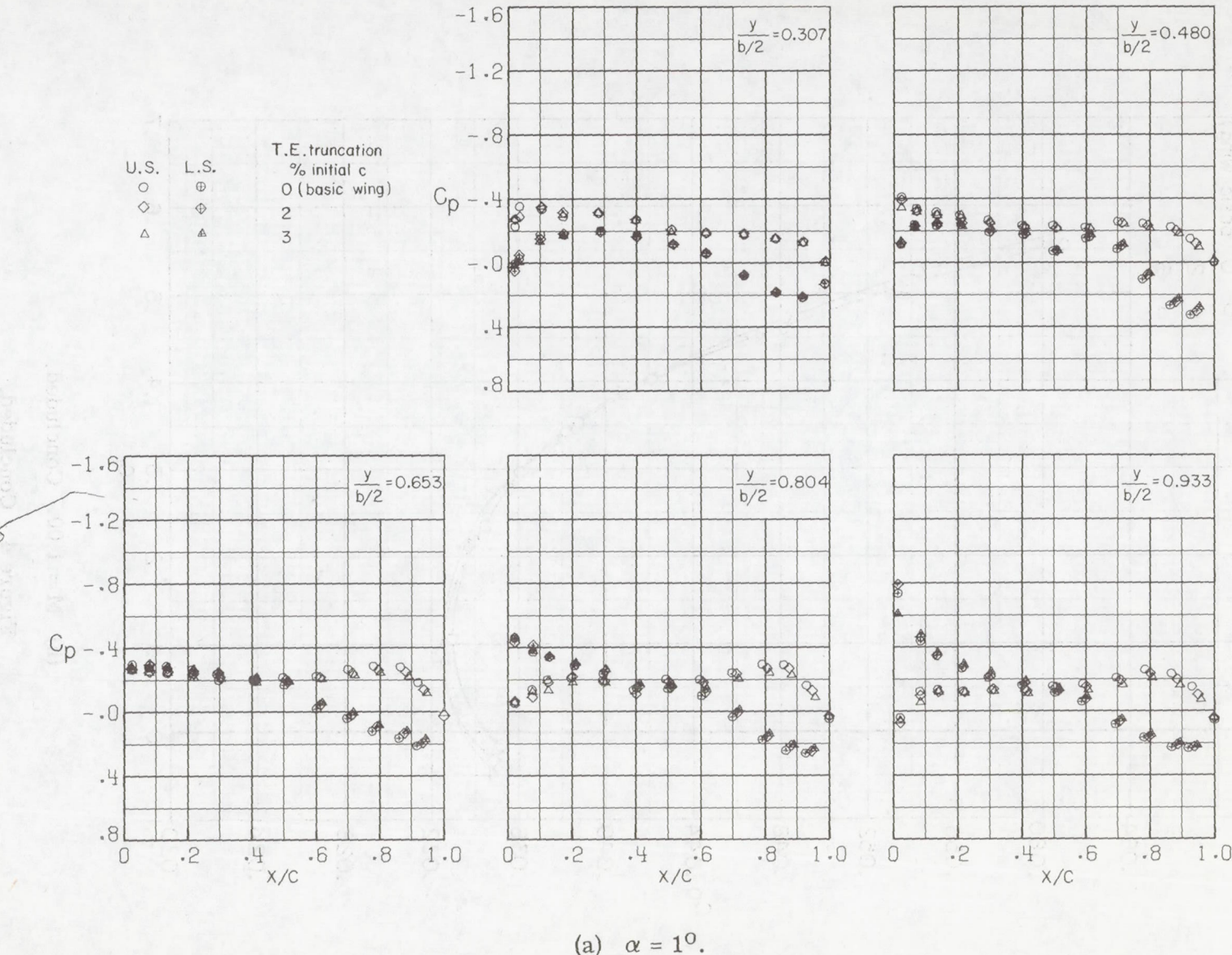


Figure 5.- Effect of wing trailing-edge truncation on wing pressure distributions at Mach number 0.80. $\beta = 0^\circ$; $\delta_h = -2.5^\circ$.

CONFIDENTIAL

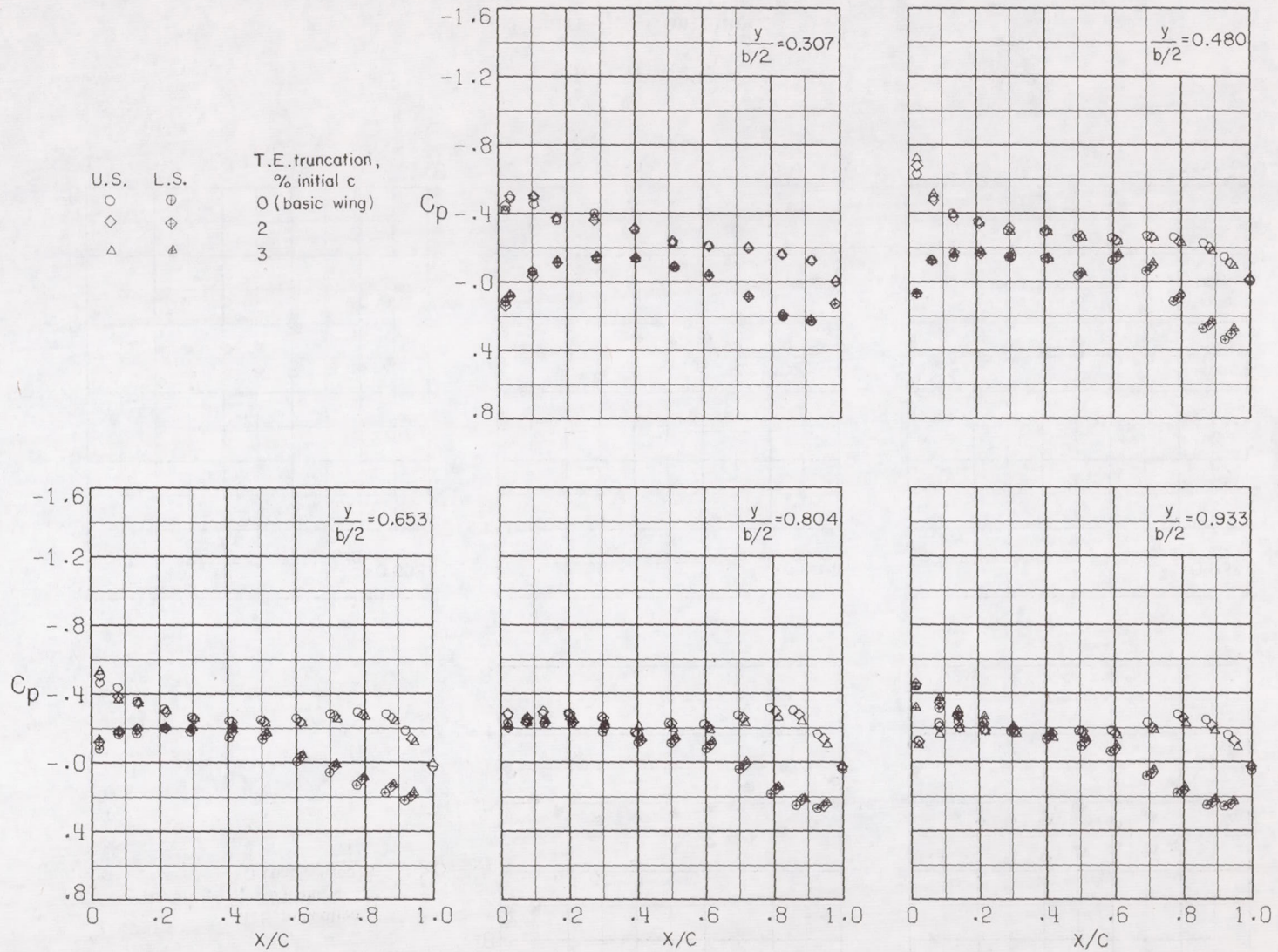
(b) $\alpha = 20^\circ$.

Figure 5.- Continued.

49

CONFIDENTIAL

CONFIDENTIAL

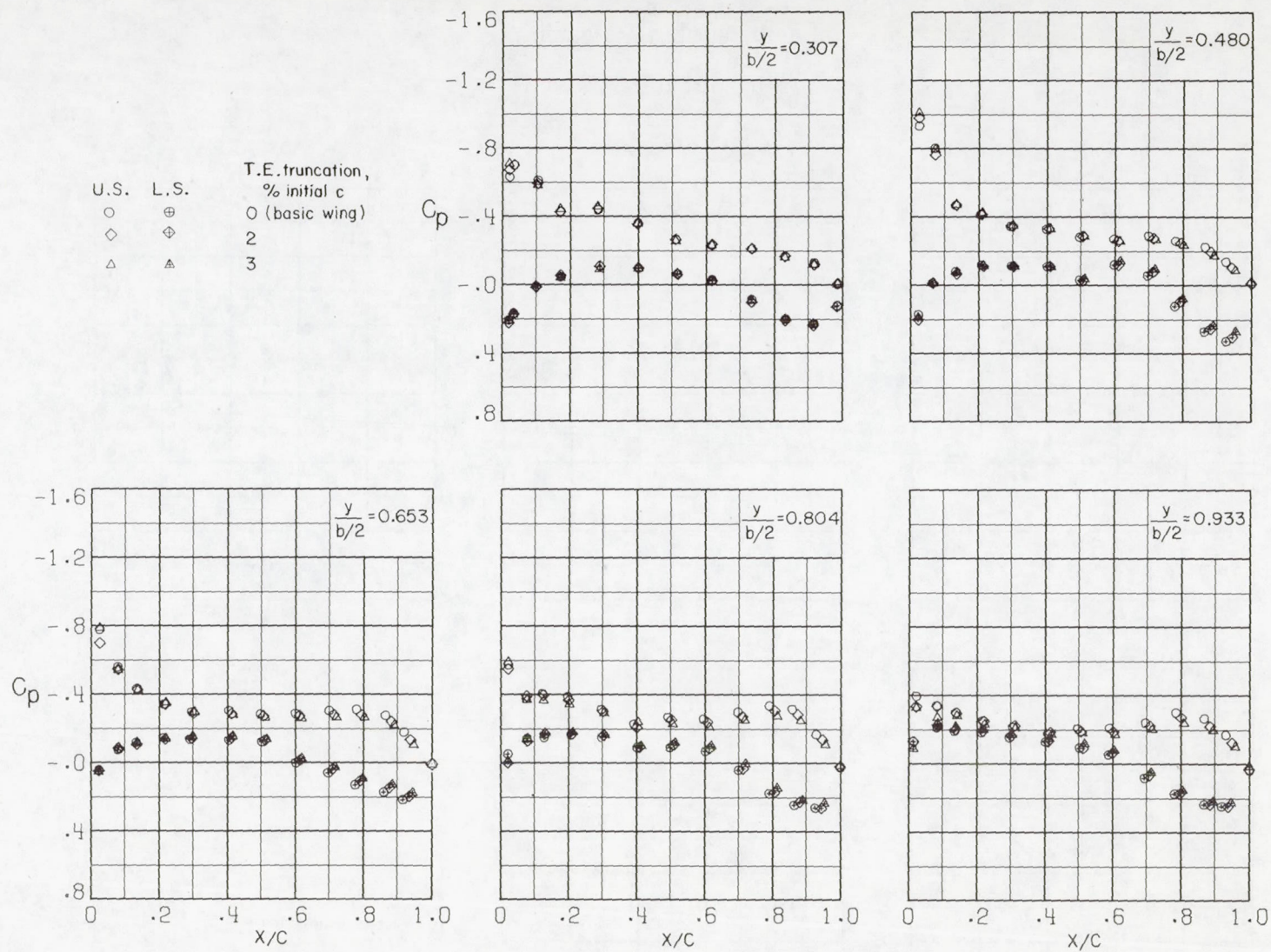
(c) $\alpha = 30^\circ$.

Figure 5.- Continued.

CONFIDENTIAL

CONFIDENTIAL

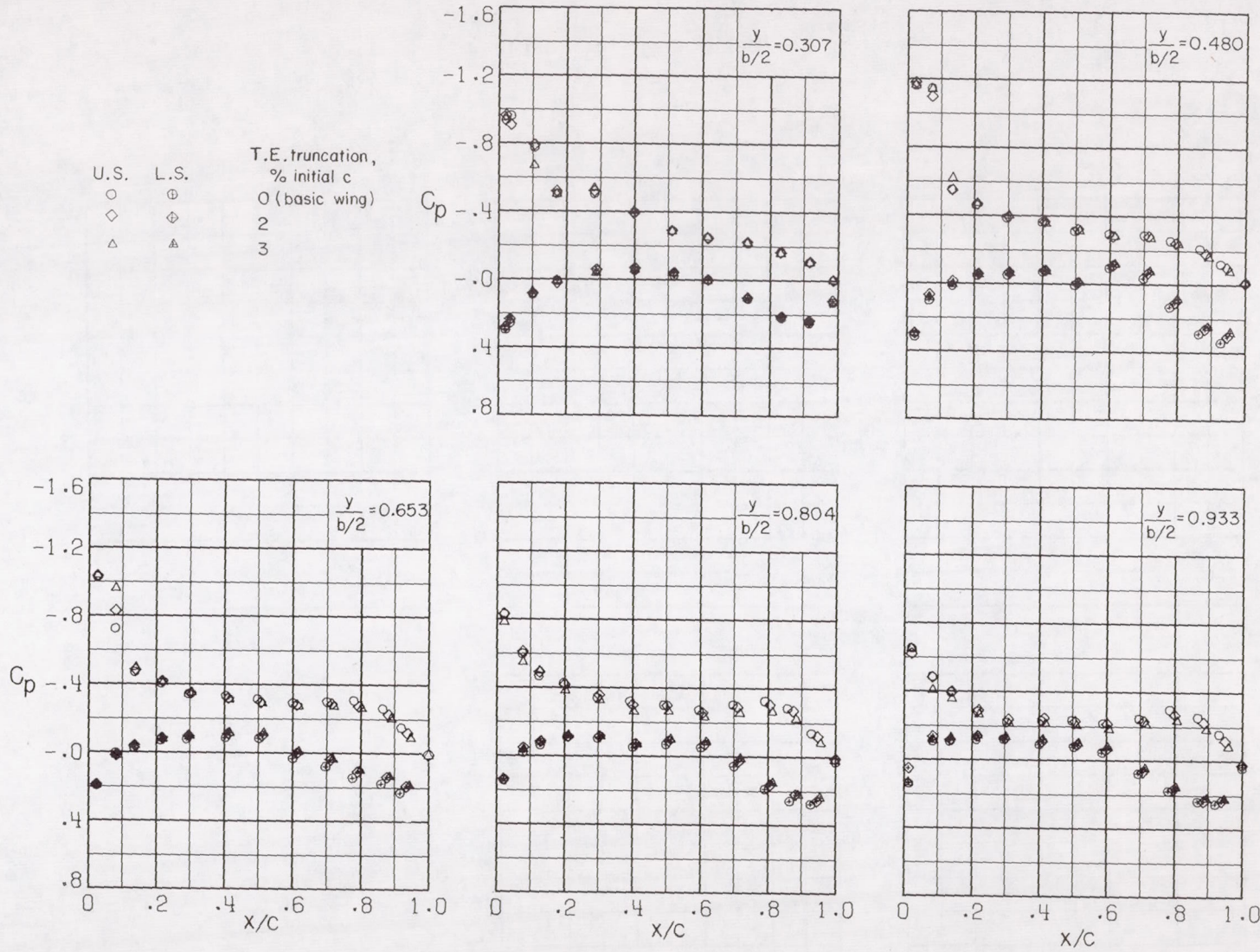
(d) $\alpha = 4^\circ$.

Figure 5.- Continued.

CONFIDENTIAL

CONFIDENTIAL

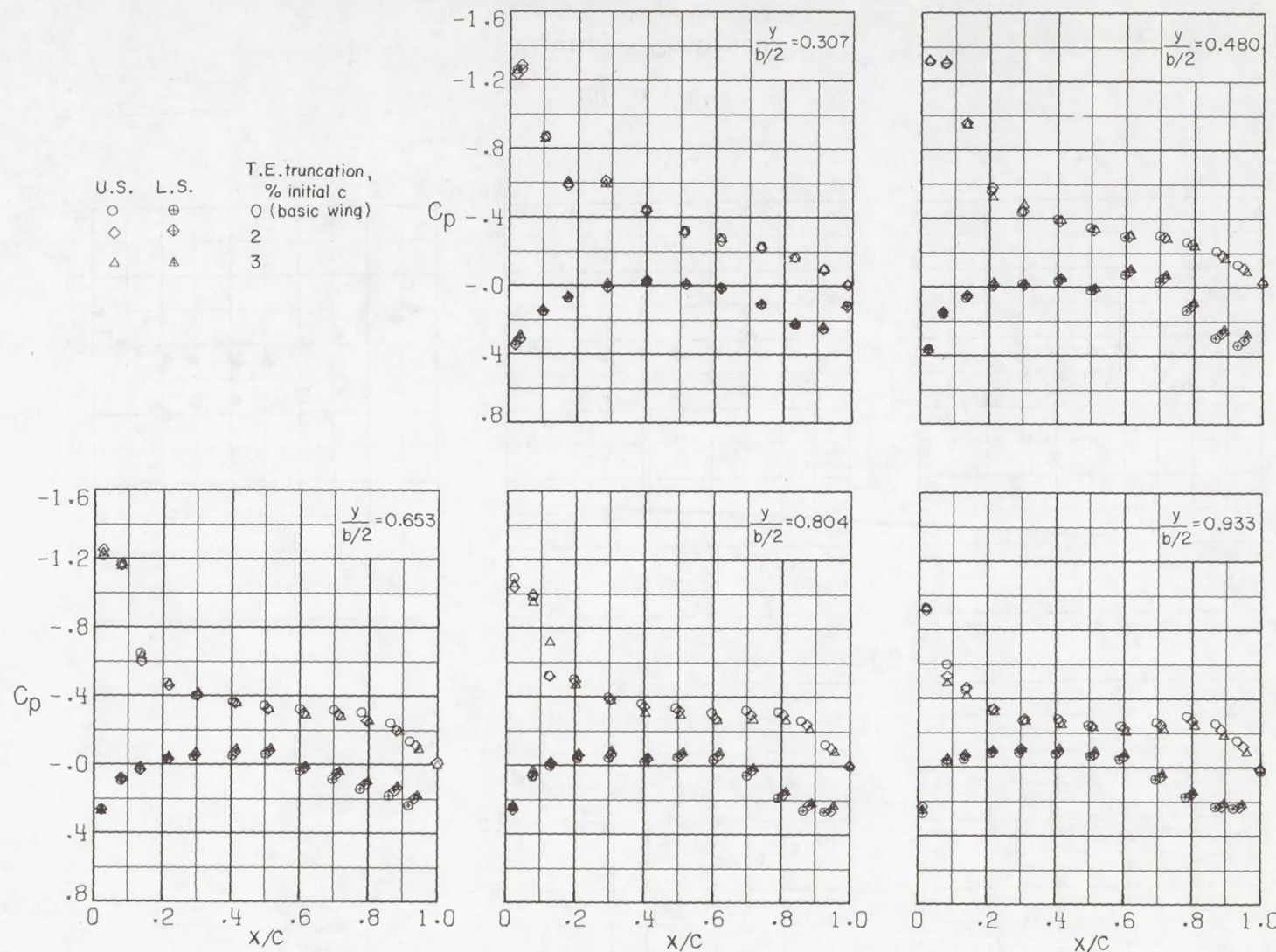
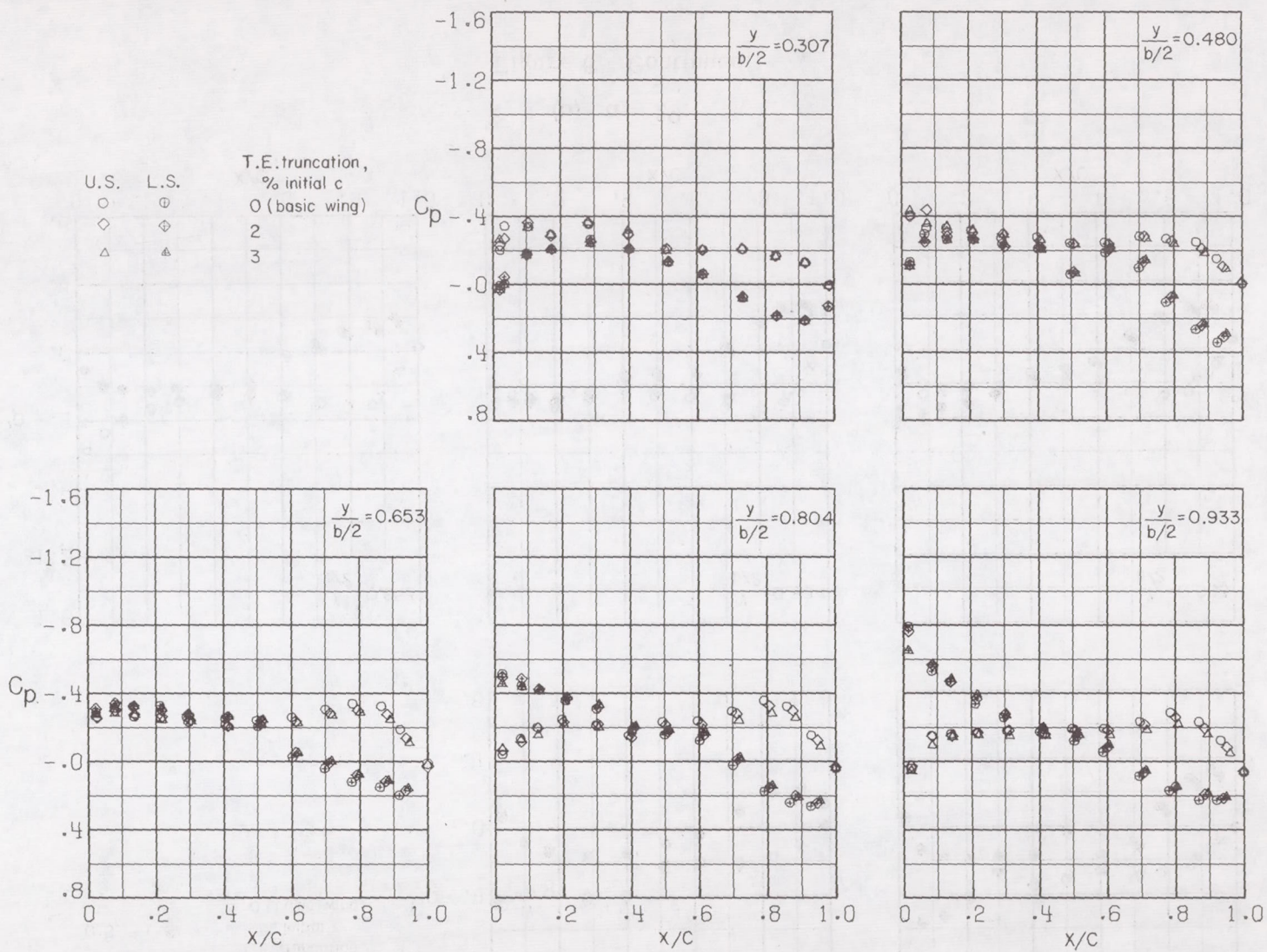
(e) $\alpha = 5^\circ$.

Figure 5.- Concluded.

CONFIDENTIAL

~~CONFIDENTIAL~~



(a) $\alpha = 1^\circ$.

Figure 6.- Effect of wing trailing-edge truncation on wing pressure distributions at Mach number 0.90. $\beta = 0^\circ$;
 $\delta_h = -2.5^\circ$.

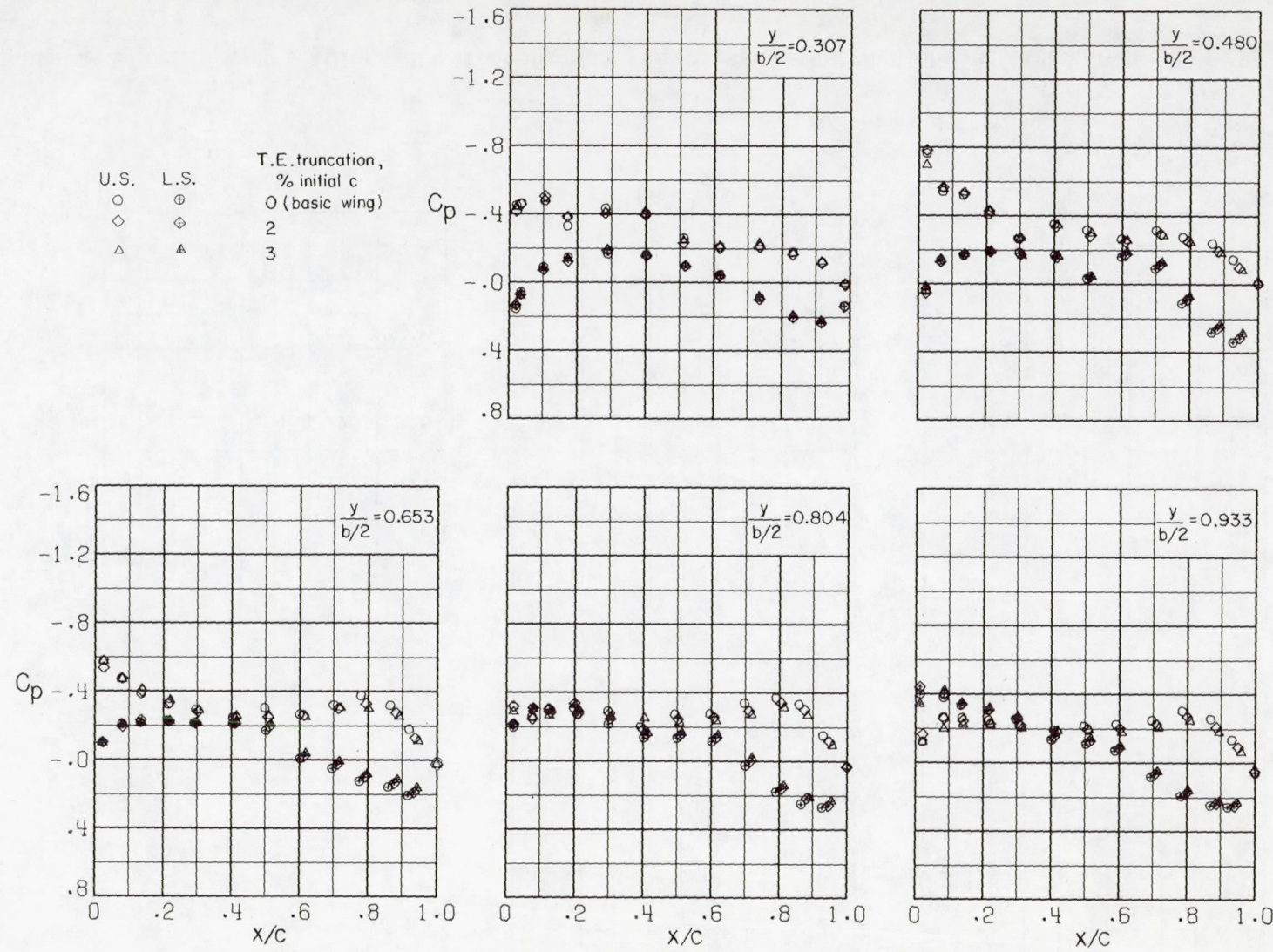
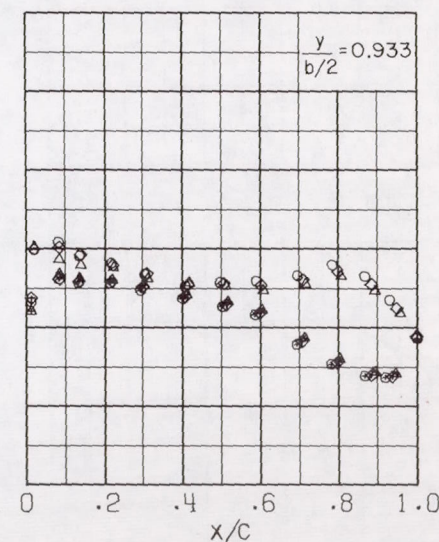
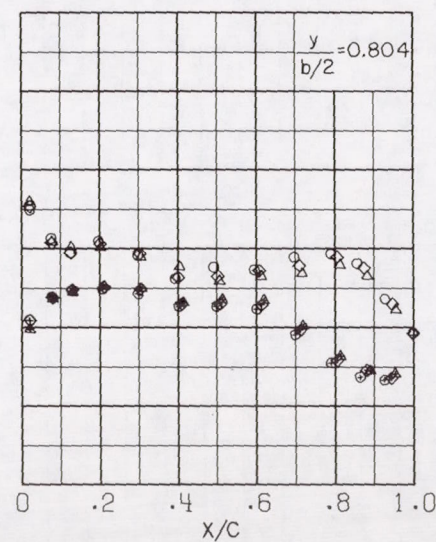
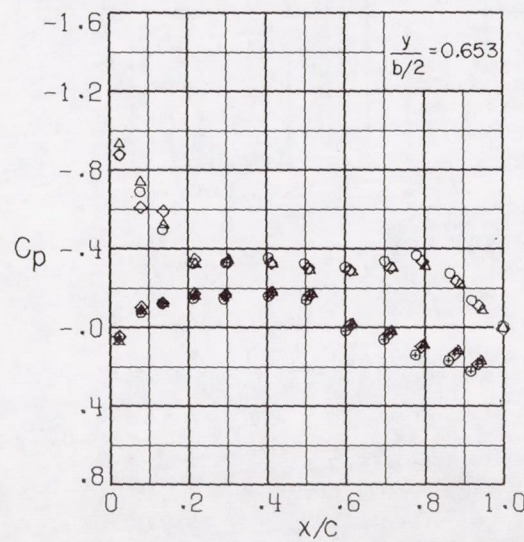
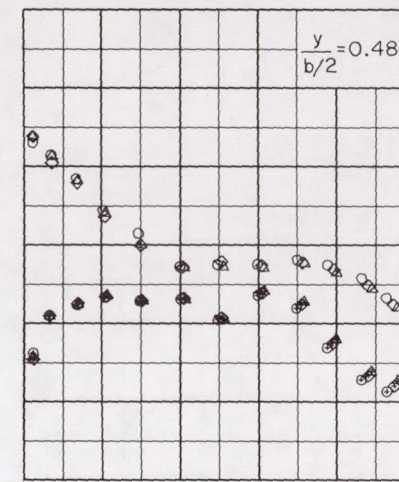
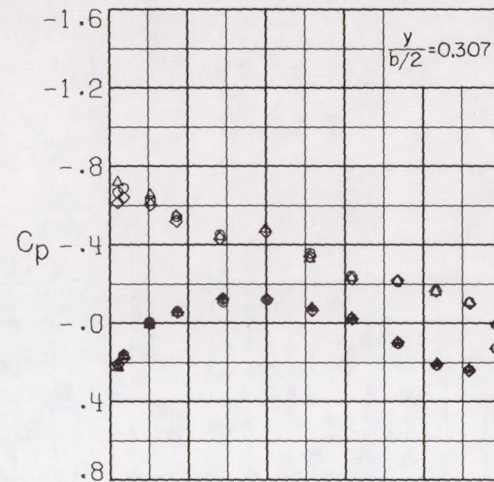
~~CONFIDENTIAL~~(b) $\alpha = 2^\circ$.

Figure 6.- Continued.

~~CONFIDENTIAL~~

~~CONFIDENTIAL~~

U.S. L.S. T.E. truncation,
 ○ ⊕ % initial c
 ◇ ⊖ 0 (basic wing)
 △ □ 2
 ▲ △ 3



(c) $\alpha = 3^{\circ}$.

Figure 6.- Continued.

~~CONFIDENTIAL~~

CONFIDENTIAL

CONFIDENTIAL

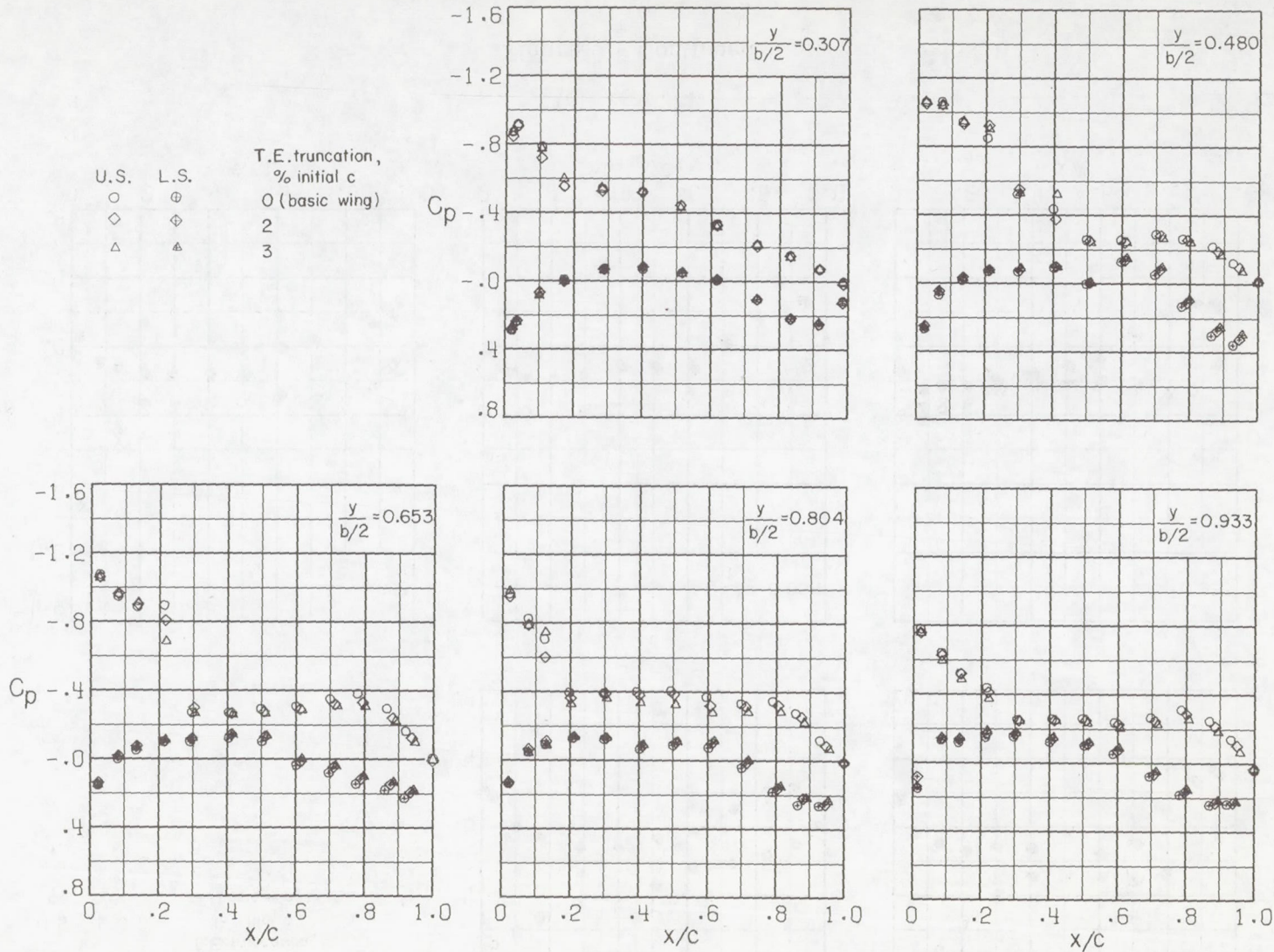
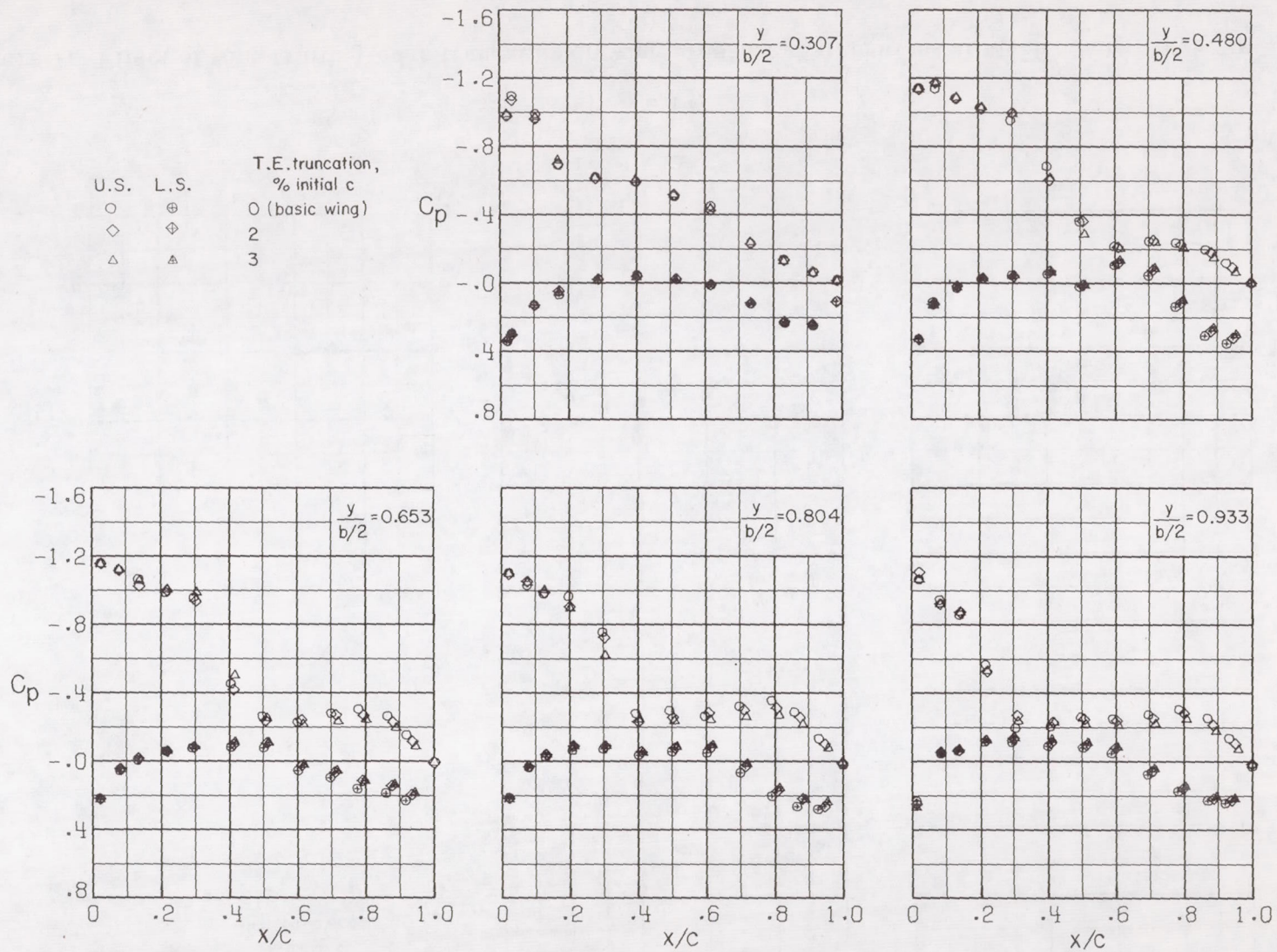
(d) $\alpha = 4^{\circ}$.

Figure 6.- Continued.

CONFIDENTIAL



(e) $\alpha = 5^\circ$.

Figure 6.- Concluded.

CONFIDENTIAL

CONFIDENTIAL

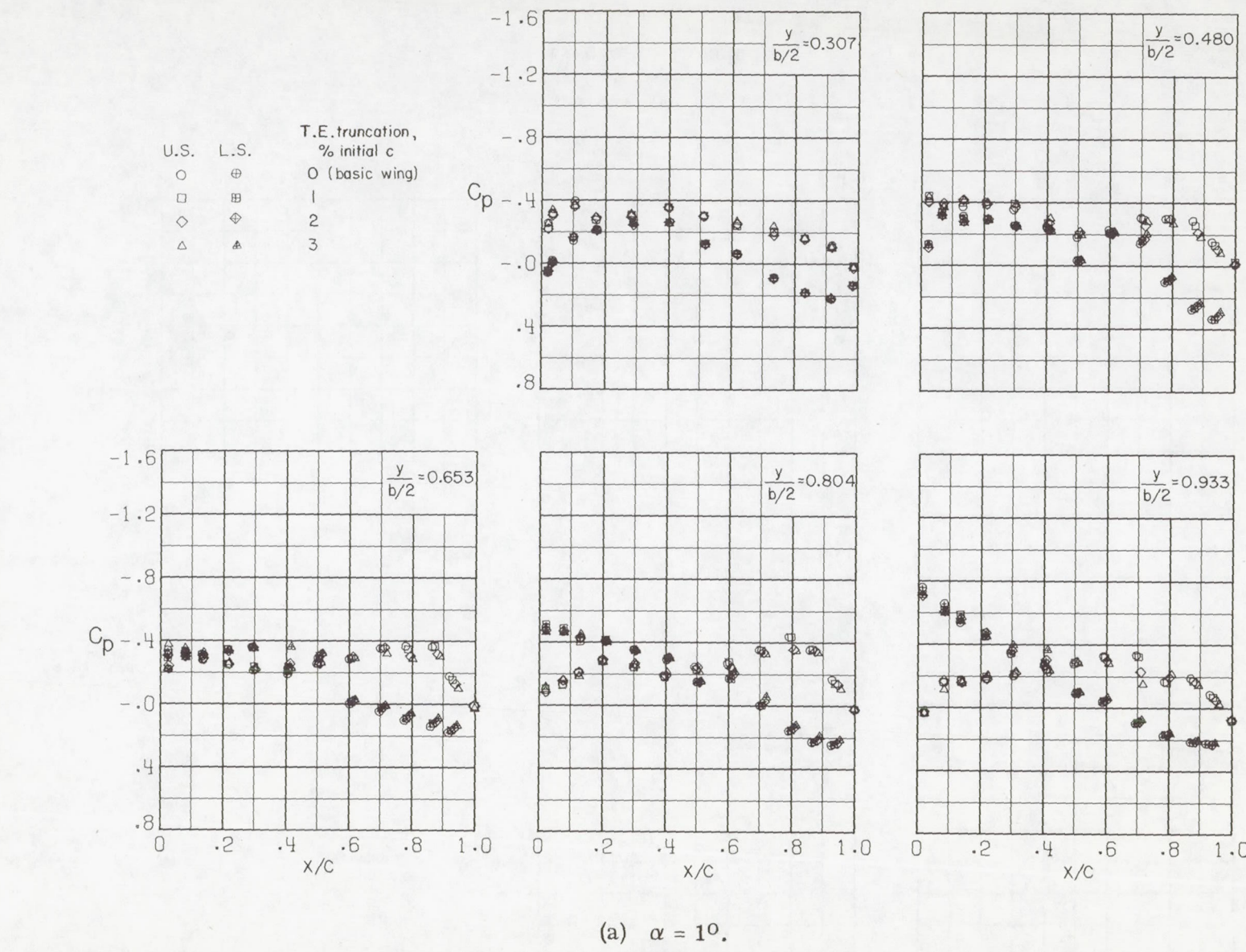


Figure 7.- Effect of wing trailing-edge truncation on wing pressure distributions at Mach number 0.95. $\beta = 0^\circ$;
 $\delta_h = -2.5^\circ$.

CONFIDENTIAL

CONFIDENTIAL

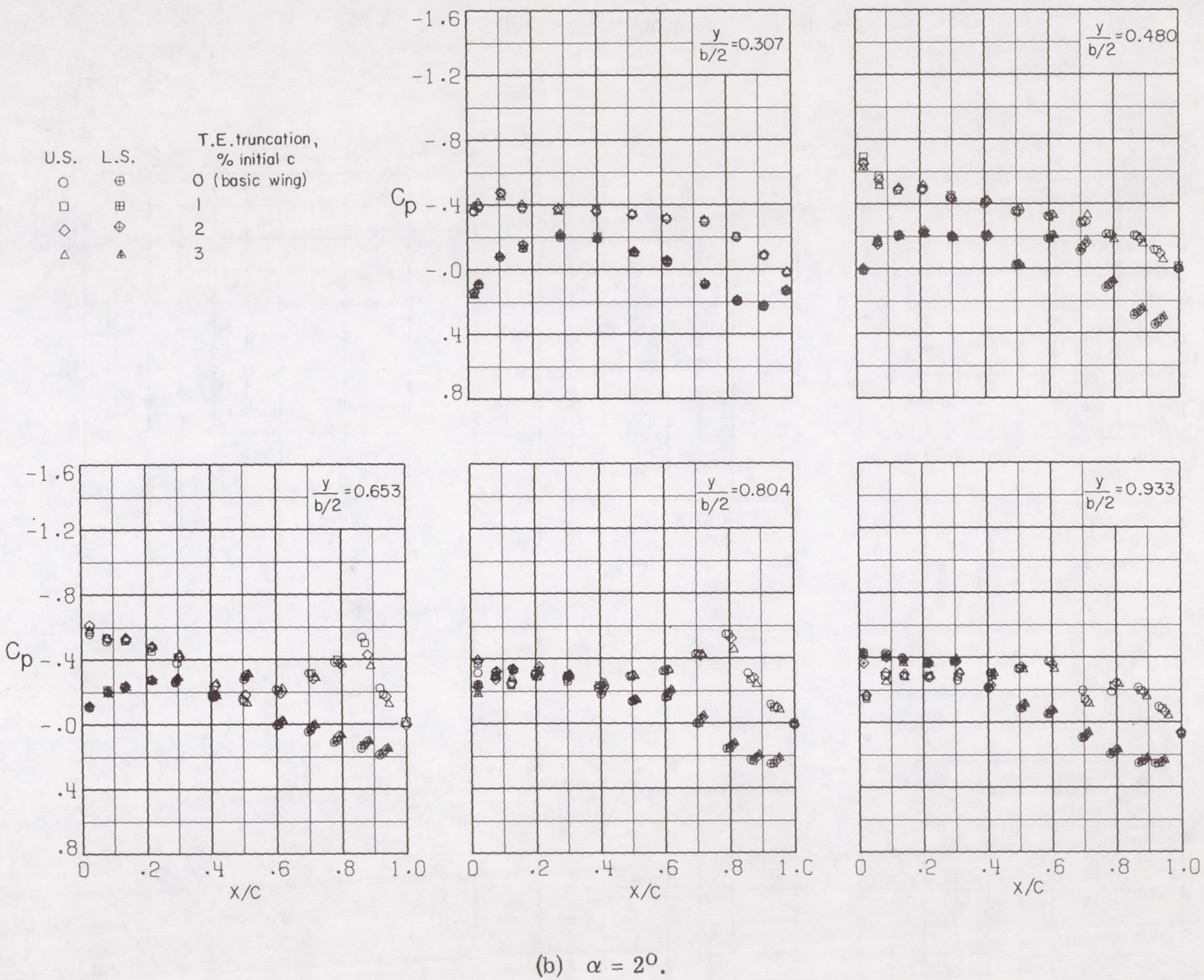


Figure 7.- Continued.

CONFIDENTIAL

CONFIDENTIAL

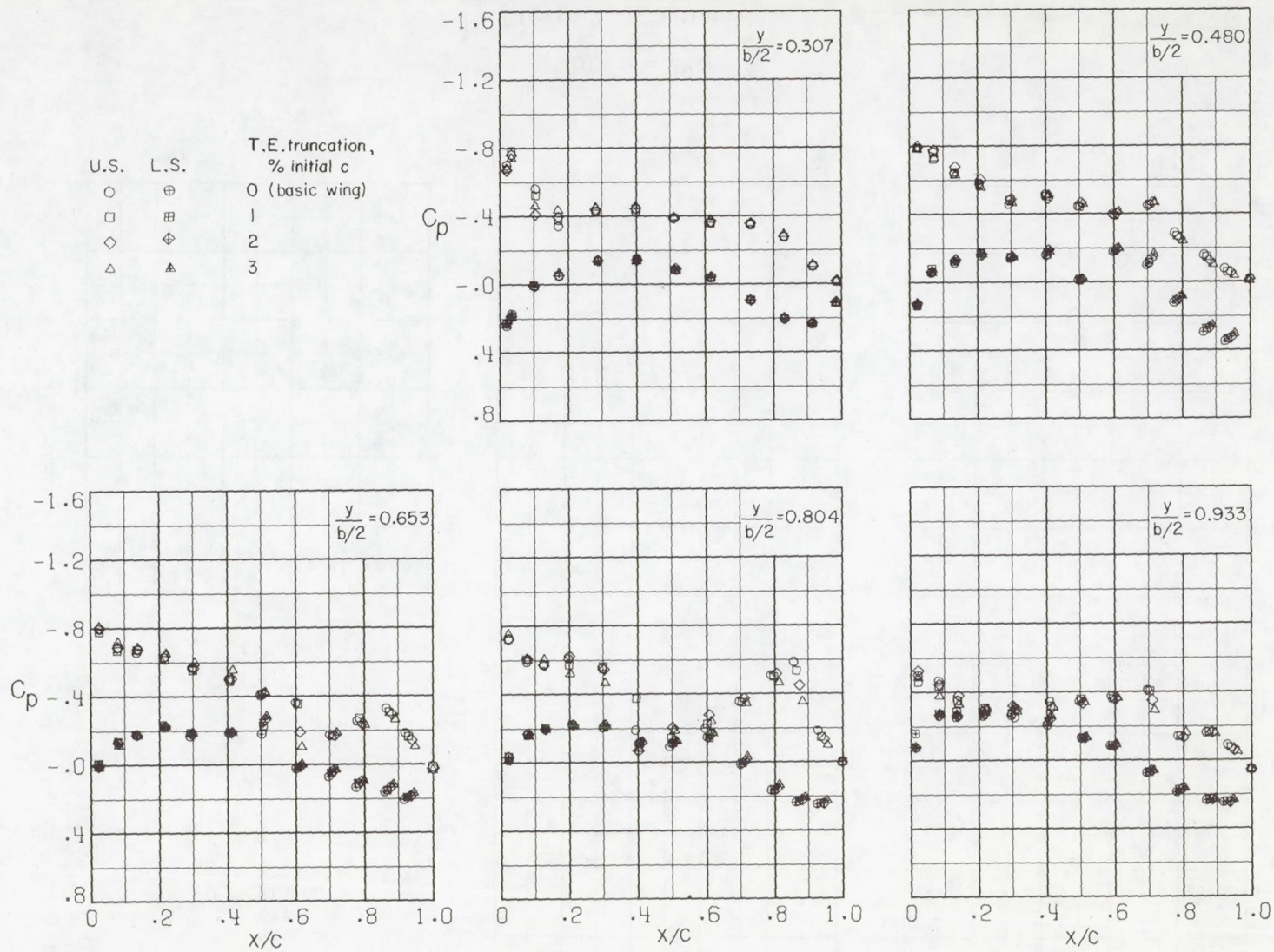
(c) $\alpha = 3^\circ$.

Figure 7.- Continued.

CONFIDENTIAL

CONFIDENTIAL

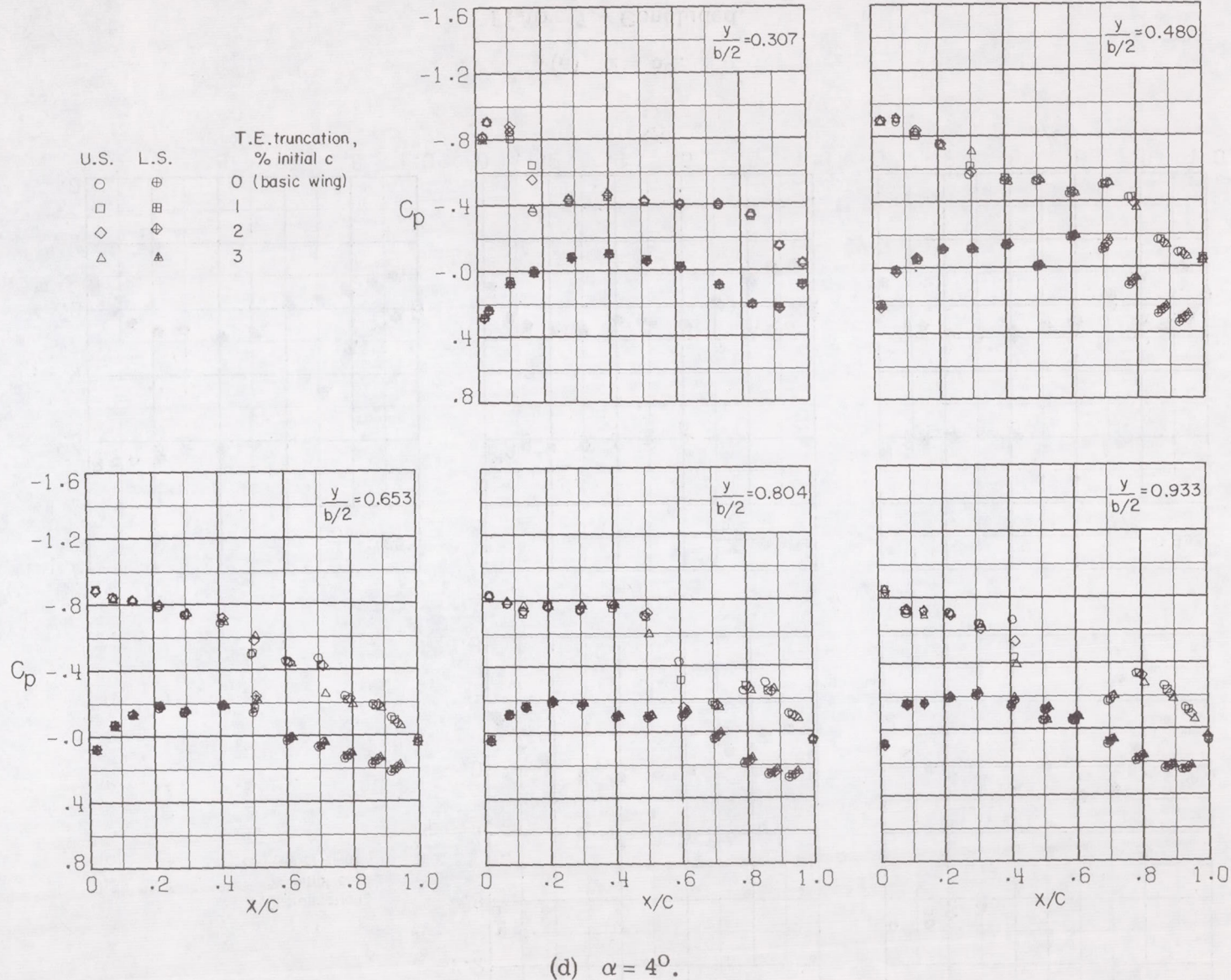


Figure 7.- Continued.

CONFIDENTIAL

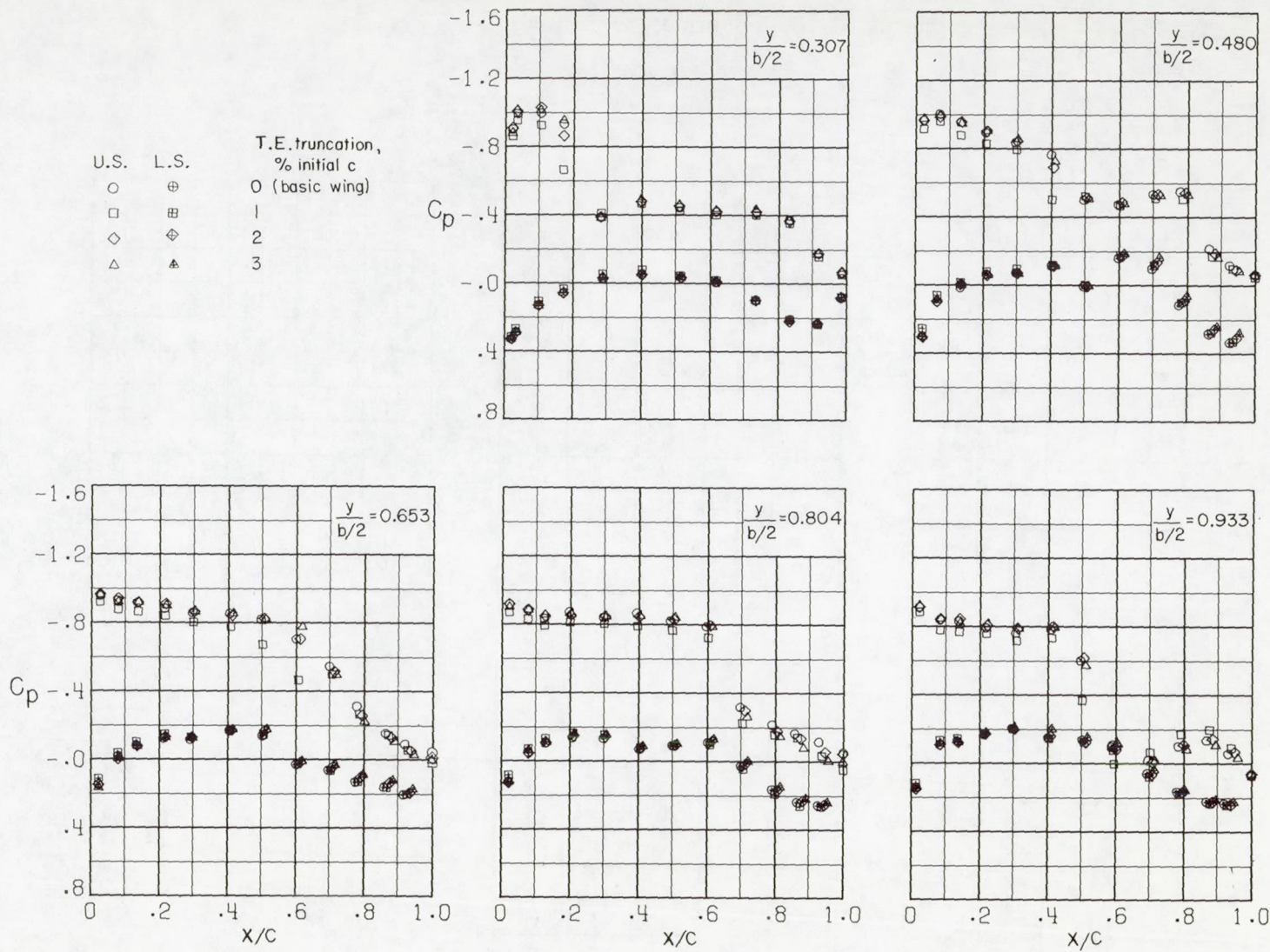
~~CONFIDENTIAL~~~~CONFIDENTIAL~~(e) $\alpha = 5^\circ$.

Figure 7.- Concluded.

CONFIDENTIAL

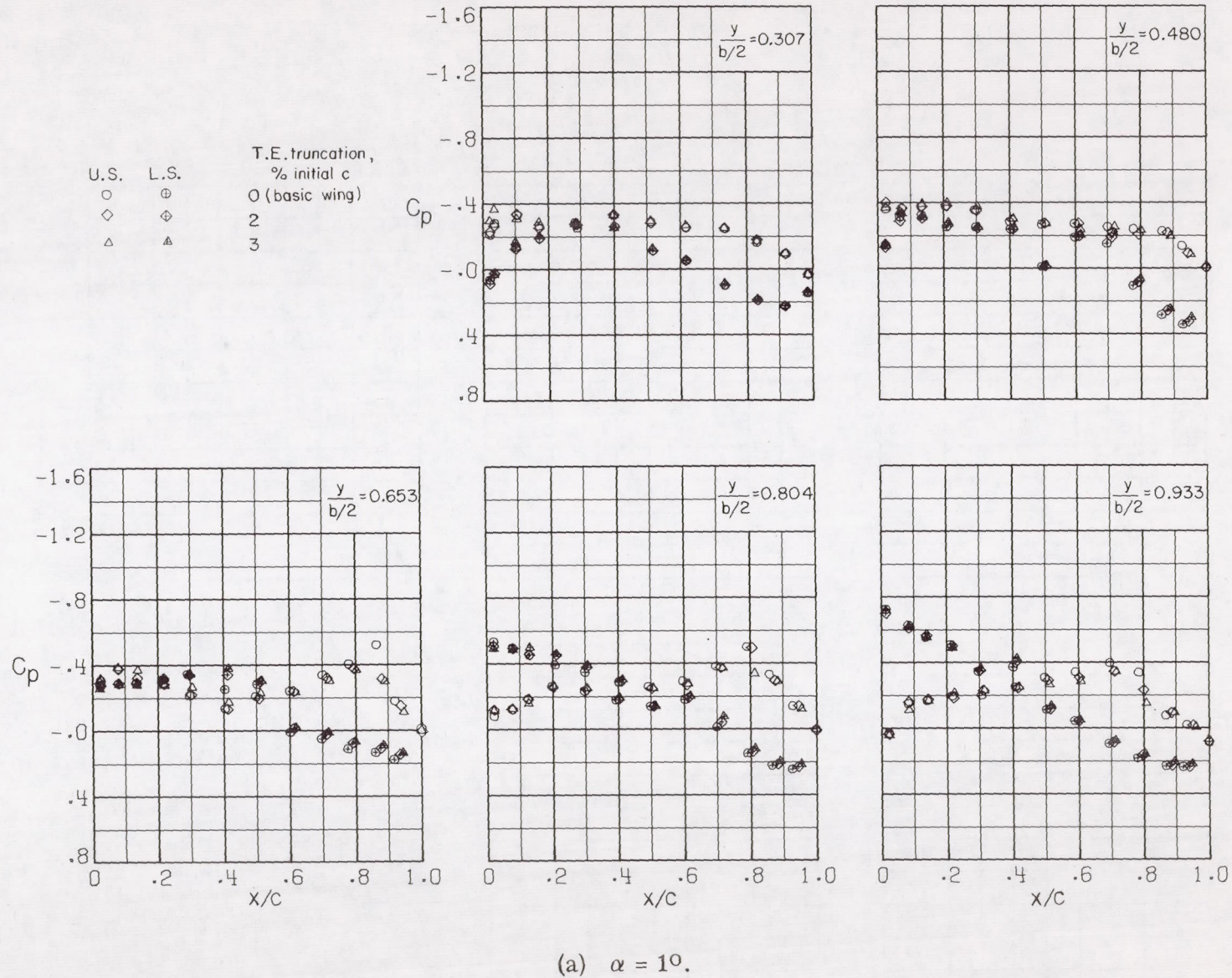
(a) $\alpha = 1^\circ$.

Figure 8.- Effect of wing trailing-edge truncation on wing pressure distributions at Mach number 0.96. $\beta = 0^\circ$; $\delta_h = -2.5^\circ$.

CONFIDENTIAL

CONFIDENTIAL

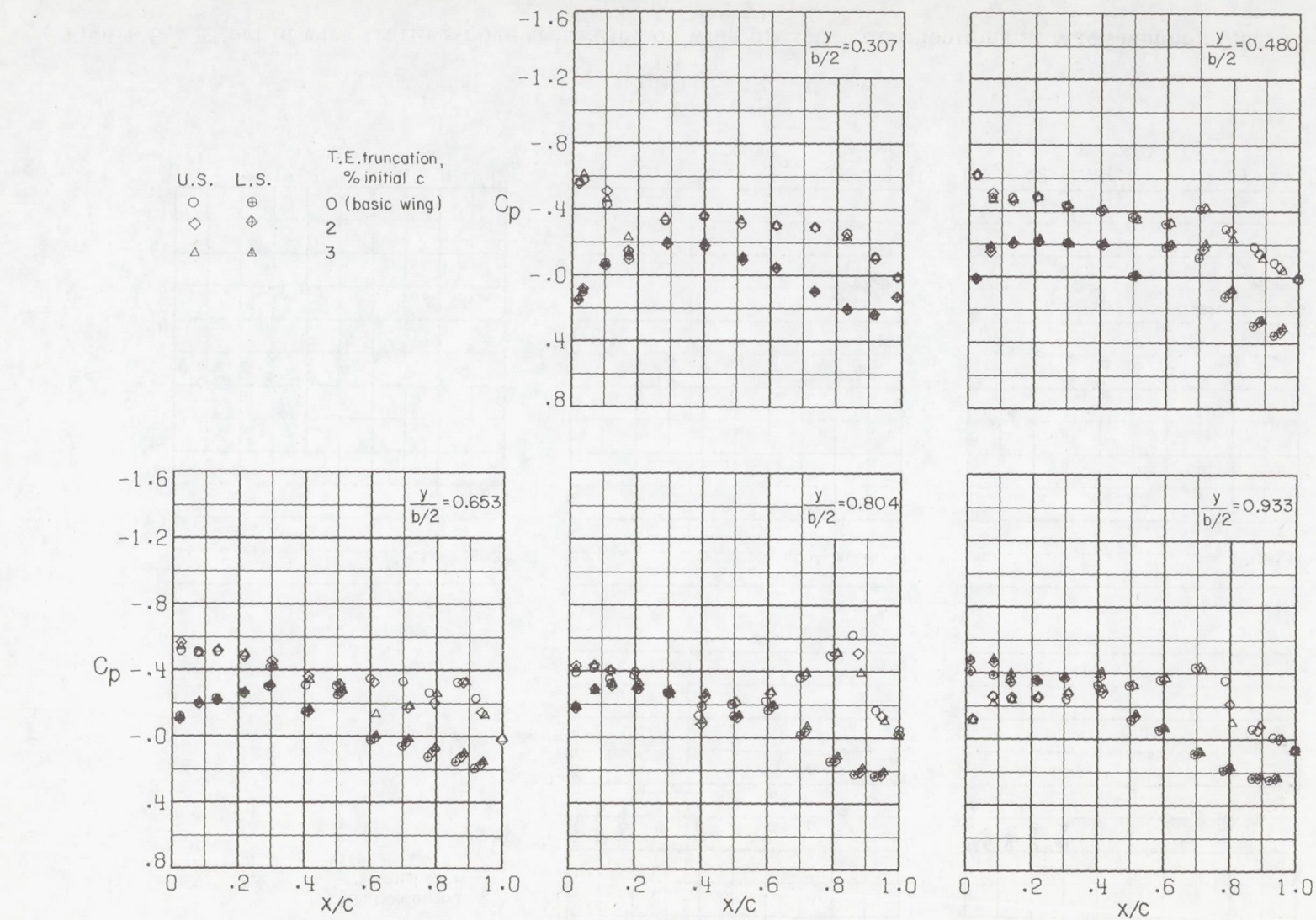
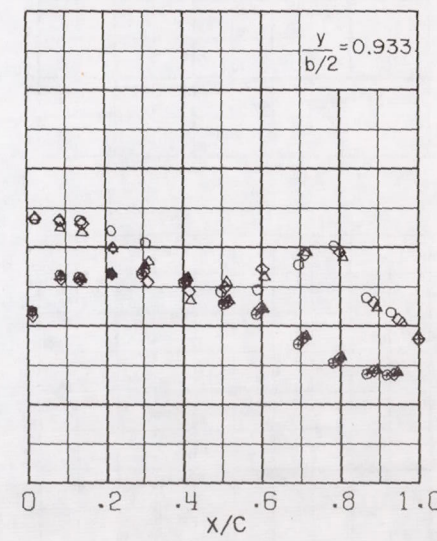
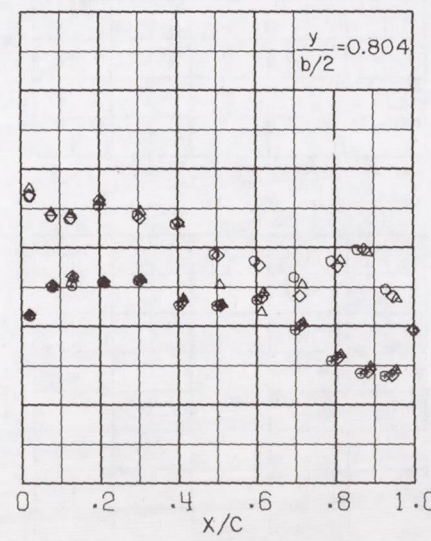
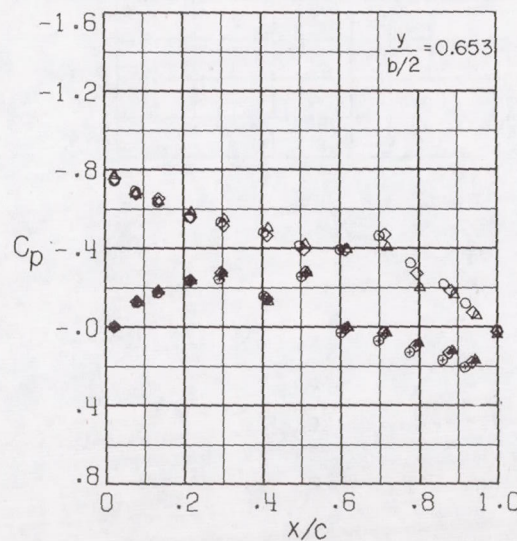
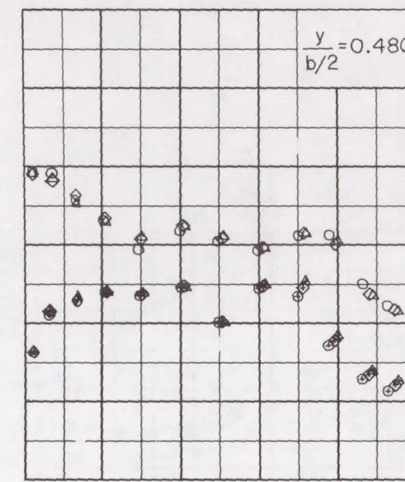
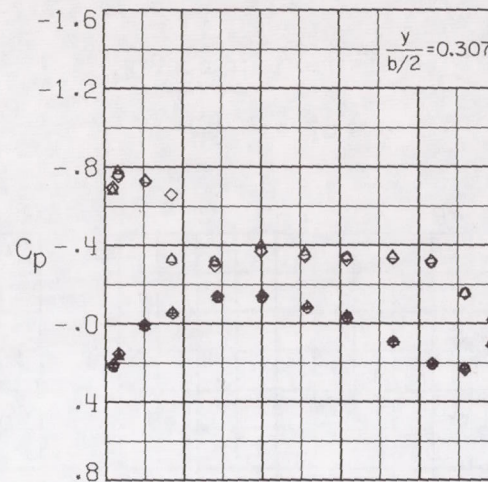
(b) $\alpha = 2^{\circ}$.

Figure 8.- Continued.

CONFIDENTIAL

~~CONFIDENTIAL~~

U.S. L.S.
○ ⊕ 0 (basic wing)
◇ ⊖ 2
△ ▲ 3
T.E. truncation,
% initial c



(c) $\alpha = 3^{\circ}$.

Figure 8.- Continued.

~~CONFIDENTIAL~~

CONFIDENTIAL

CONFIDENTIAL

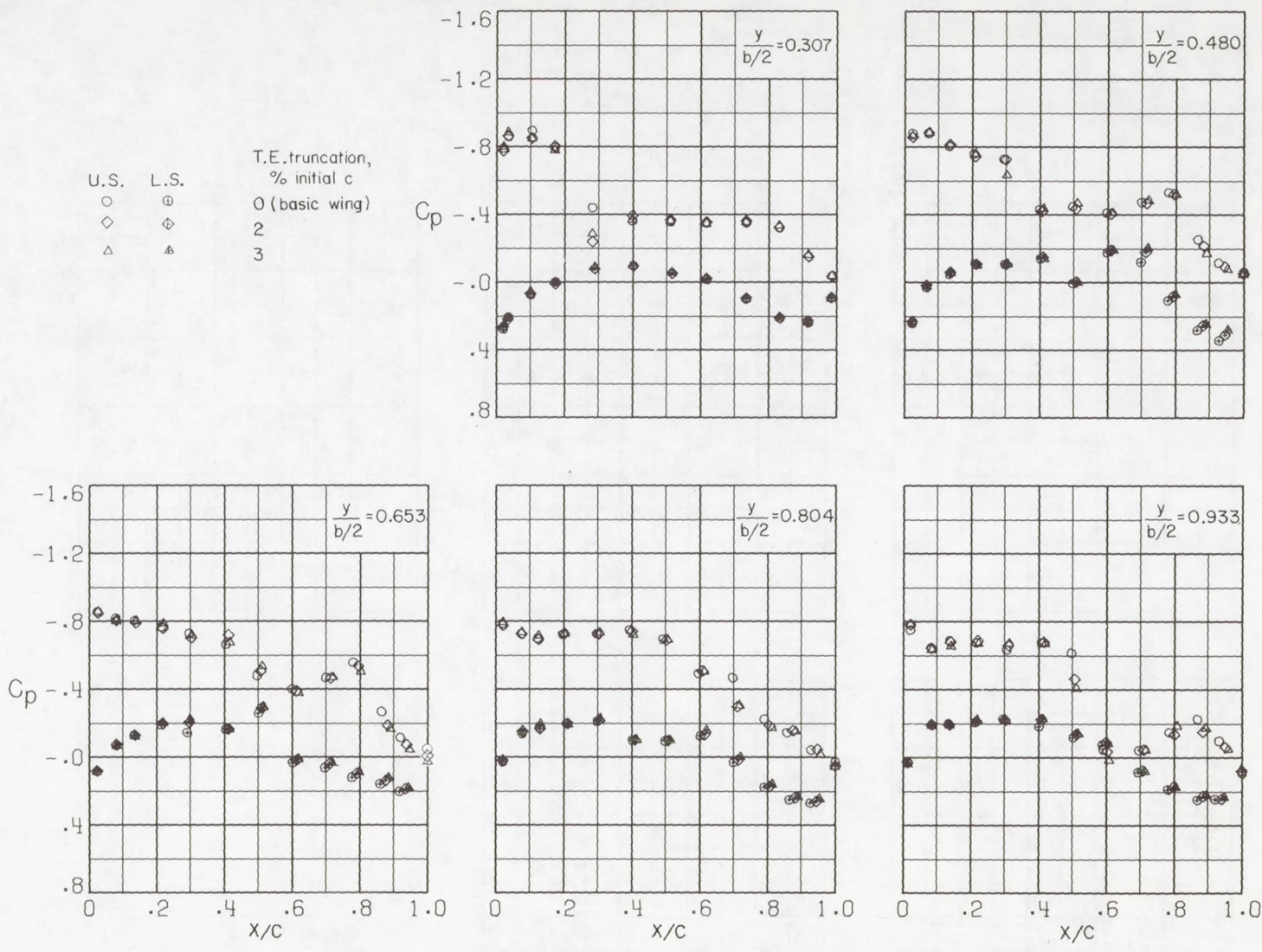
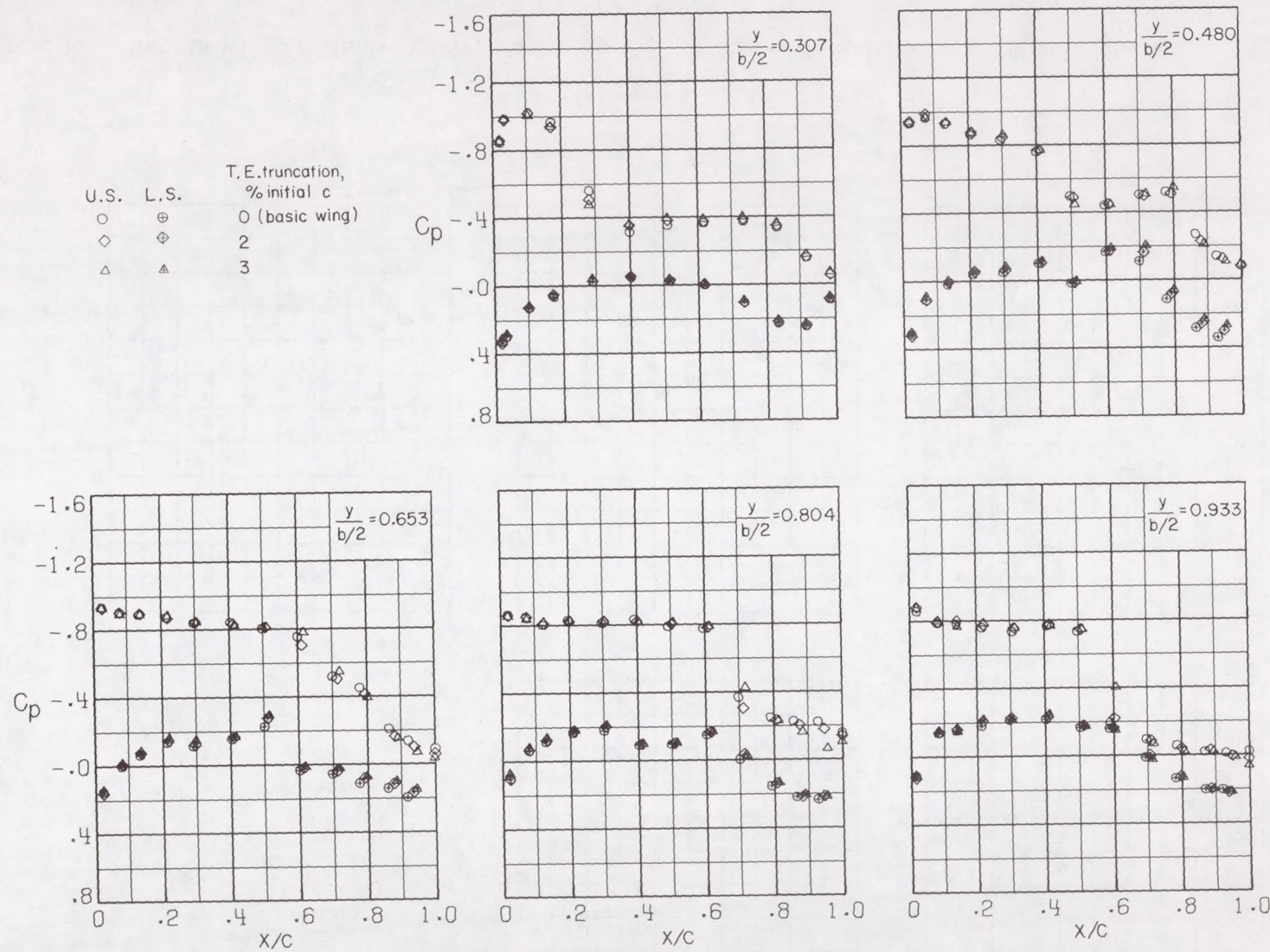
(d) $\alpha = 4^\circ$.

Figure 8.- Continued.

~~CONFIDENTIAL~~



(e) $\alpha = 5^{\circ}$.

Figure 8.- Concluded.

~~CONFIDENTIAL~~

CONFIDENTIAL

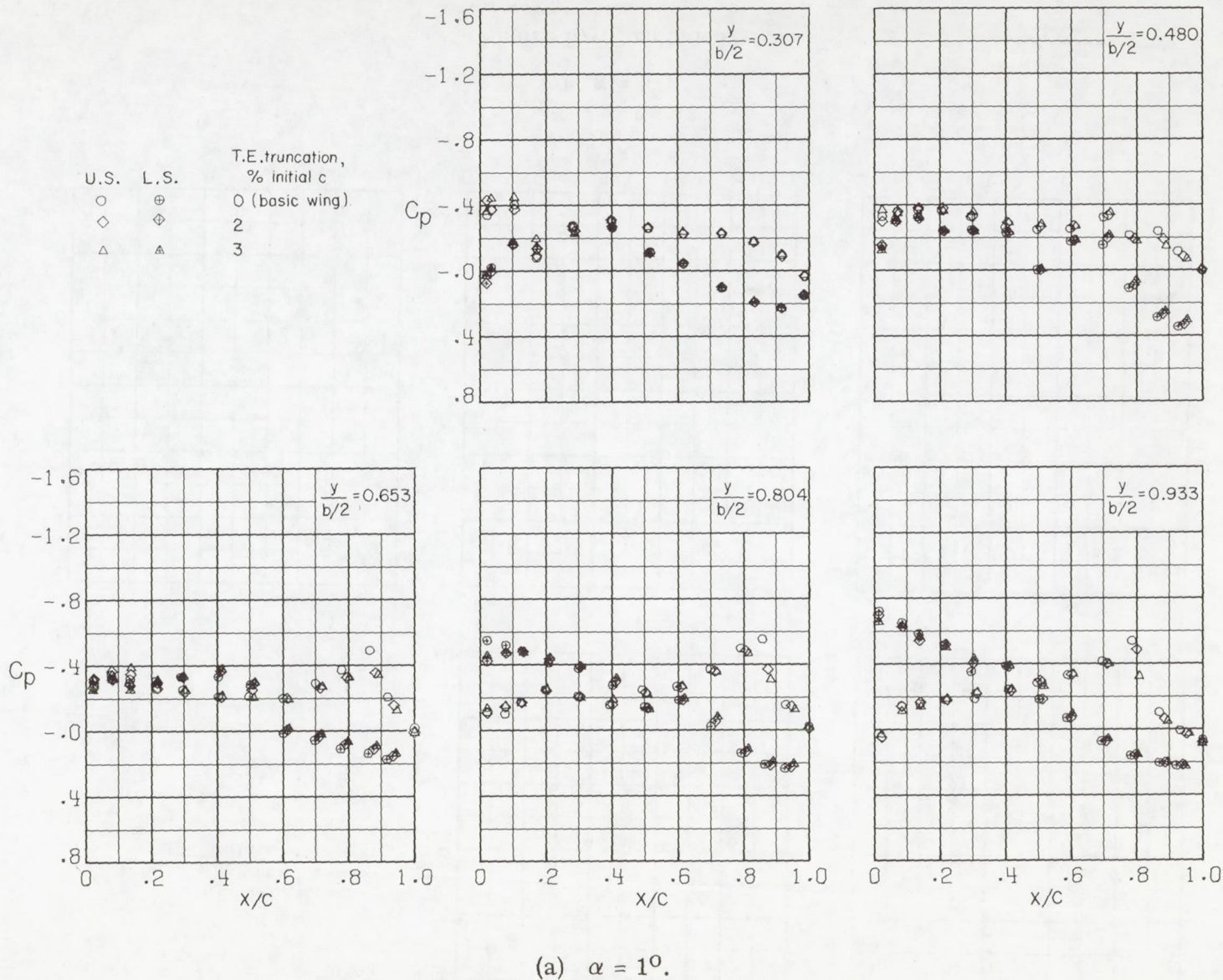


Figure 9.- Effect of wing trailing-edge truncation on wing pressure distributions at Mach number 0.97. $\beta = 0^\circ$;
 $\delta_h = -2.5^\circ$.

CONFIDENTIAL

CONFIDENTIAL

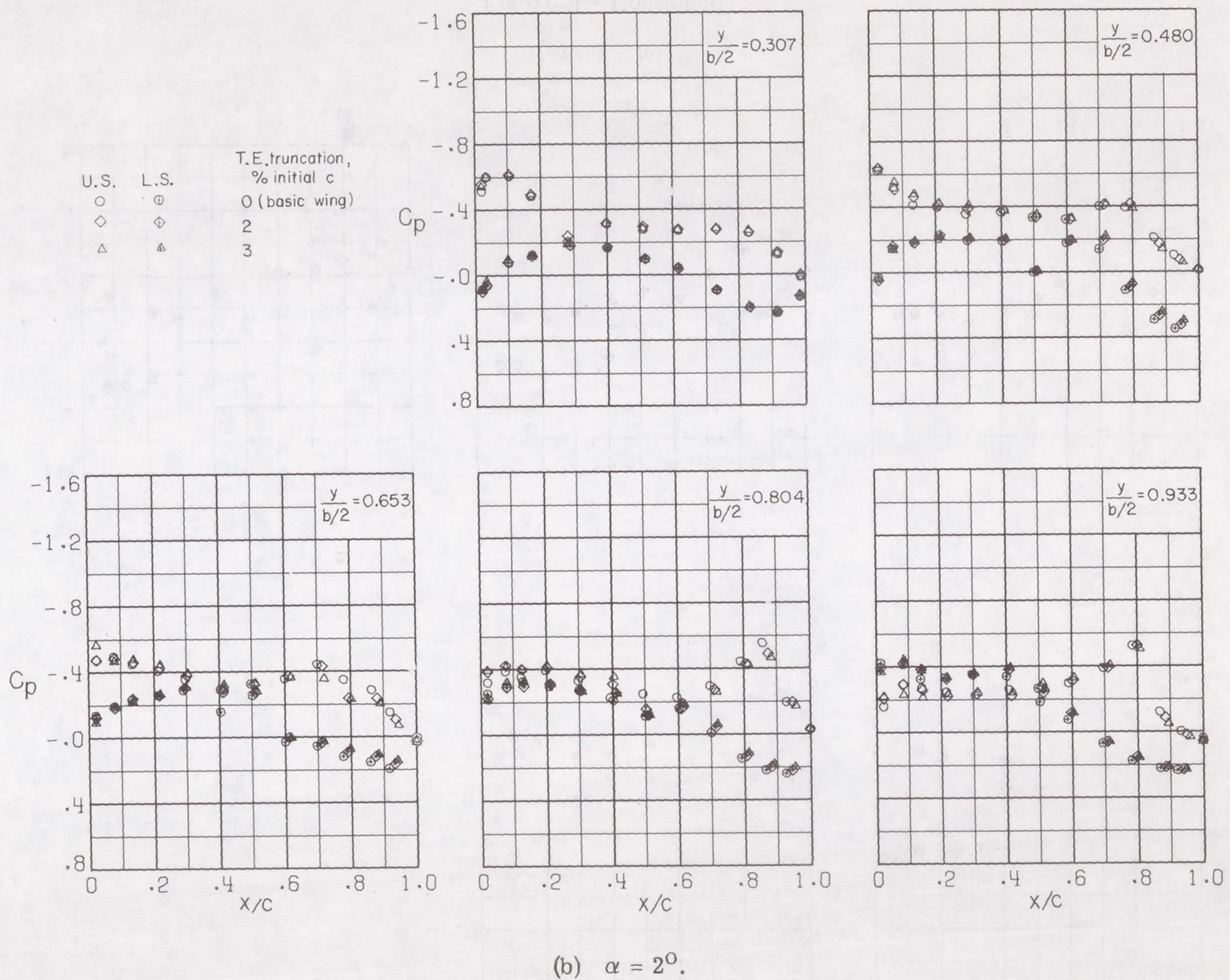


Figure 9.- Continued.

CONFIDENTIAL

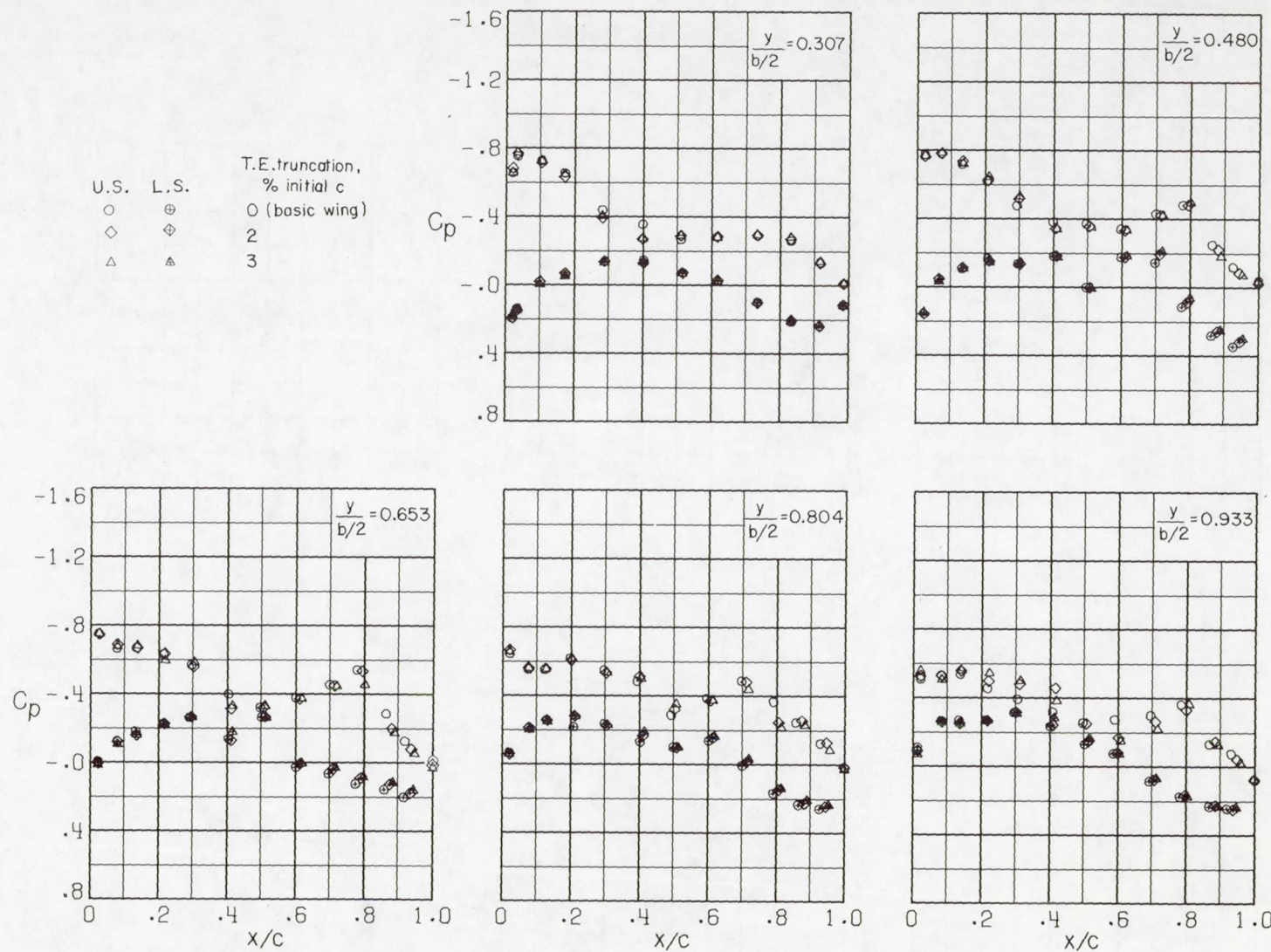
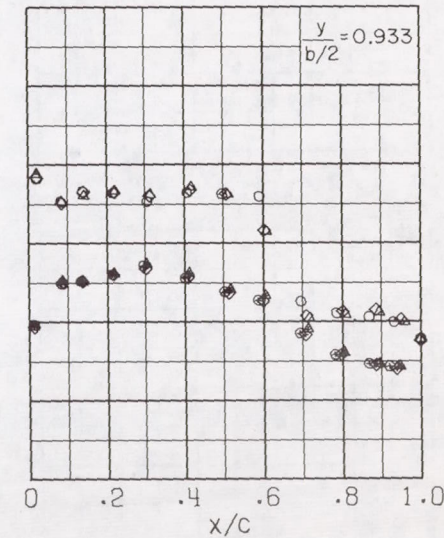
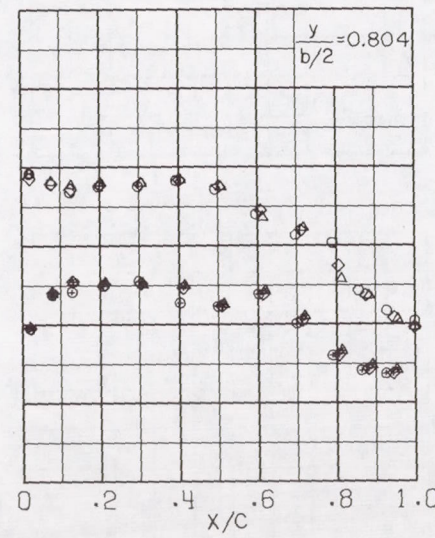
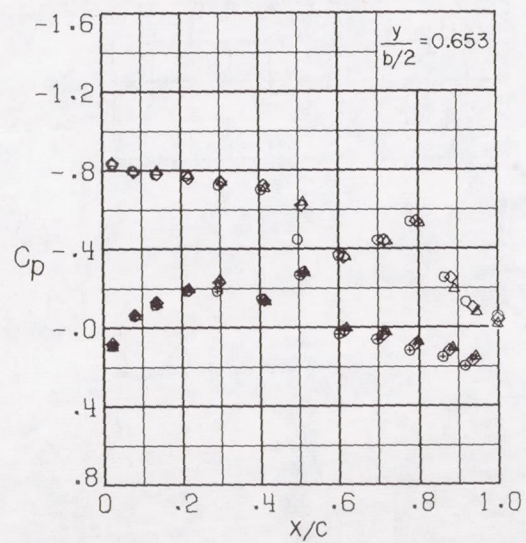
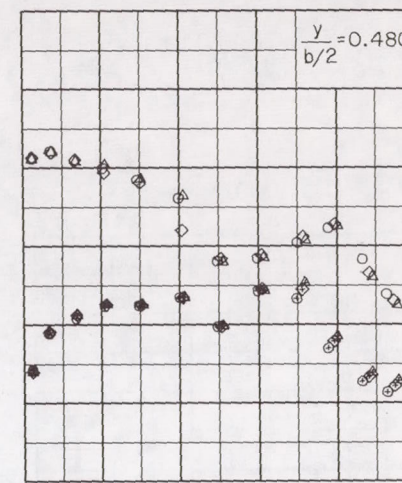
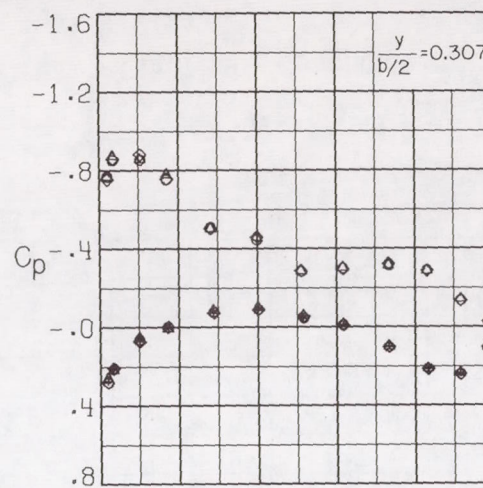
~~CONFIDENTIAL~~~~CONFIDENTIAL~~(c) $\alpha = 3^\circ$.

Figure 9.- Continued.

~~CONFIDENTIAL~~

U.S. L.S.
○ ⊕
◇ ◇
△ △
T.E. truncation,
% initial c
○ (basic wing)
2
3



(d) $\alpha = 4^\circ$.

Figure 9.- Continued.

~~CONFIDENTIAL~~

CONFIDENTIAL

CONFIDENTIAL

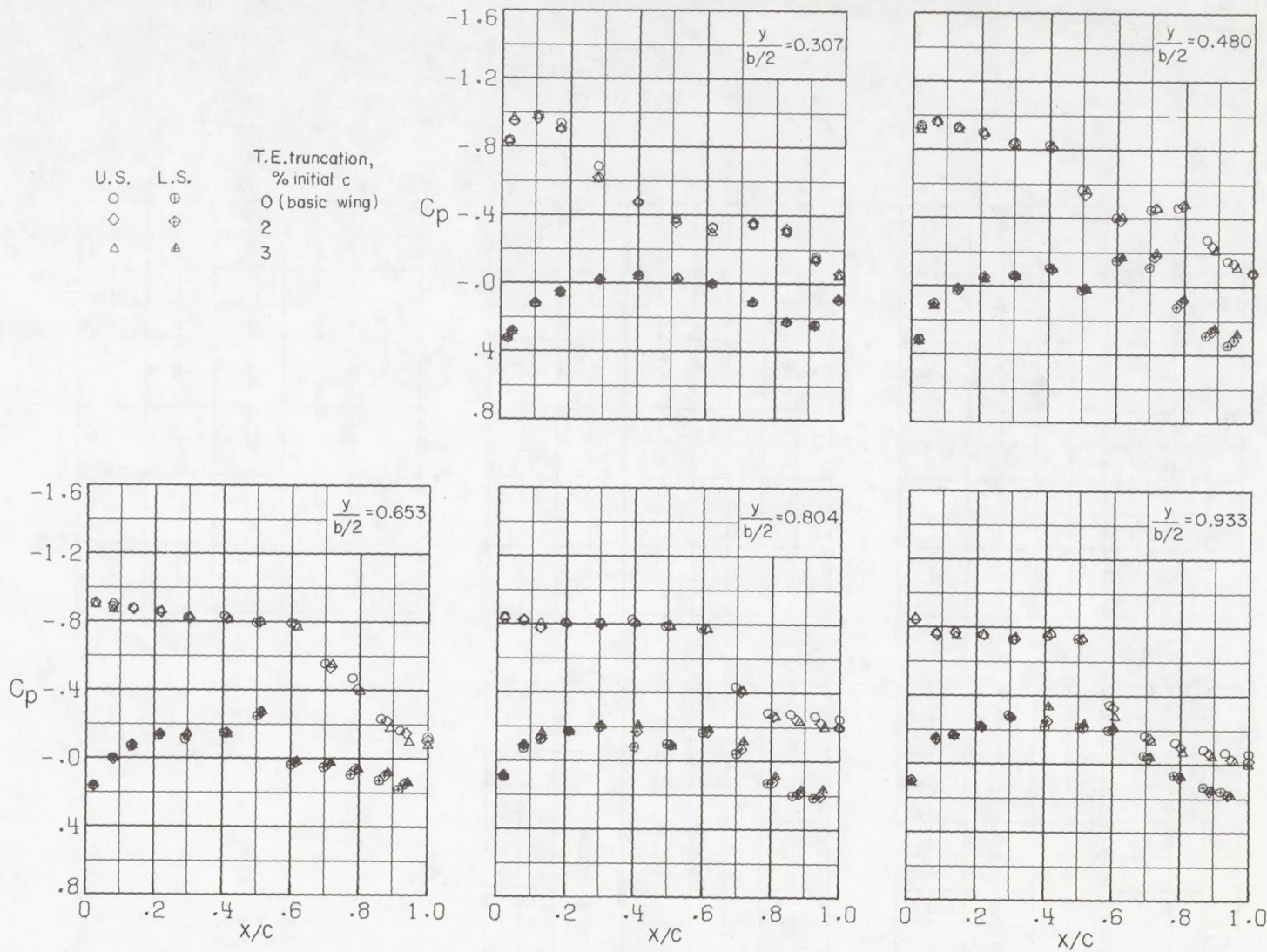
(e) $\alpha = 5^\circ$.

Figure 9.- Concluded.

CONFIDENTIAL

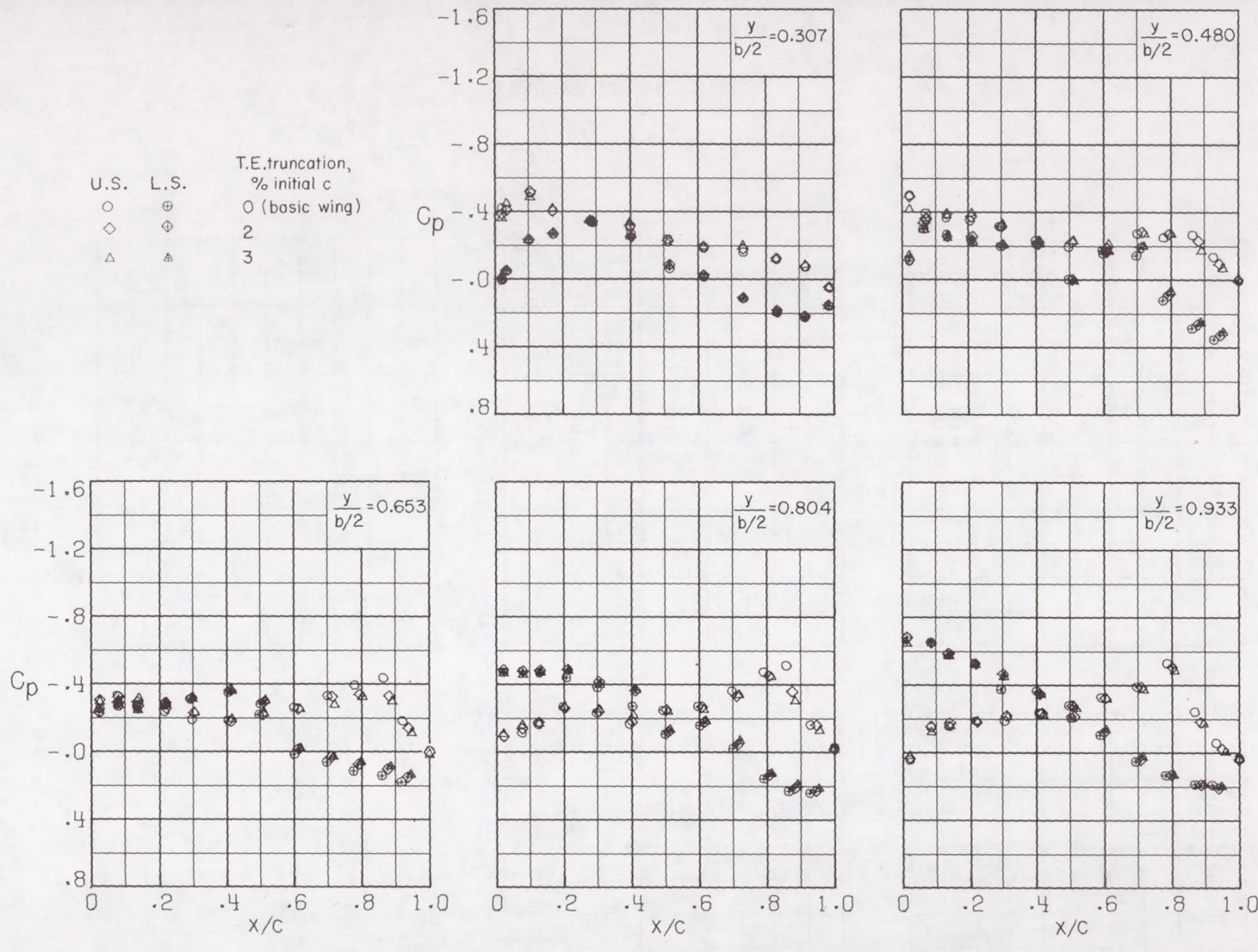
(a) $\alpha = 1^{\circ}$.

Figure 10.- Effect of wing trailing-edge truncation on wing pressure distributions at Mach number 0.98. $\beta = 0^{\circ}$;
 $\delta_h = -2.5^{\circ}$.

CONFIDENTIAL

CONFIDENTIAL

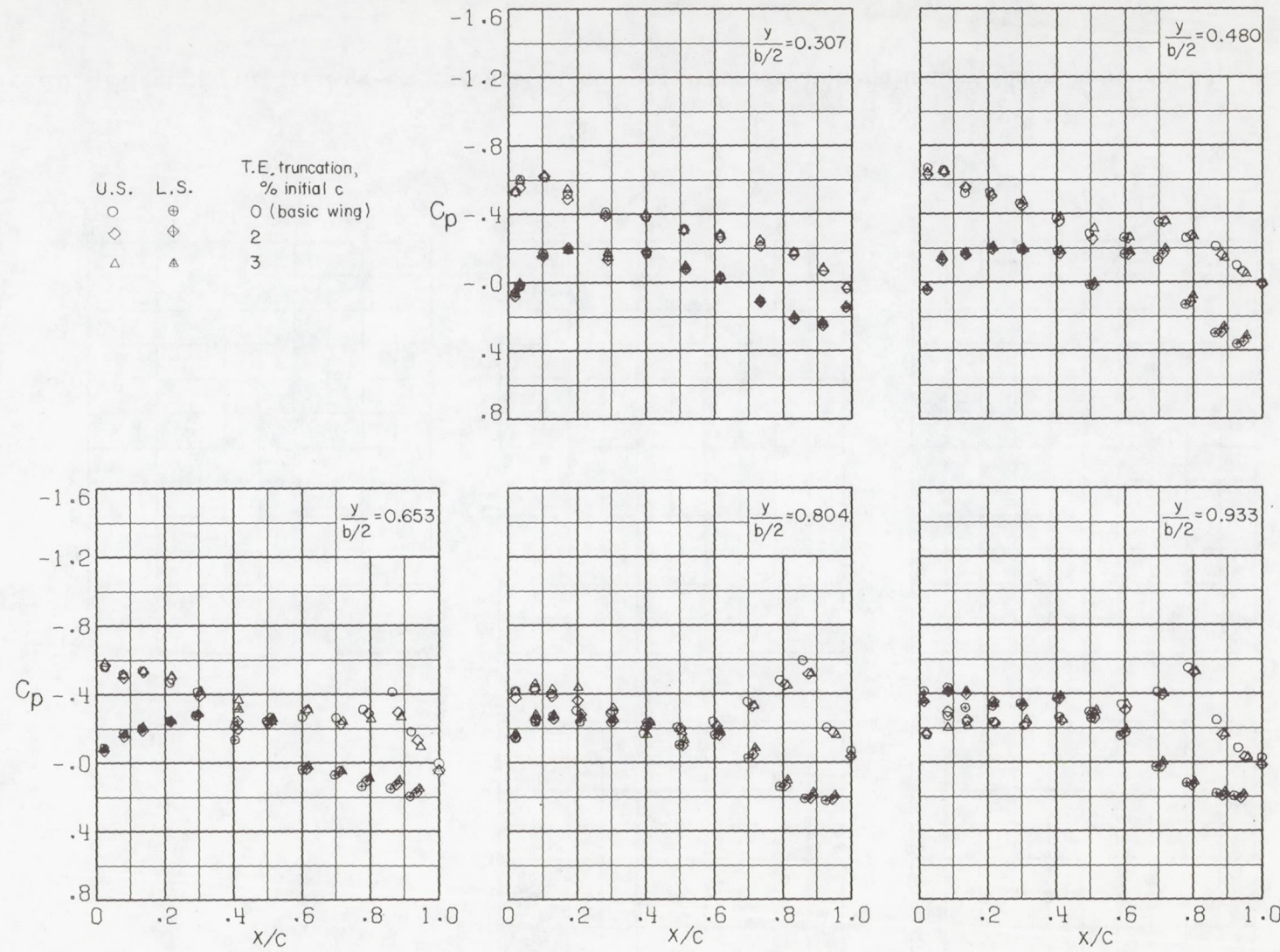
(b) $\alpha = 2^\circ$.

Figure 10.- Continued.

CONFIDENTIAL

~~CONFIDENTIAL~~

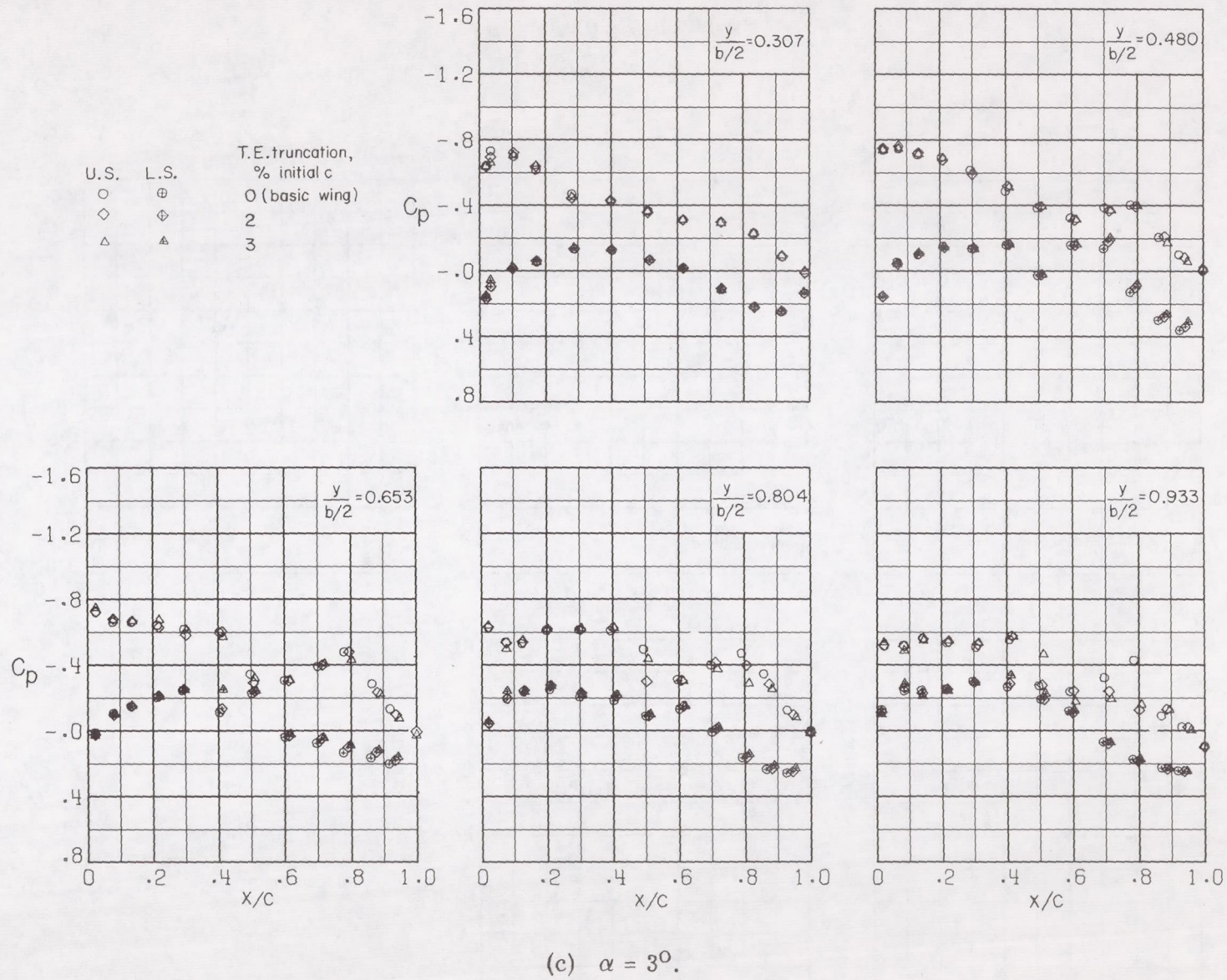


Figure 10.- Continued.

~~CONFIDENTIAL~~

CONFIDENTIAL

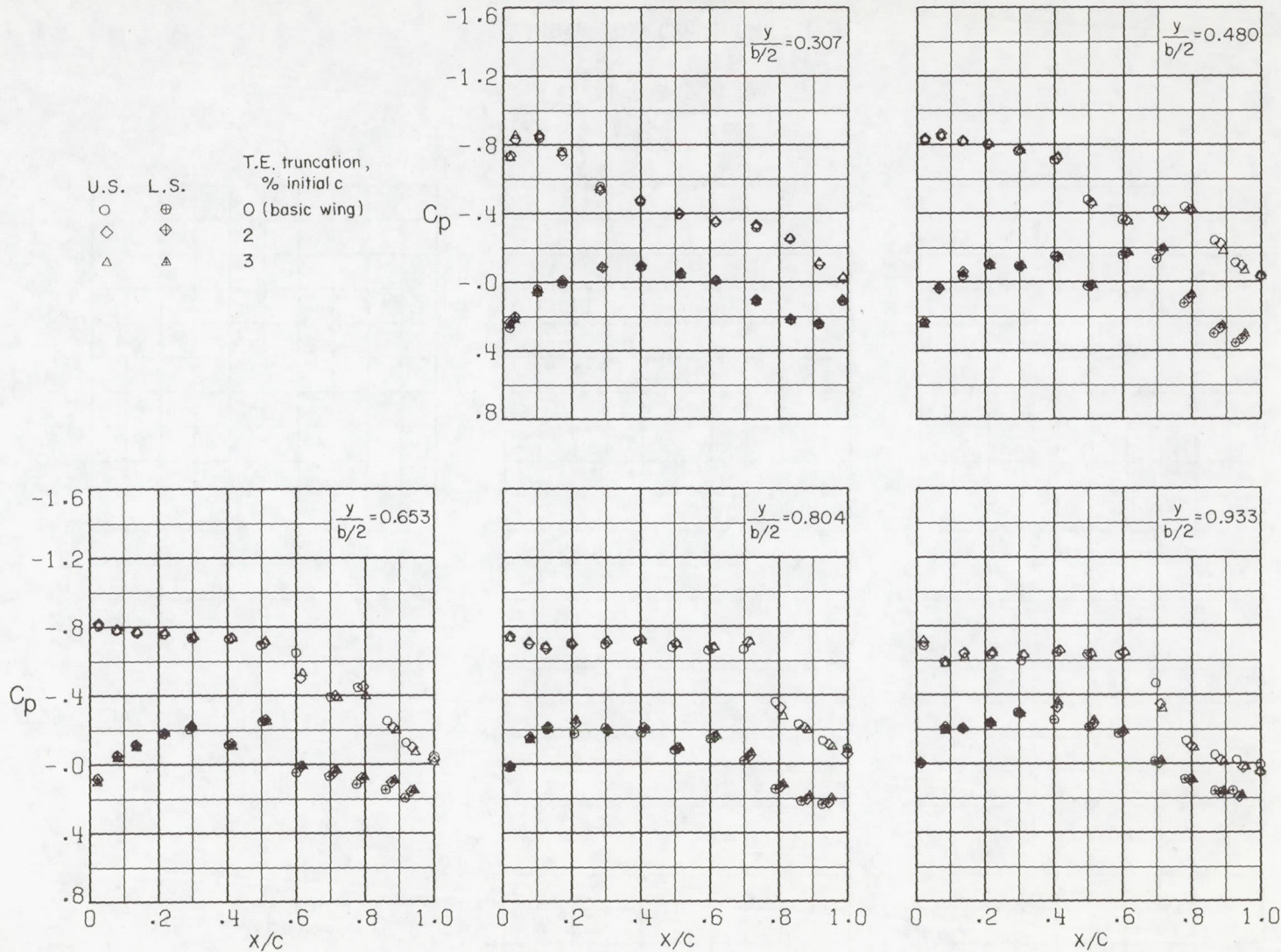
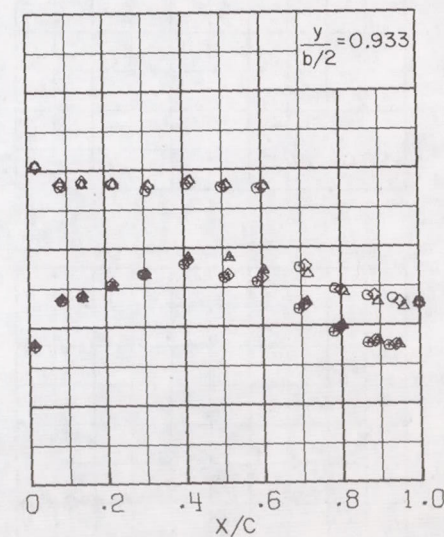
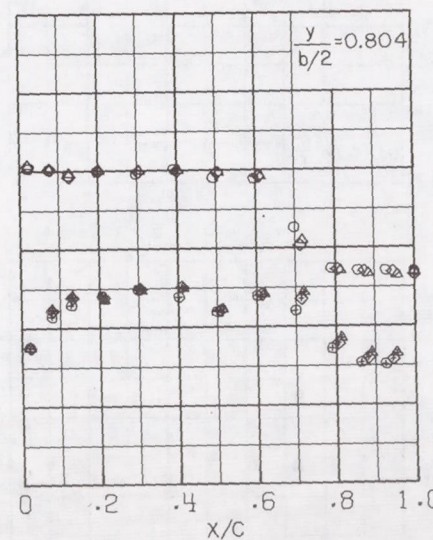
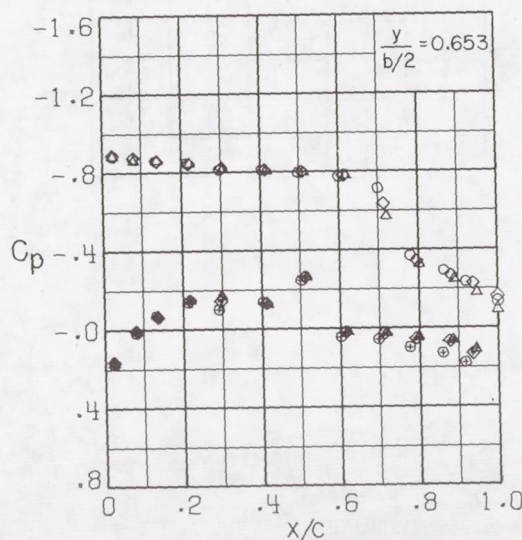
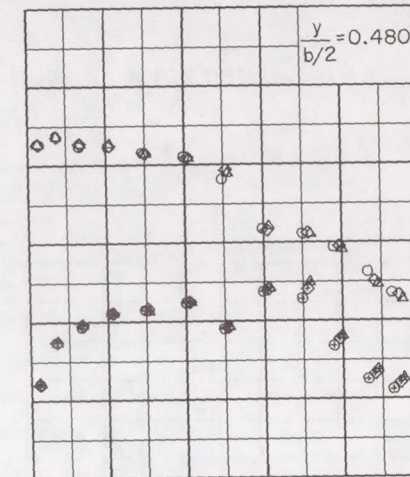
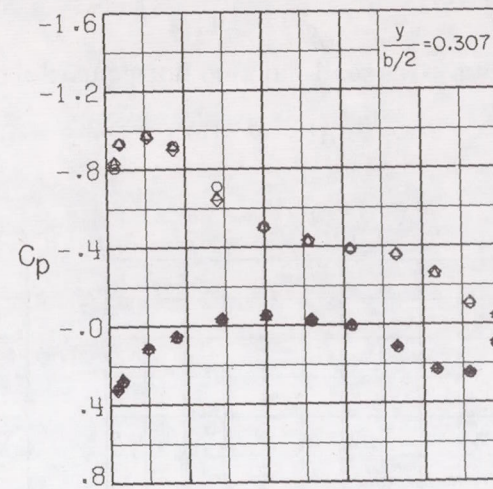
(d) $\alpha = 4^{\circ}$.

Figure 10.- Continued.

CONFIDENTIAL

~~CONFIDENTIAL~~

U.S. L.S.
○ ⊖
◇ ◇
△ △
T.E., truncation,
% initial c
0 (basic wing)
2
3



(e) $\alpha = 5^\circ$.

Figure 10.- Concluded.

~~CONFIDENTIAL~~

CONFIDENTIAL

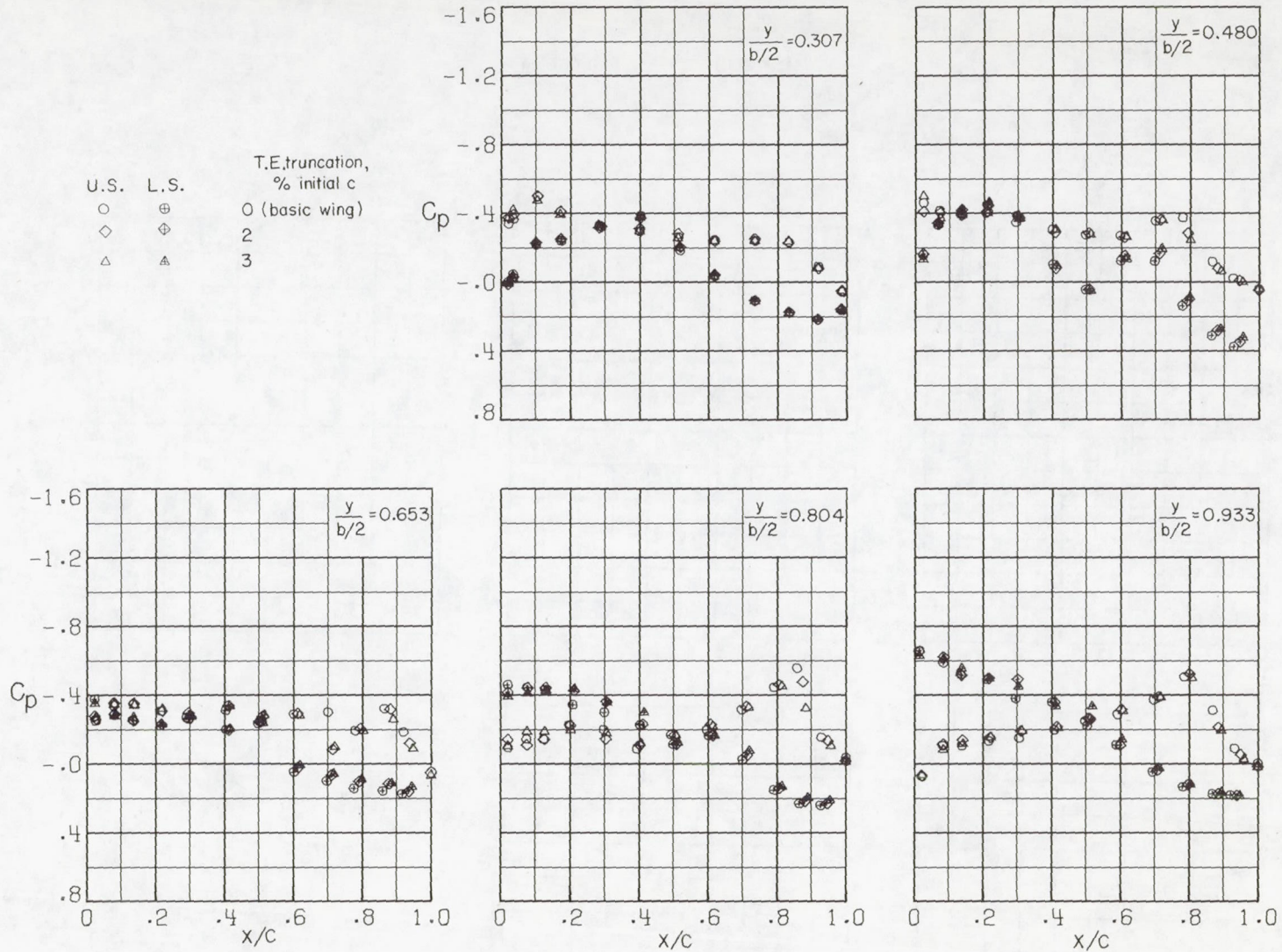
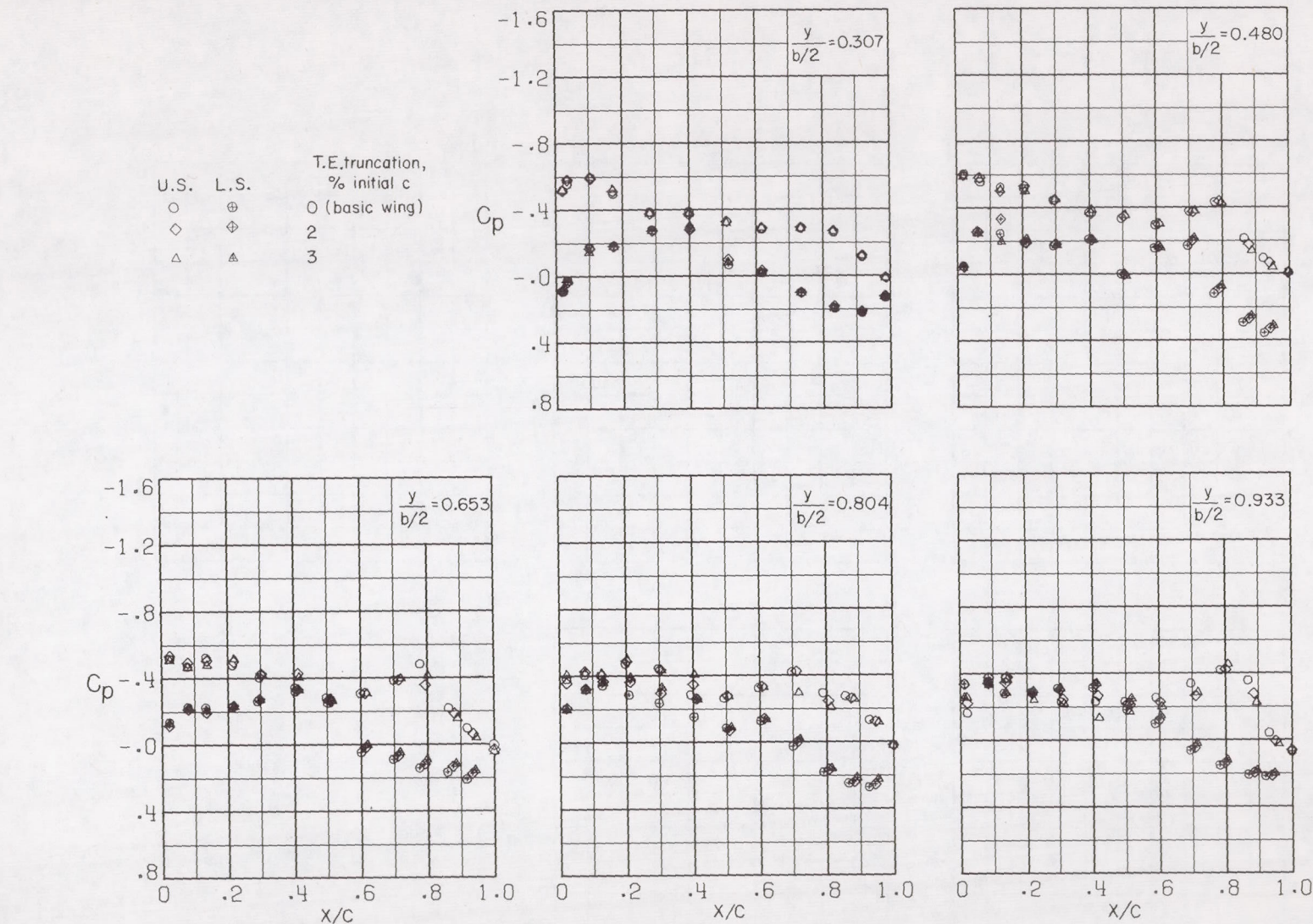
(a) $\alpha = 1^\circ$.

Figure 11.- Effect of wing trailing-edge truncation on wing pressure distributions at Mach number 0.99. $\beta = 0^\circ$; $\delta_h = -2.5^\circ$.

CONFIDENTIAL

~~CONFIDENTIAL~~



(b) $\alpha = 2^\circ$.

Figure 11.- Continued.

~~CONFIDENTIAL~~

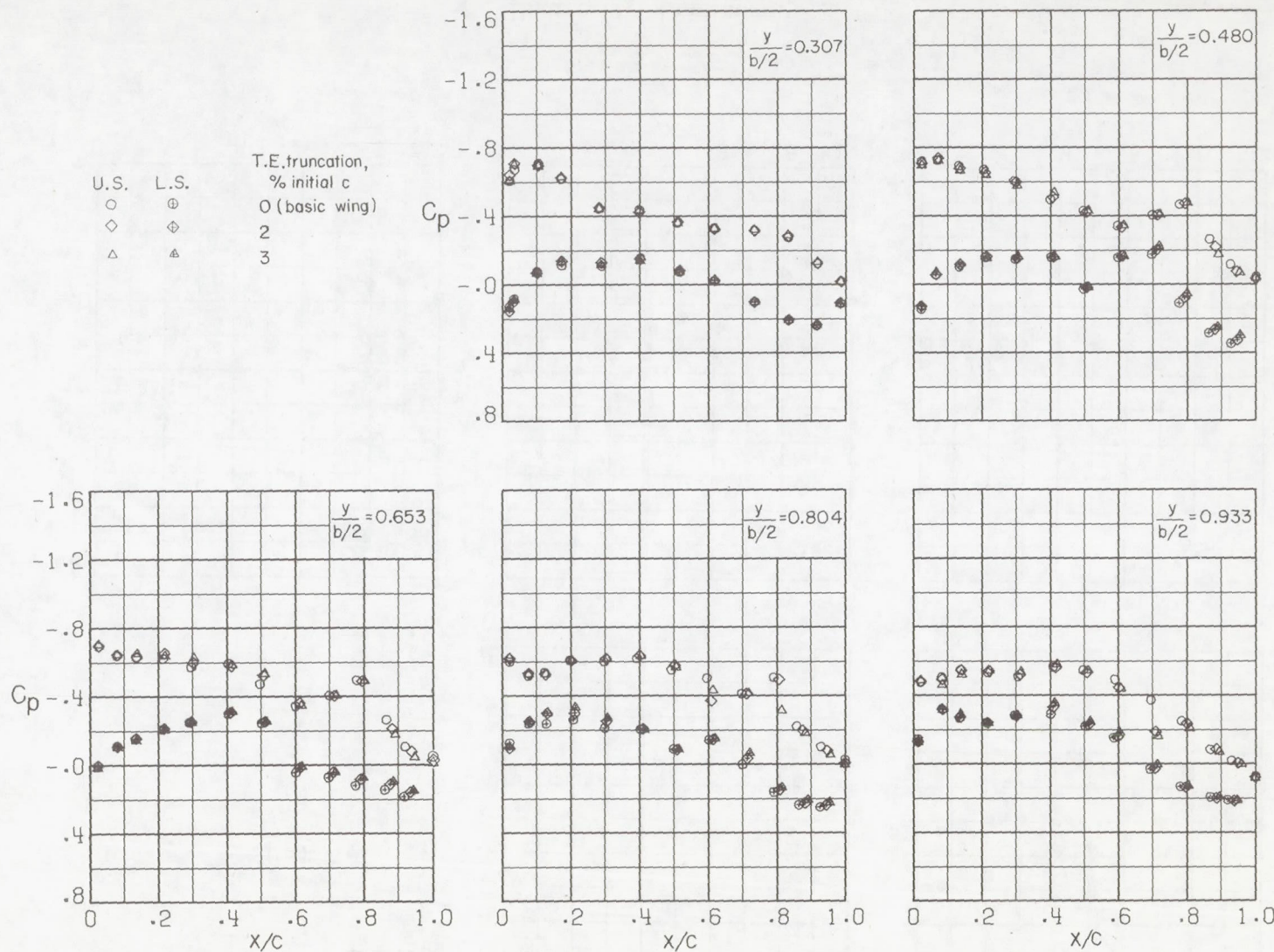
(c) $\alpha = 3^{\circ}$.

Figure 11.- Continued.

CONFIDENTIAL

CONFIDENTIAL

U.S.	L.S.	T.E. truncation, % initial c
○	⊕	O (basic wing)
◇	◊	2
△	▲	3

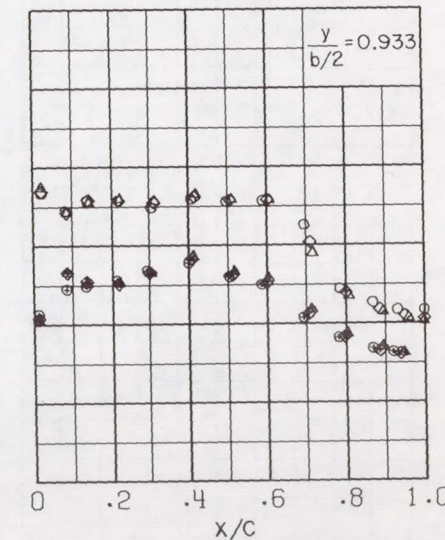
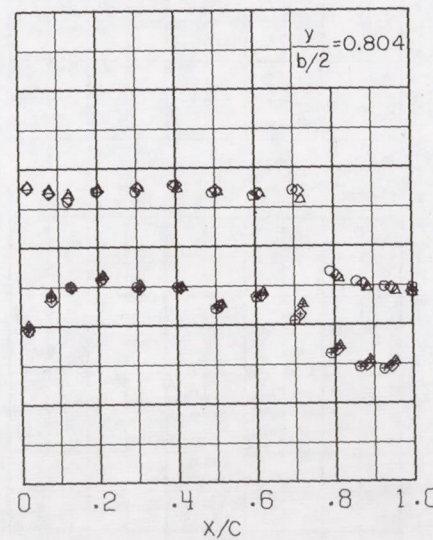
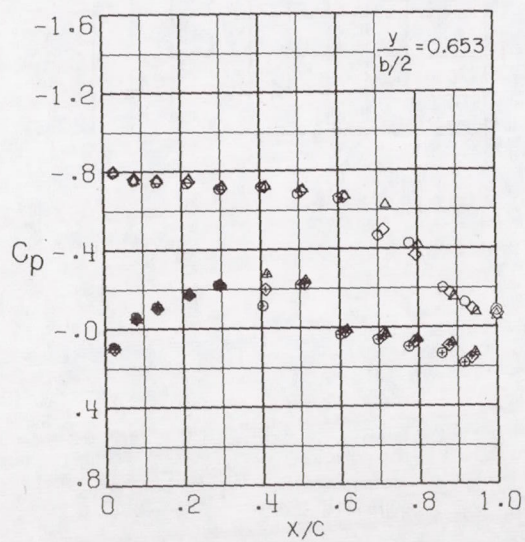
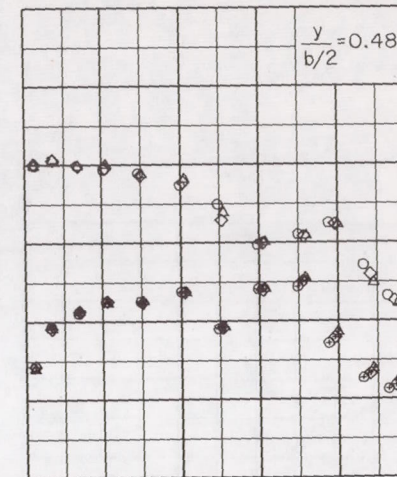
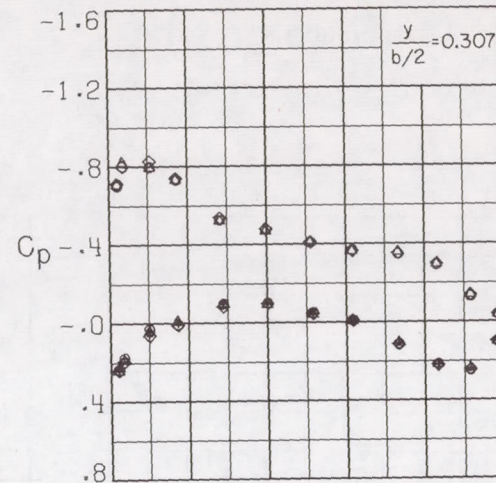
(d) $\alpha = 4^\circ$.

Figure 11.- Continued.

CONFIDENTIAL

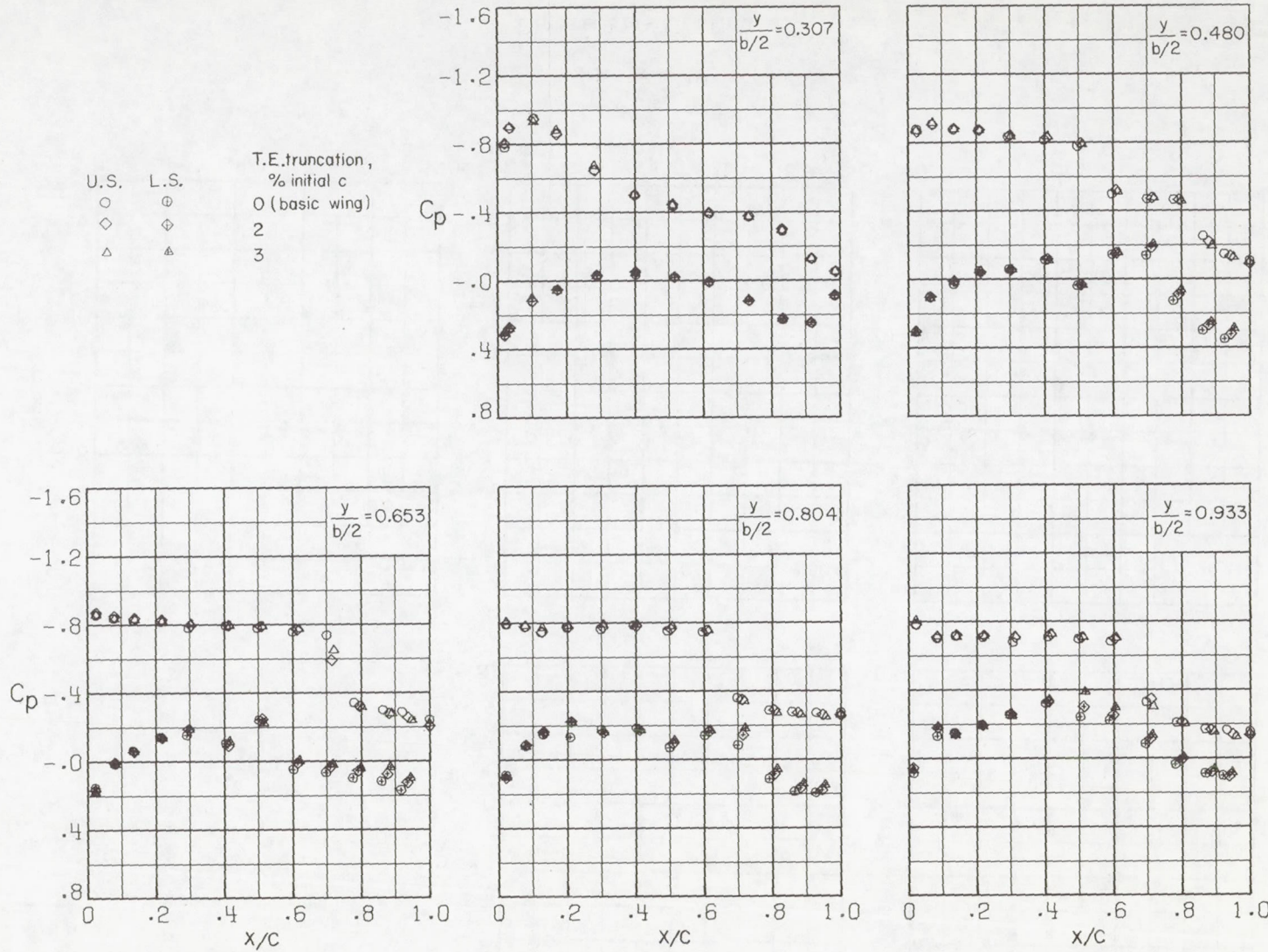
~~CONFIDENTIAL~~~~CONFIDENTIAL~~(e) $\alpha = 5^\circ$.

Figure 11.- Concluded.

CONFIDENTIAL

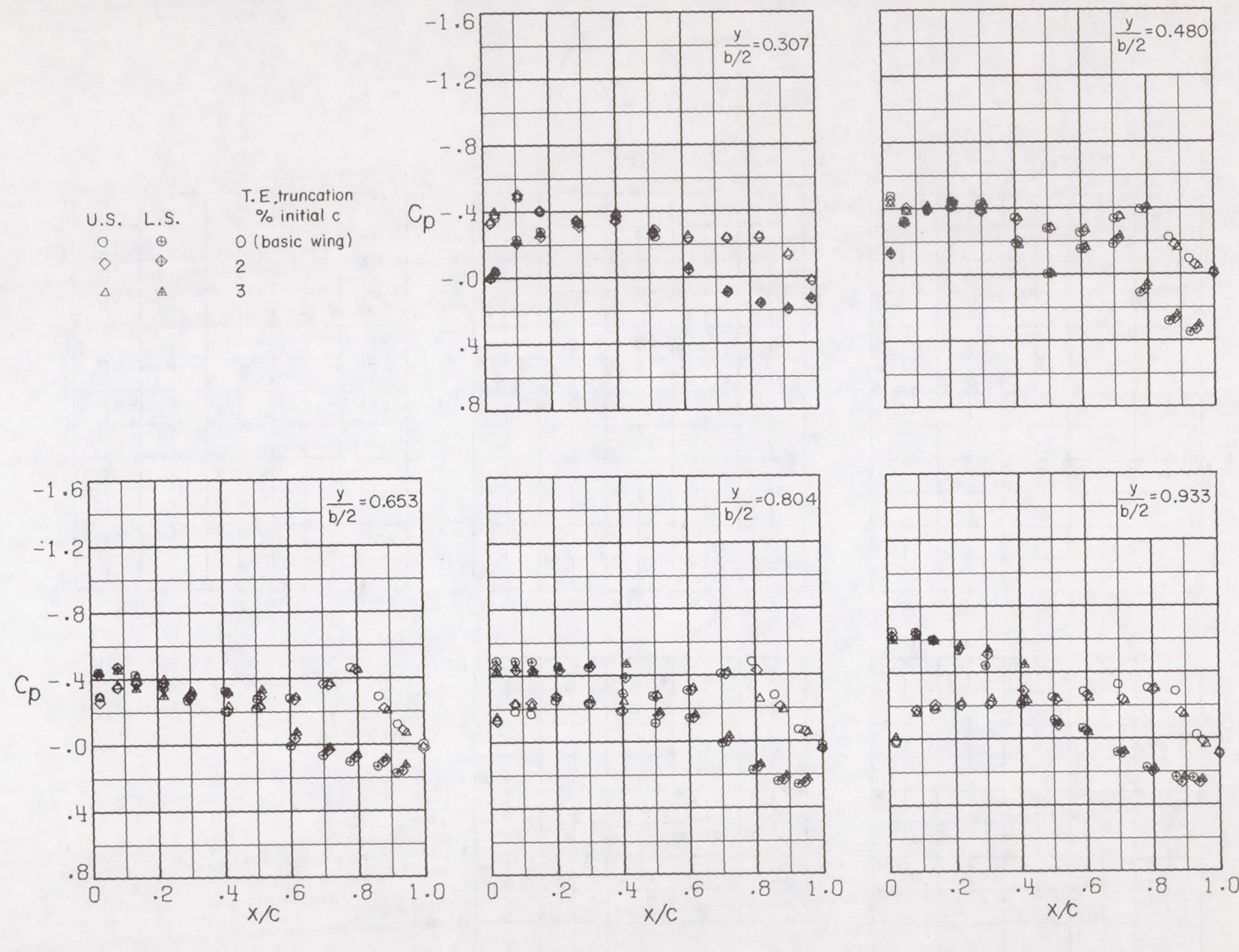
(a) $\alpha = 1^\circ$.

Figure 12.- Effect of wing trailing-edge truncation on wing pressure distributions at Mach number 1.00. $\beta = 0^\circ$; $\delta_h = -2.5^\circ$.

CONFIDENTIAL

CONFIDENTIAL

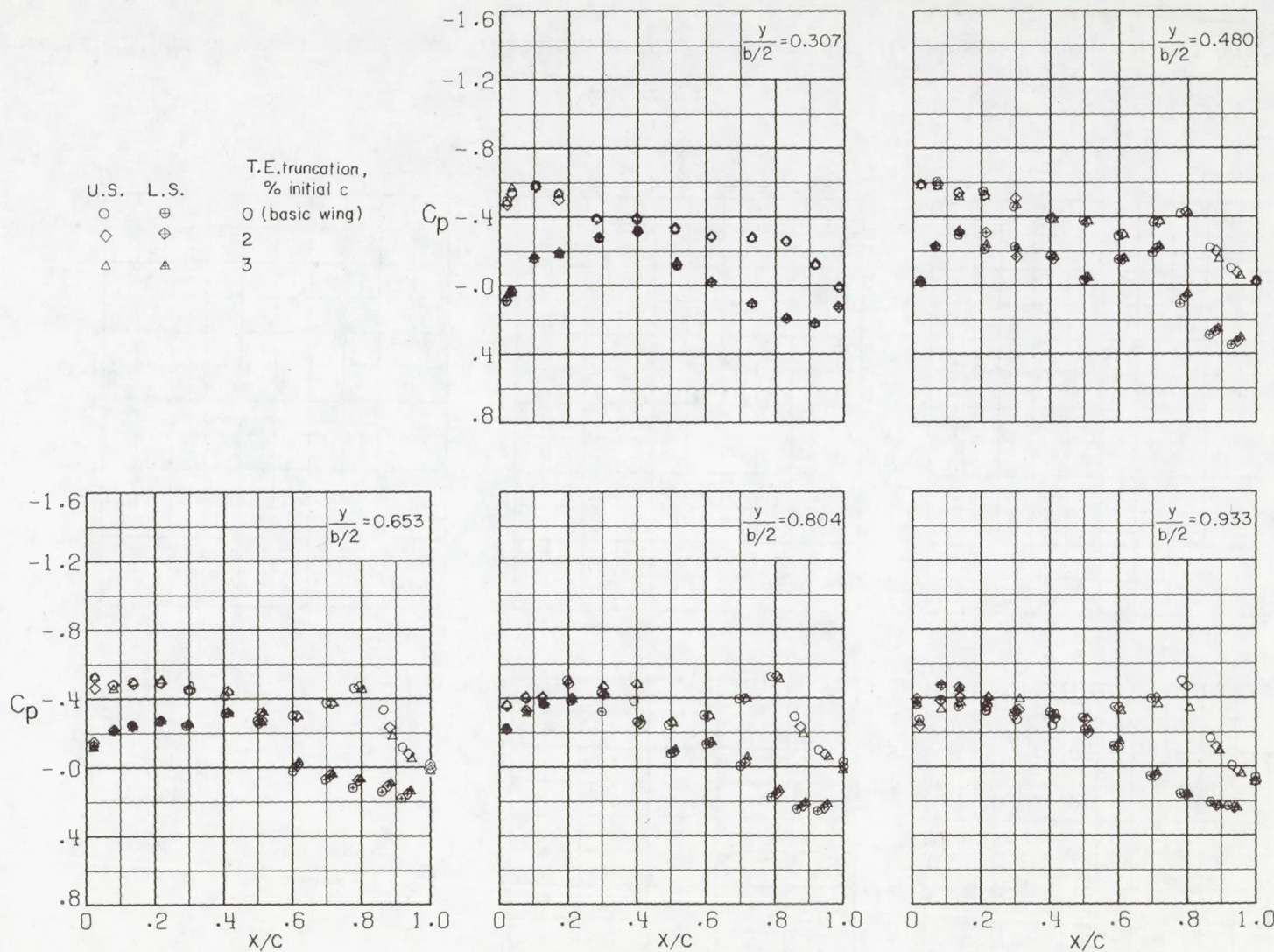
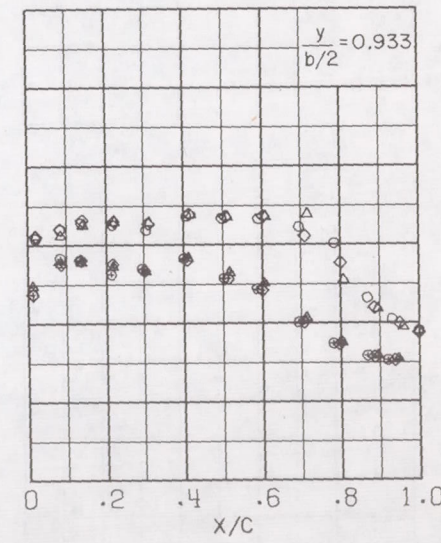
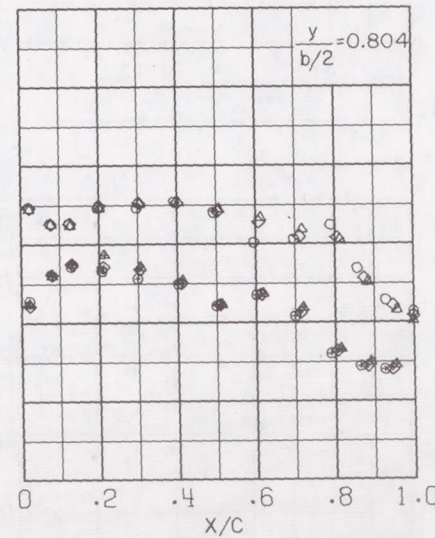
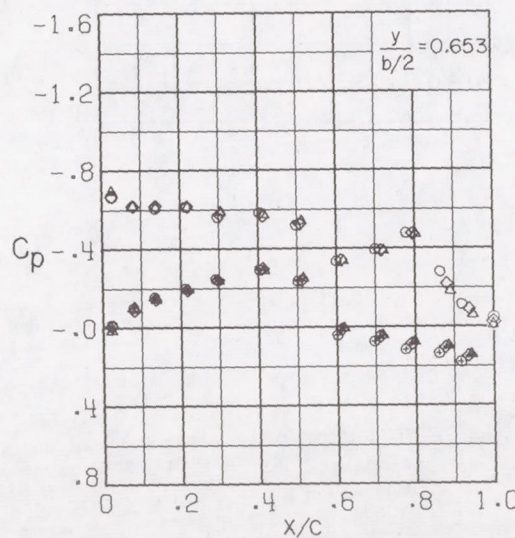
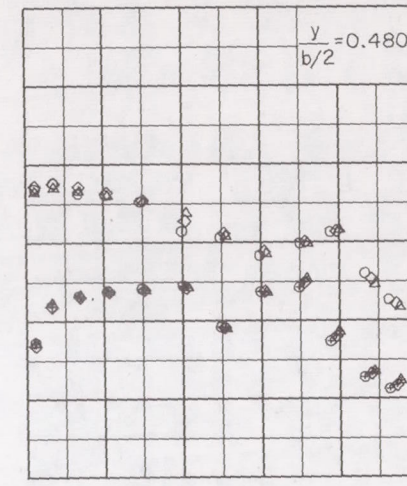
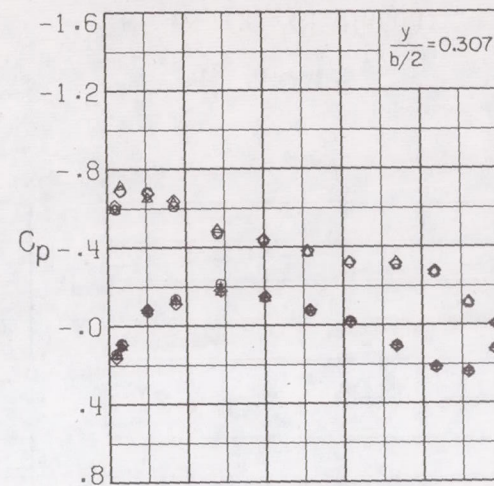
(b) $\alpha = 2^{\circ}$.

Figure 12.- Continued.

~~CONFIDENTIAL~~

U.S. L.S.
○ ⊕ T.E., truncation,
◊ ⊖ % initial c
△ ⊙ 0 (basic wing)
2
3



(c) $\alpha = 3^\circ$.

Figure 12.- Continued.

~~CONFIDENTIAL~~

CONFIDENTIAL

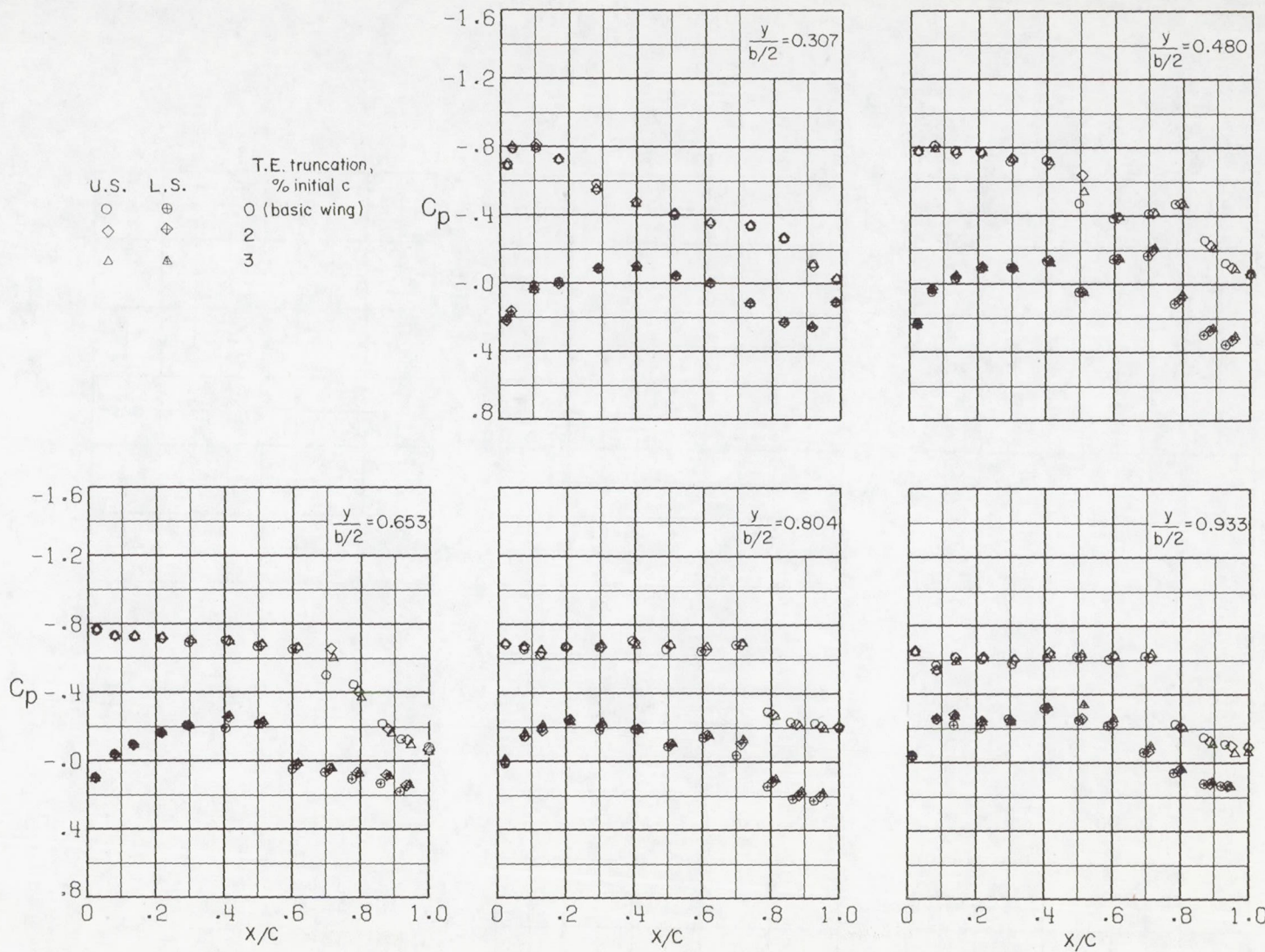
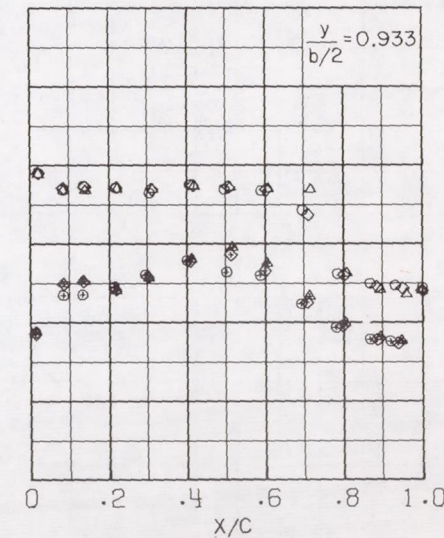
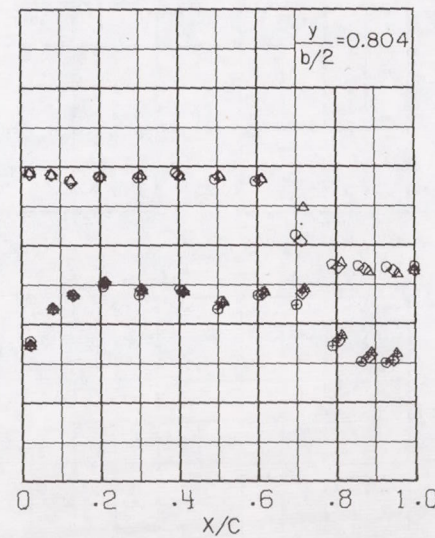
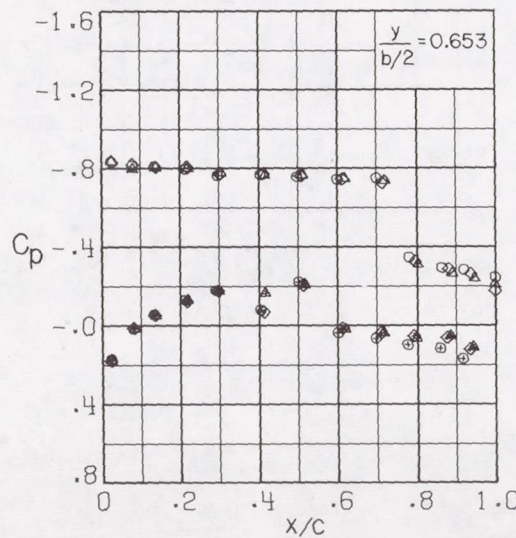
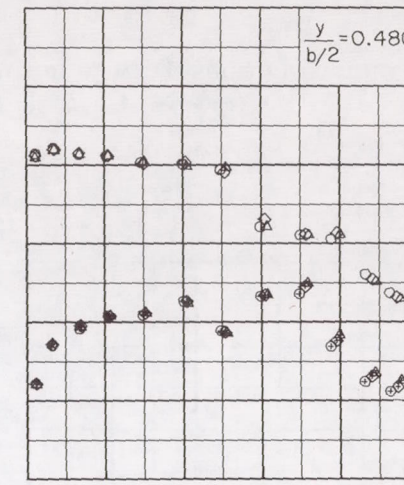
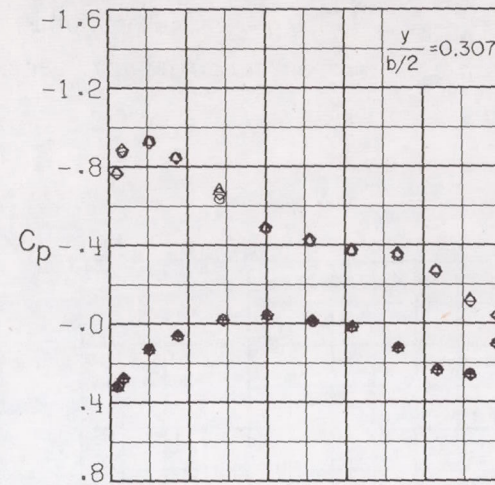
(d) $\alpha = 4^{\circ}$.

Figure 12.- Continued.

CONFIDENTIAL

~~CONFIDENTIAL~~

U.S. L.S.
○ ⊕ T.E., truncation,
◇ ◆ % initial c
△ ▲ 0 (basic wing)
2
3



(e) $\alpha = 5^\circ$.

Figure 12.- Concluded.

~~CONFIDENTIAL~~

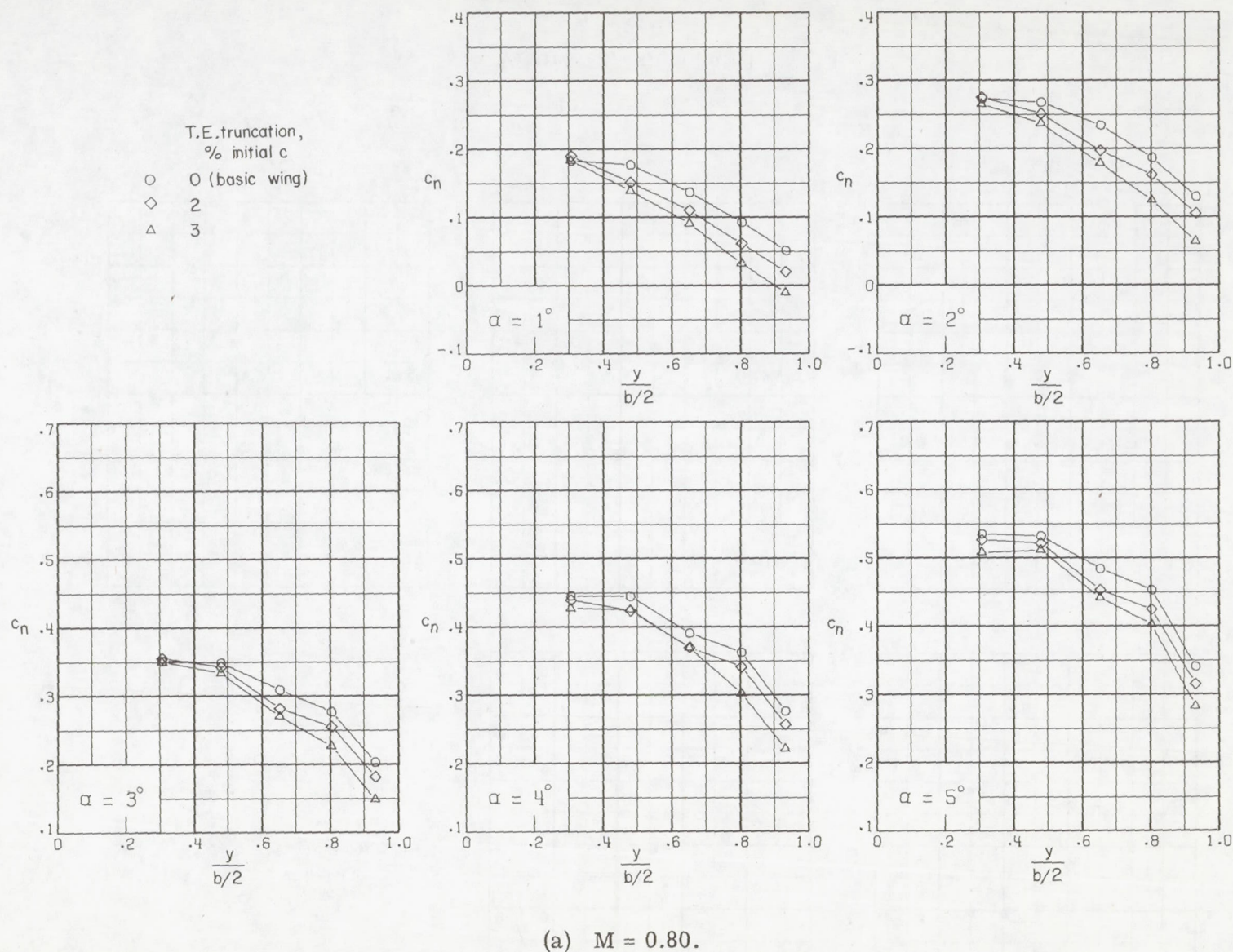
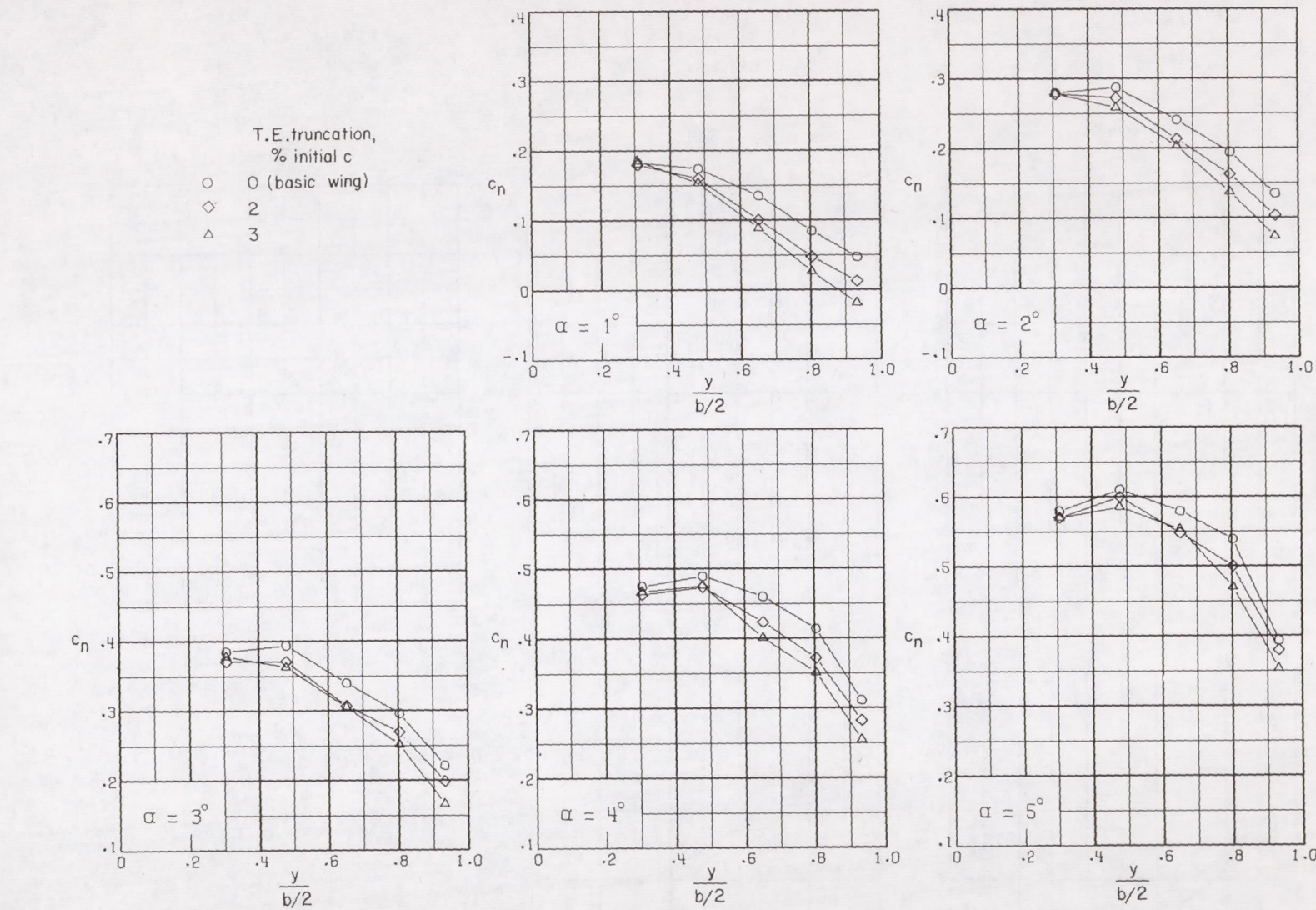


Figure 13. - Effect of wing trailing-edge truncation on the spanwise distribution of wing-section normal-force coefficient. $\beta = 0^\circ$; $\delta_h = -2.5^\circ$

CONFIDENTIAL



(b) $M = 0.90$.

Figure 13.- Continued.

CONFIDENTIAL

CONFIDENTIAL

T.E. truncation,
% initial c
 ○ 0 (basic wing)
 □ 1
 ◇ 2
 △ 3

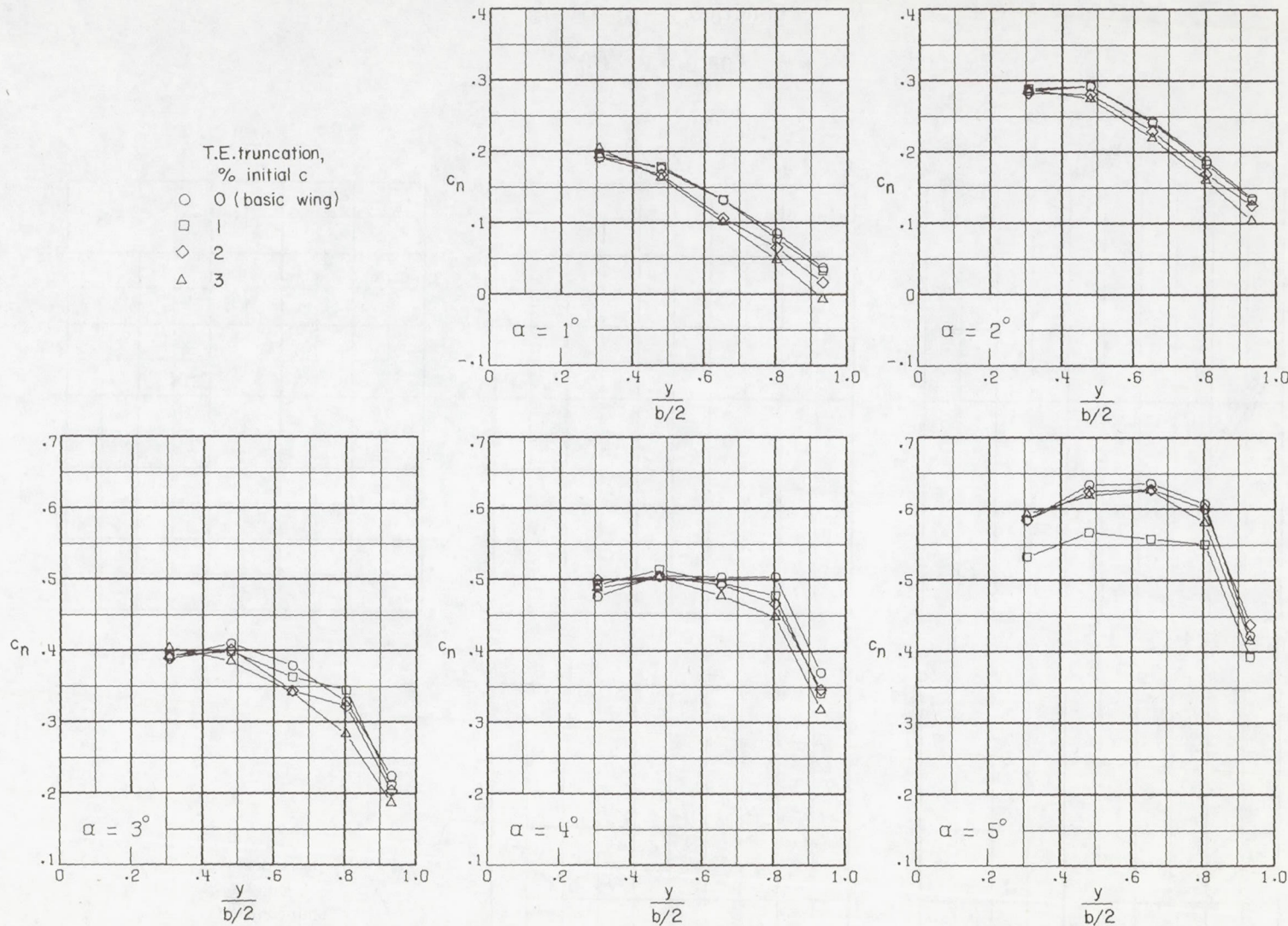
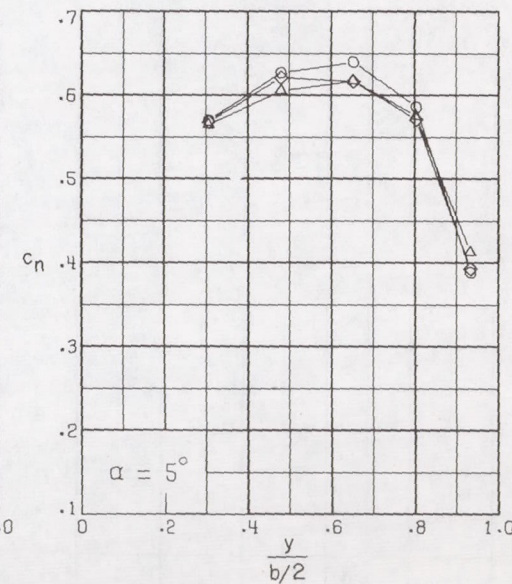
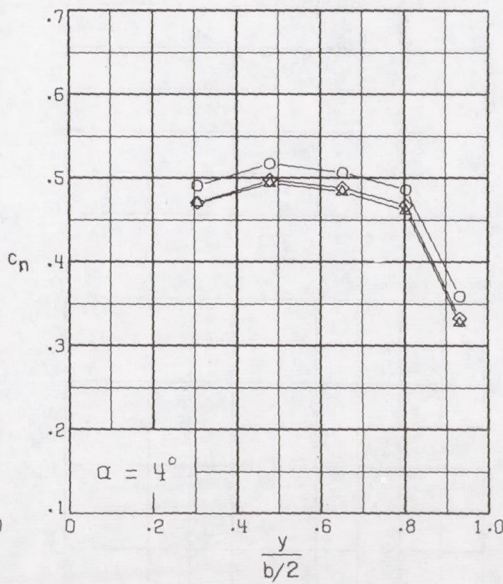
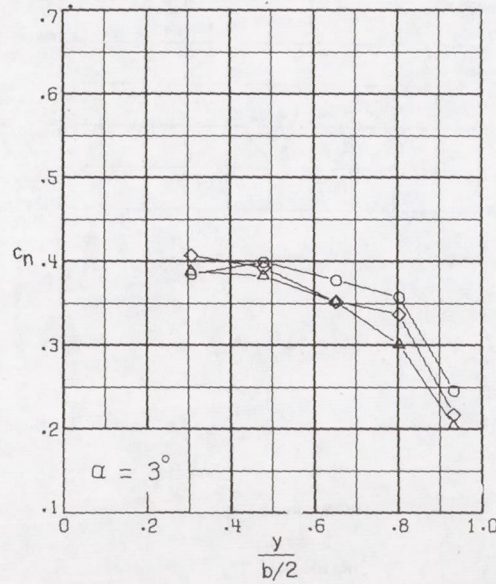
(c) $M = 0.95$.

Figure 13.- Continued.

CONFIDENTIAL

~~CONFIDENTIAL~~

T.E. truncation,
% initial c
○ 0 (basic wing)
◇ 2
△ 3



(d) $M = 0.96$.

Figure 13.- Continued.

~~CONFIDENTIAL~~

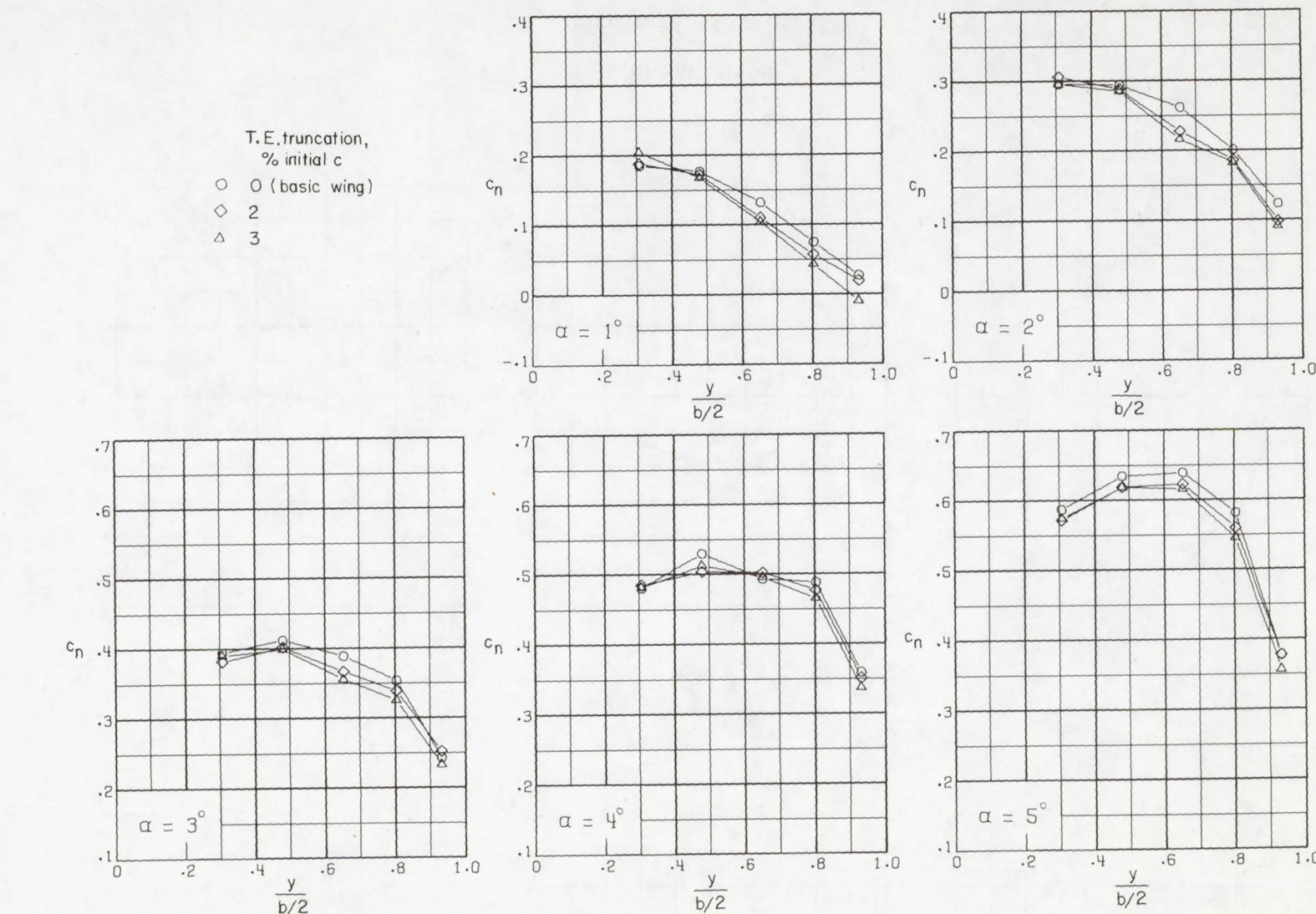
~~CONFIDENTIAL~~(e) $M = 0.97$.

Figure 13.- Continued.

~~CONFIDENTIAL~~

CONFIDENTIAL

T.E. truncation,
% initial c

- 0 (basic wing)
- ◇ 2
- △ 3

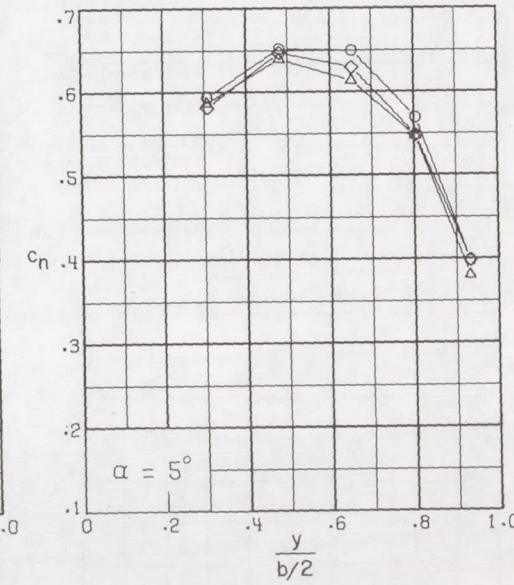
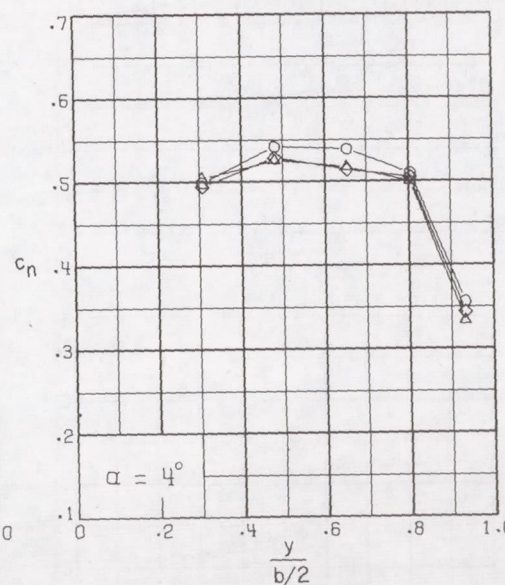
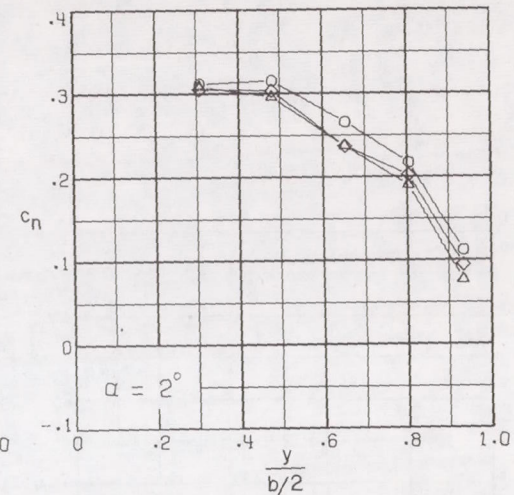
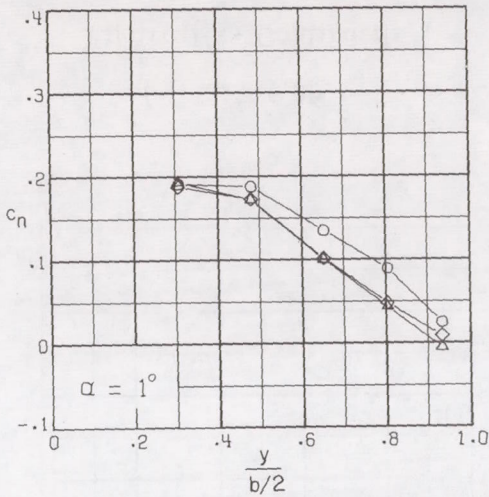
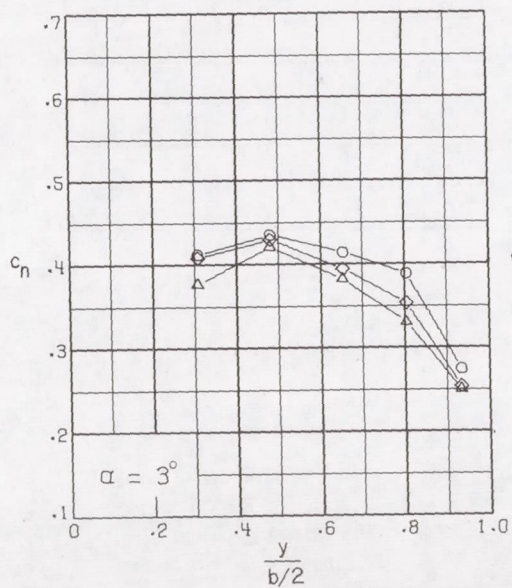
(f) $M = 0.98$.

Figure 13.- Continued.

CONFIDENTIAL

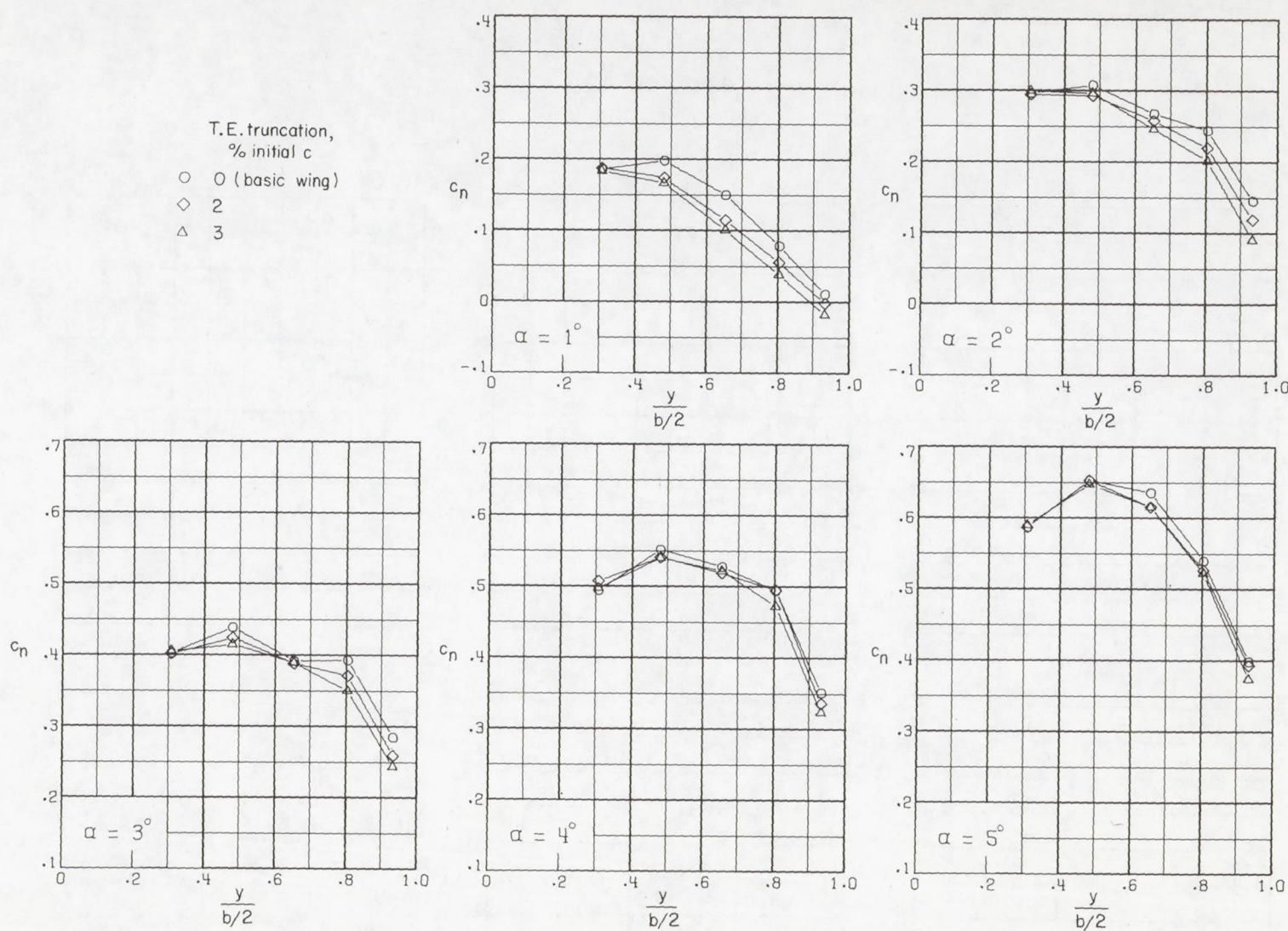
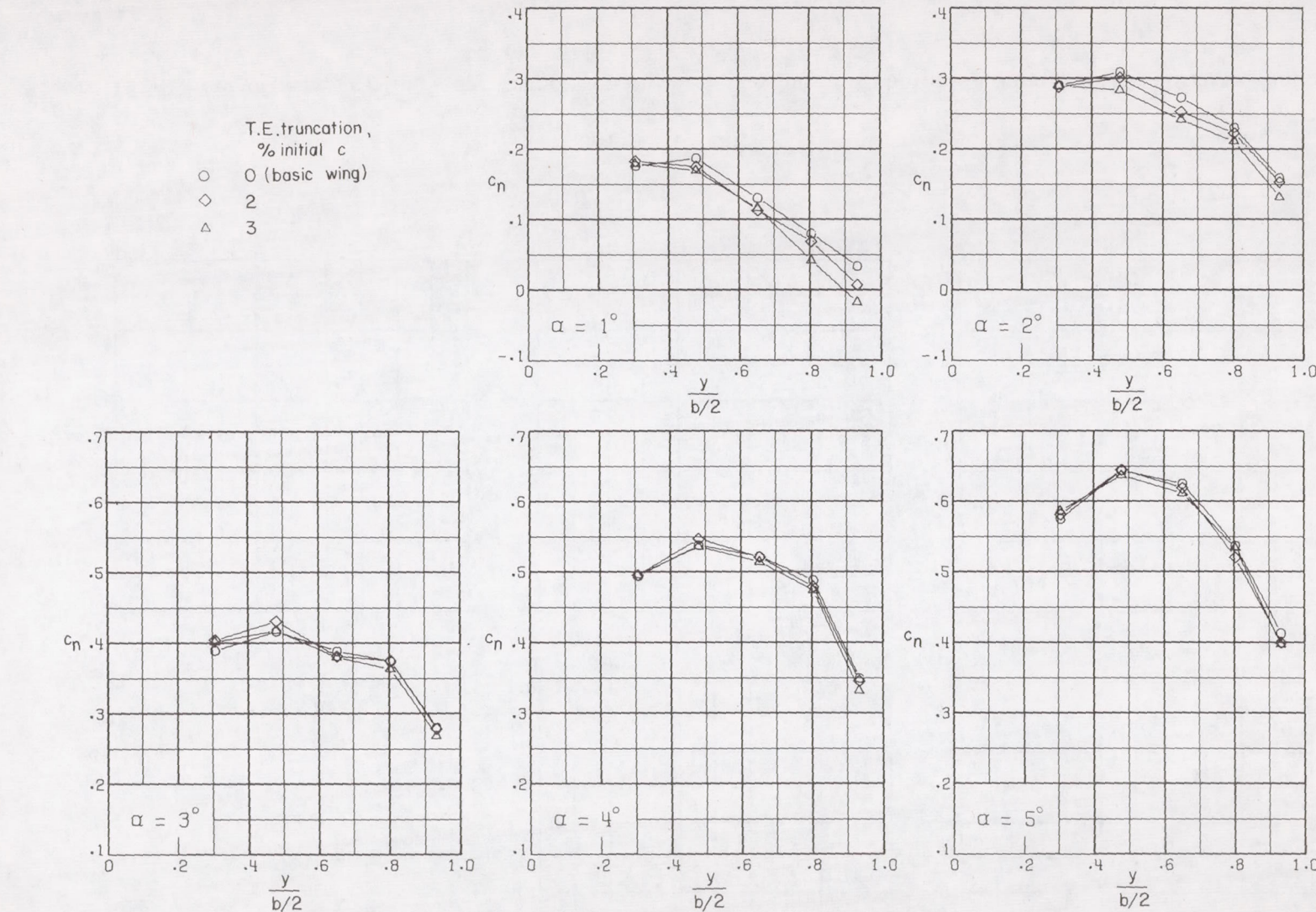
(g) $M = 0.99$.

Figure 13.- Continued.

CONFIDENTIAL

CONFIDENTIAL

~~CONFIDENTIAL~~



(h) $M = 1.00$.

Figure 13.- Concluded.

~~CONFIDENTIAL~~

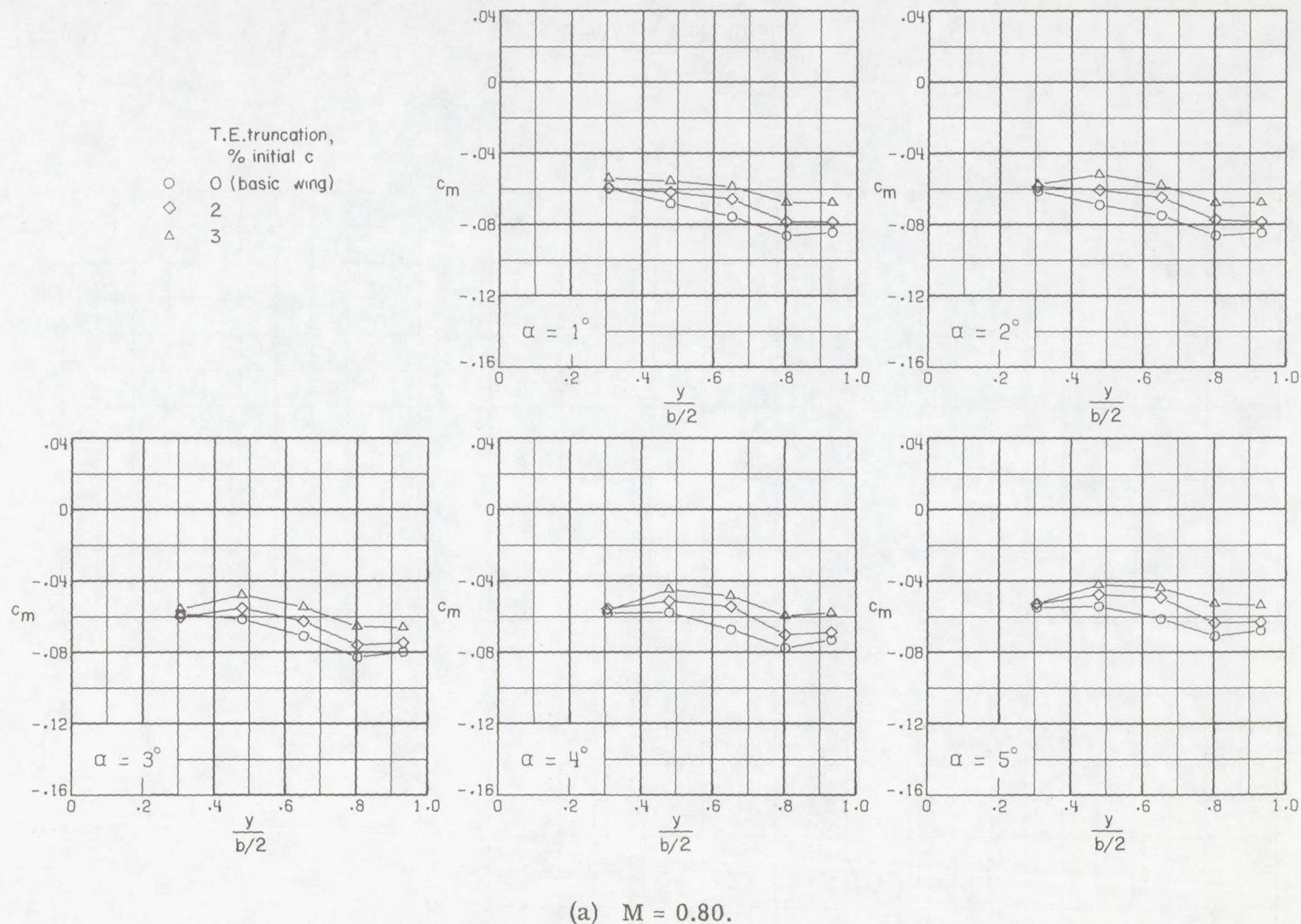


Figure 14.- Effect of wing trailing-edge truncation on the spanwise distribution of wing-section pitching-moment coefficient. $\beta = 0^\circ$; $\delta_h = -2.5^\circ$.

CONFIDENTIAL

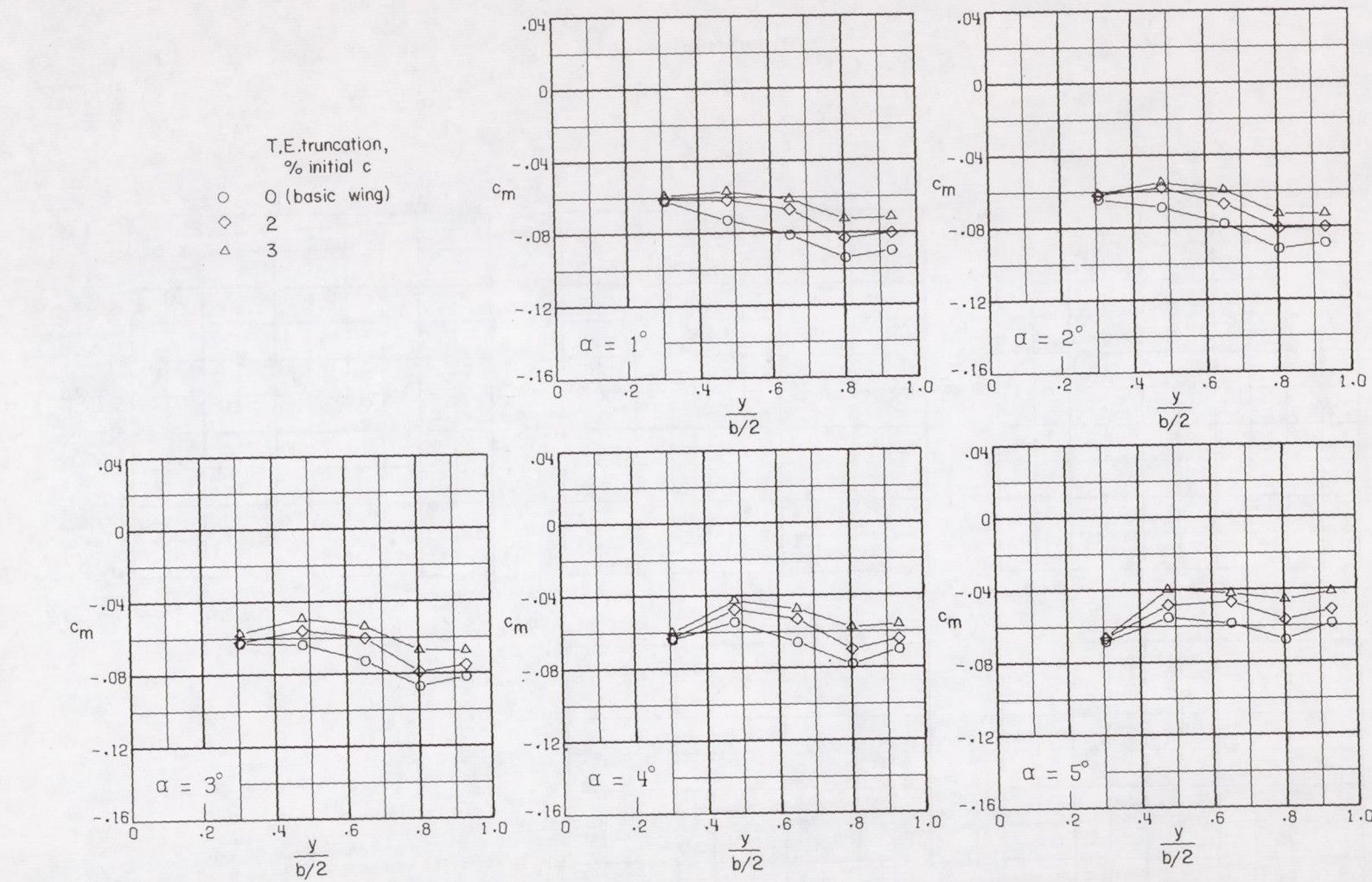
(b) $M = 0.90$.

Figure 14.- Continued.

CONFIDENTIAL

CONFIDENTIAL

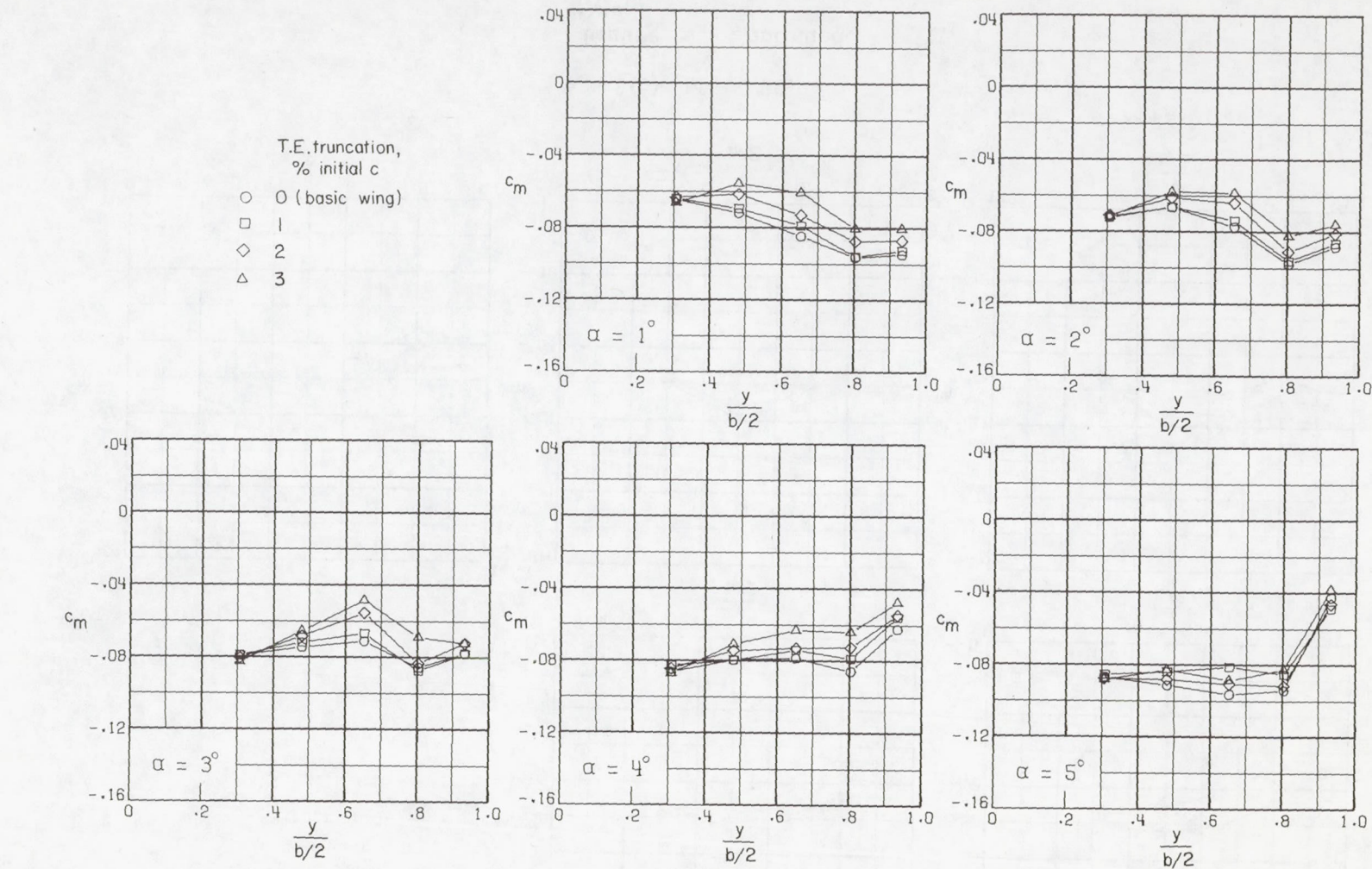
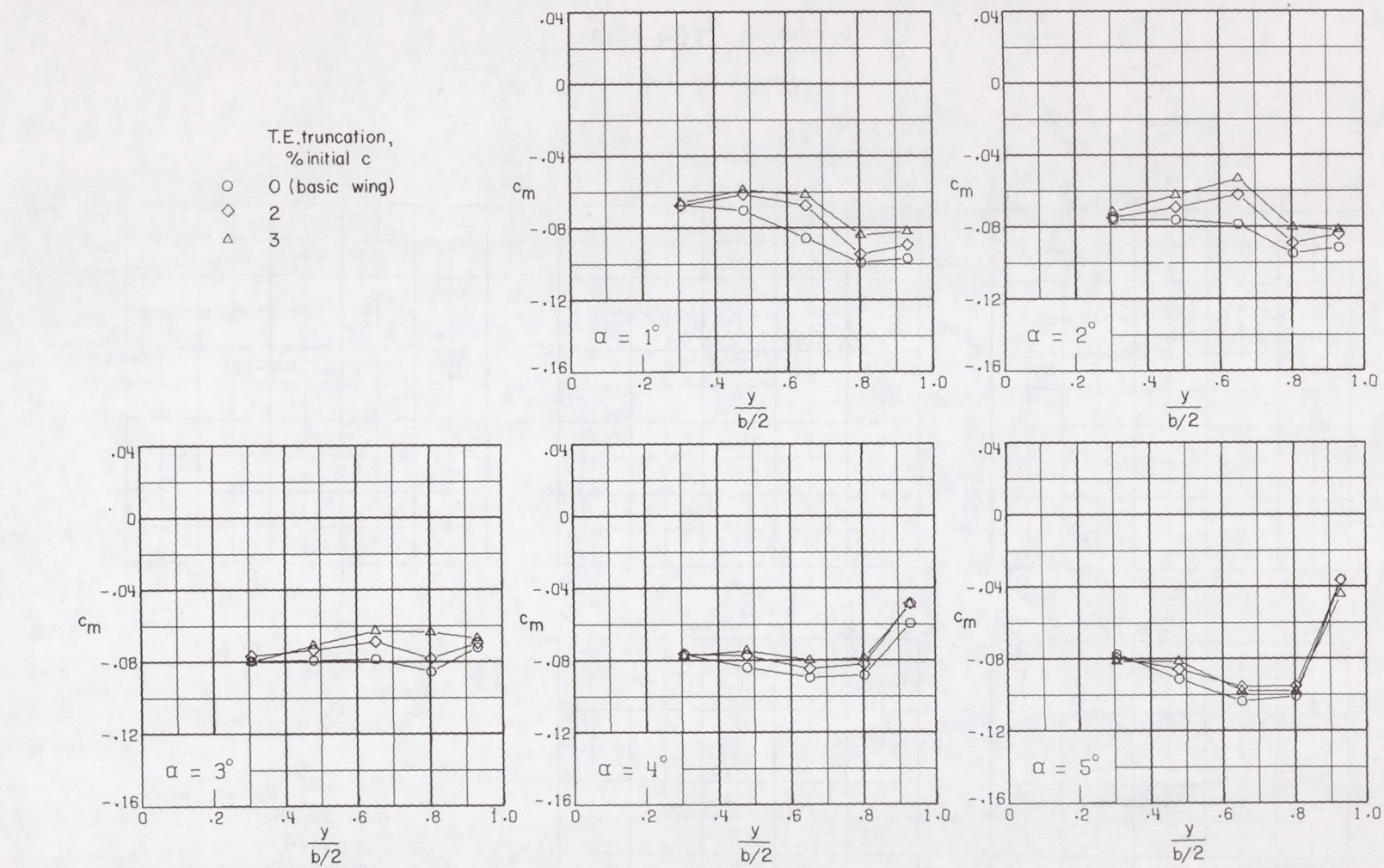
(c) $M = 0.95$.

Figure 14.- Continued.

CONFIDENTIAL

~~CONFIDENTIAL~~



(d) $M = 0.96$.

Figure 14.- Continued.

~~CONFIDENTIAL~~

CONFIDENTIAL

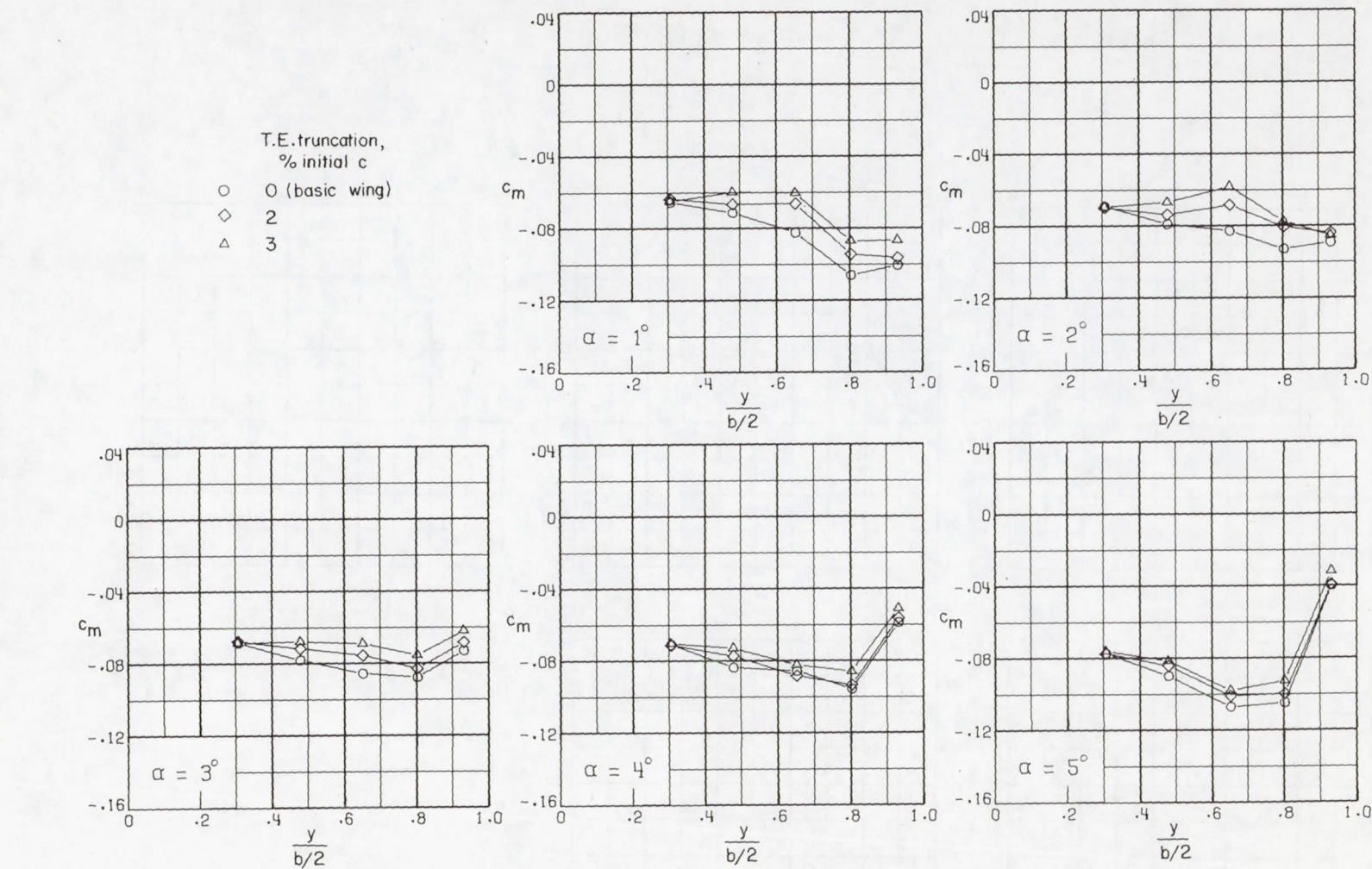
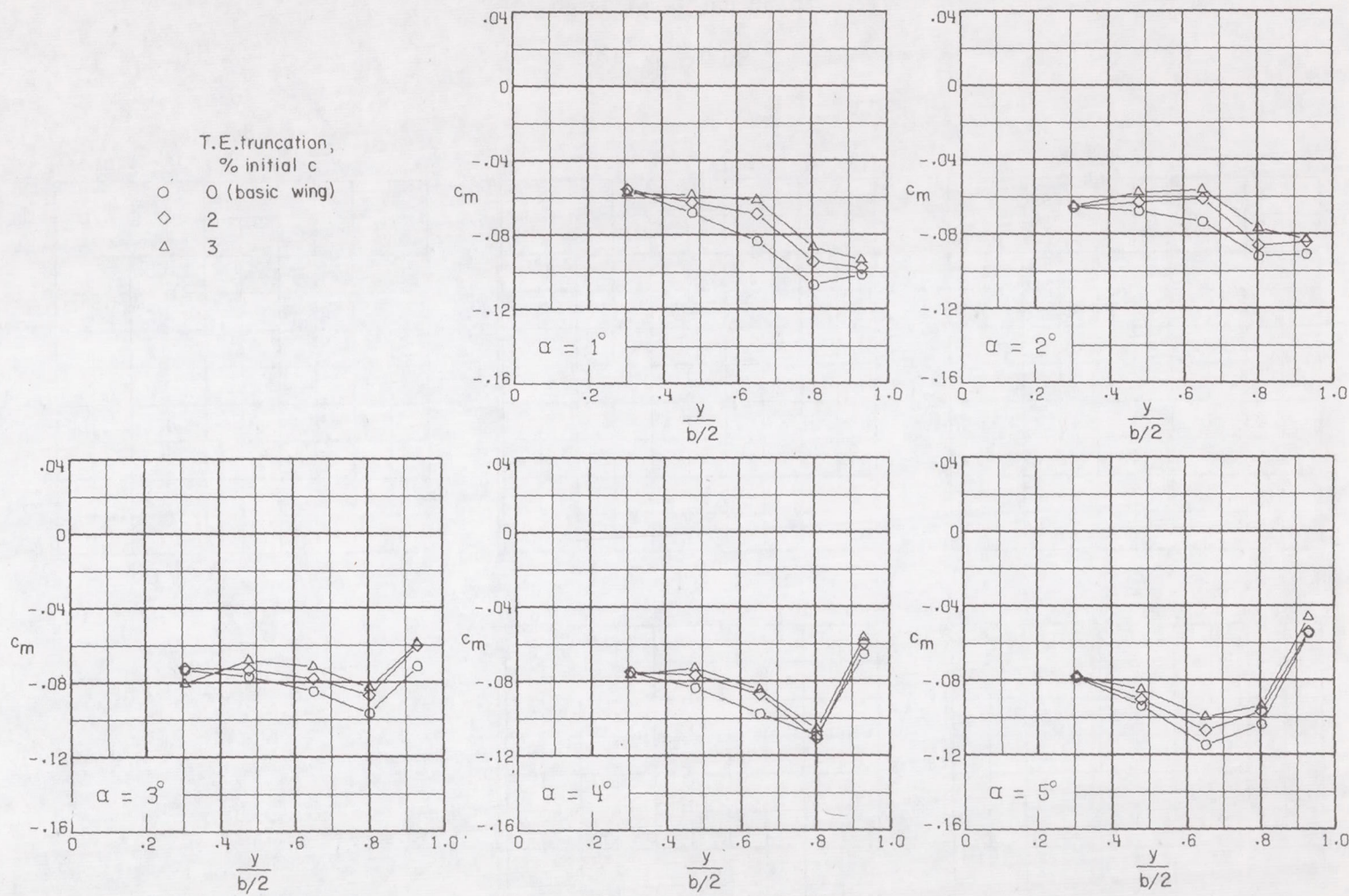
(e) $M = 0.97$.

Figure 14.- Continued.

CONFIDENTIAL

CONFIDENTIAL



(f) $M = 0.98$.

Figure 14.- Continued.

CONFIDENTIAL

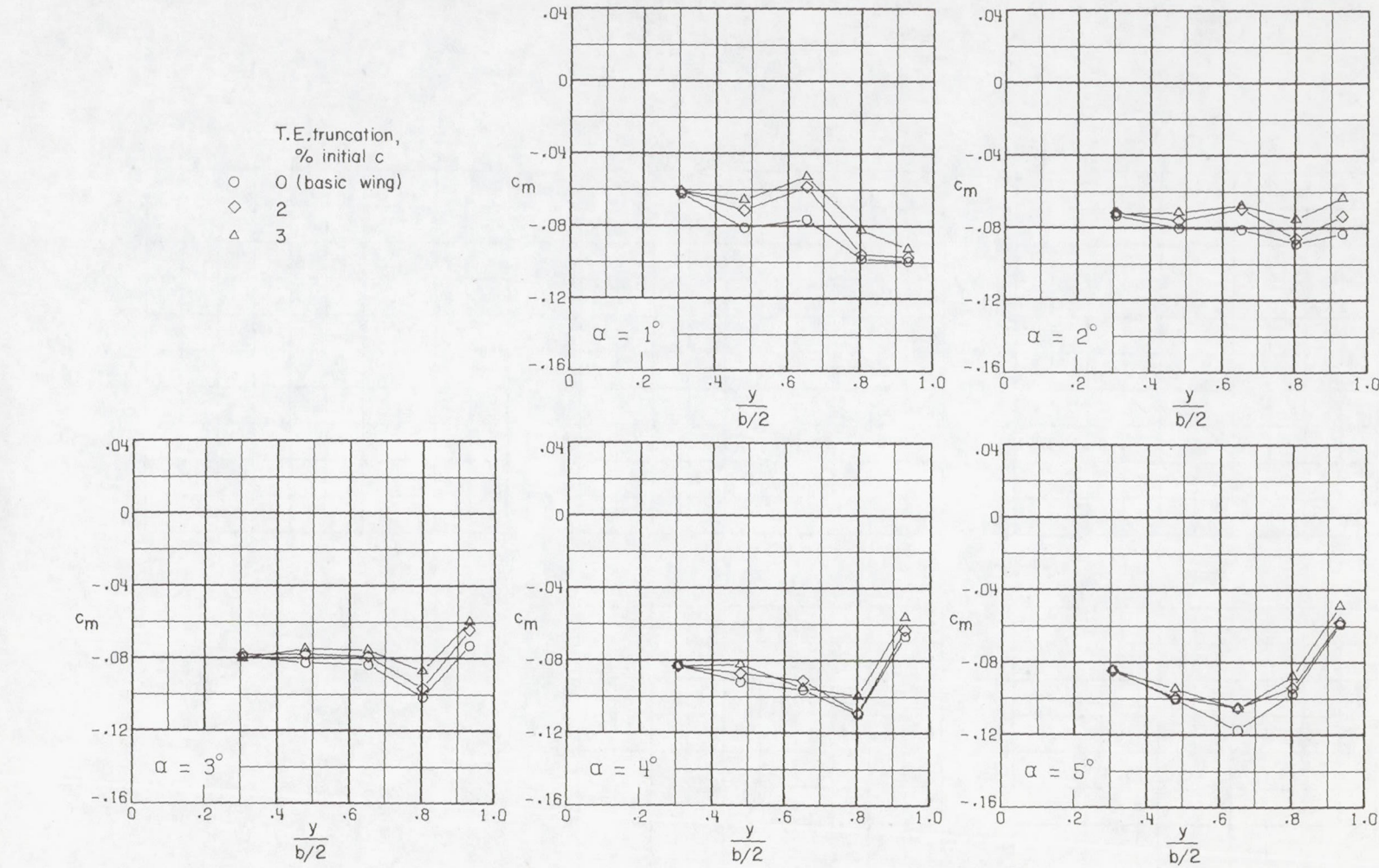
~~CONFIDENTIAL~~(g) $M = 0.99$.

Figure 14.- Continued.

~~CONFIDENTIAL~~

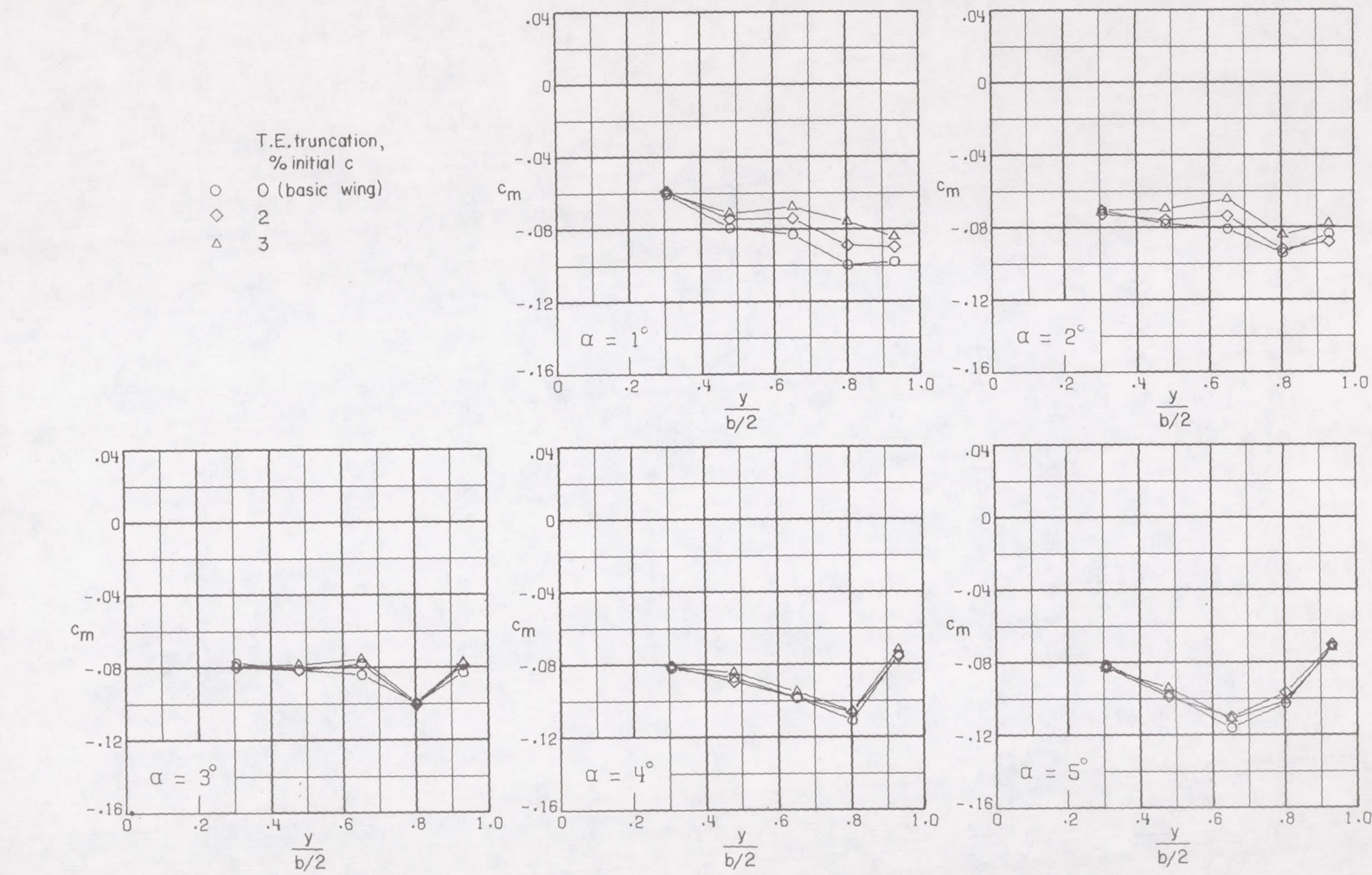
~~CONFIDENTIAL~~(h) $M = 1.00.$

Figure 14.- Concluded.

~~CONFIDENTIAL~~

~~CONFIDENTIAL~~

~~CONFIDENTIAL~~

~~CONFIDENTIAL~~

"The aeronautical and space activities of the United States shall be conducted so as to contribute . . . to the expansion of human knowledge of phenomena in the atmosphere and space. The Administration shall provide for the widest practicable and appropriate dissemination of information concerning its activities and the results thereof."

— NATIONAL AERONAUTICS AND SPACE ACT OF 1958

NASA SCIENTIFIC AND TECHNICAL PUBLICATIONS

TECHNICAL REPORTS: Scientific and technical information considered important, complete, and a lasting contribution to existing knowledge.

TECHNICAL NOTES: Information less broad in scope but nevertheless of importance as a contribution to existing knowledge.

TECHNICAL MEMORANDUMS: Information receiving limited distribution because of preliminary data, security classification, or other reasons.

CONTRACTOR REPORTS: Scientific and technical information generated under a NASA contract or grant and considered an important contribution to existing knowledge.

TECHNICAL TRANSLATIONS: Information published in a foreign language considered to merit NASA distribution in English.

SPECIAL PUBLICATIONS: Information derived from or of value to NASA activities. Publications include conference proceedings, monographs, data compilations, handbooks, sourcebooks, and special bibliographies.

TECHNOLOGY UTILIZATION

PUBLICATIONS: Information on technology used by NASA that may be of particular interest in commercial and other non-aerospace applications. Publications include Tech Briefs, Technology Utilization Reports and Notes, and Technology Surveys.

Details on the availability of these publications may be obtained from:

**SCIENTIFIC AND TECHNICAL INFORMATION OFFICE
NATIONAL AERONAUTICS AND SPACE ADMINISTRATION
Washington, D.C. 20546**

~~CONFIDENTIAL~~